KTH Aeronautical
and Vehicle Engineering

# *INVESTIGATION OF NONLINEAR ACOUSTICAL PROPERTIES OF PERFORATED PLATE SAMPLES AND SAMPLES OF AIRCRAFT ENGINE LINERS*

*Master of Science Thesis at MWL, KTH*

by

**Daniel Pimenov**

Supervisor: Hans Boden
Stockholm, Sweden 2010

# Abstract


Five samples, three perforated plates and two more realistic samples used in aircraft engine liners have been investigated.
All the samples when exposed to high amplitude sound waves show nonlinear acoustic behavior which depends on acoustic velocity at the plate position. Velocity dependent sound absorption and acoustic energy transfer to higher harmonics are the consequence.

In the literature there is a lack of systematic experimental approach to determine these energy transfers to other frequencies considering harmonics.

In this thesis a one-port model for measurements in impedance tube is chosen with sound pressure at the frequency of excitation and two and three times higher than that as variables. The samples are tested at single tone and two tone excitation involving harmonics at 110Hz, 220Hz and 330Hz with varying particle velocity at the sample position. In the case of realistic samples an excitation frequency of 990Hz was also used because these samples are designed for higher frequencies and higher sound levels.

For single tone excitation both low and high sound levels are used to see linear and nonlinear behavior of acoustic properties.
A part of investigation for two tone excitation is to analyze acoustical properties when the tones are not exactly harmonics but are slightly different from that, 330Hz combined with 100Hz or 110HZ or 120HZ.
The effect of shifting the phase of one of two signals on impedance measurement for three perforated samples has also been studied.

Results from experimental tests using these techniques give a good understanding of the acoustical behavior of the samples at both low and high sound levels.

Two different methods, the two-microphone method and sound intensity probe (p-u probe) method, are used to obtain the results in order to compare the reliability of both methods.

# Table of Contents

# 1. Introduction

This paper presents the results of a study of non-linear acoustic properties of perforated plate samples and two realistic samples with more complex structure. In the range with linear behavior the perforate acoustic properties as reflection coefficient and acoustic impedance in form of resistance and reactance are independent of the sound field but when the sound pressure level is high they will be dependent on the acoustic particle velocity in the holes. It is assumed that the non-linearity occurs locally at constrictions or sharp corners and is caused by turbulence consisting of vortices produced at edges of holes which leads to energy transferring between frequencies. The structure of the samples influences the turbulence character and so acoustical properties which in that way depends on the size of holes in the perforate, thickness of the plate, number of holes as well as the percentage open area.

For pure tone excitation the acoustic properties will be controlled by the acoustic particle velocity at that frequency. If the acoustic excitation includes signals at other frequencies the acoustic properties at a certain frequency will depend on the particle velocity at other frequencies. This thesis investigates harmonic interaction effects by using single pure tone excitation and two-tone pure excitation. Also effect of shifting the phase on one of two tones will be studied.

The choice of harmonics considering two-tone excitation was 110Hz, 220Hz and 330Hz, but for the realistic samples which are designed for working conditions at higher frequencies and even higher sound levels, the combinations of 110Hz, 330Hz and 990Hz are chosen.

The influence on the acoustic properties of not having exact harmonics is also discussed. For this purpose the combinations of signals at 330Hz and 100Hz or 110Hz or 120Hz are used.

Impedance tube measurements, using two different methods in order to compare them, were made for determining the acoustic impedance of non-linear samples using sinusoidal excitation at low and high levels for better characterization of samples with non-linear properties. The range where linear behavior becomes nonlinear was of particular interest.

The study of acoustic properties of the samples especially the realistic samples gives an improved understanding of the acoustical behavior of the samples and helps to predict the actual acoustic behavior of a plate after it is installed in a system.

# 2. Samples and acoustic properties

## 2.1 Test objects

The pictures show samples of perforated plates and realistic samples used in aircraft engine liners. The realistic samples are treated with duct tape to avoid energy disappearance through the sample walls. The perforated plate are mounted in a holder at the end of impedance tube and do not need to be managed in any special way.

**Figure 1. Three perforate samples P2, P3, P4 and two realistic samples R1 and R2**

The following table covers structural properties of all five samples. The geometrical structure of realistic samples is unknown.

**Table 1. Structural parameters of test objects**

| | P2 | P3 | P4 | R1 | R2 |
|---|---|---|---|---|---|
| Thickness (mm) | 1,5 | 2 | 2 | 21 | 33 |
| Percentage open area (%) | 3,2 | 8,6 | 2,0 | 0 | 0 |
| Number of holes | 19 | 40 | 40 | 0 | 0 |
| Diameter of holes (mm) | 2 | 2 | 1 | 0 | 0 |

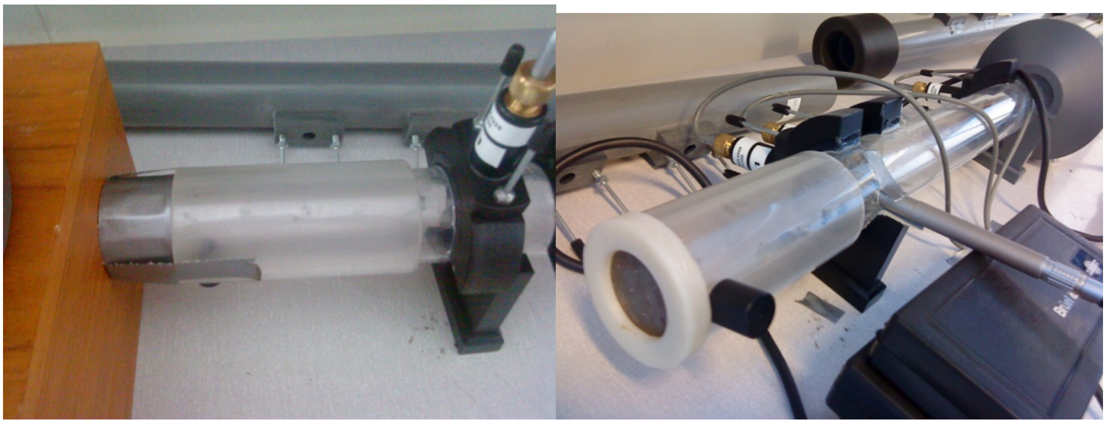

**Figure 2. Mounting of realistic sample R2 outside the impedance tube and mounting of perforate sample in a holder.**

## 2.2 Acoustic properties

Measured quantities for both methods are processed and analyzed to present results in form of following acoustic properties:

The sound pressure is decomposed into its incident and reflected waves and gives us **reflection coefficient R**, defined in terms of the component pressure wave amplitude as

$$R = {p^-}\big/{p^+} \qquad \textbf{(2.1)}$$

Since the wave amplitudes are complex, reflection coefficient is also normally a complex quantity. The results of this thesis will present reflection coefficient as its absolute value and the phase.

**Acoustic impedance, Z**:

The acoustic impedance is a complex quantity which is very useful to describe the behavior of perforated plates and other samples in our case. It is a frequency dependent parameter and is basically a relation between sound pressure and particle velocity at a surface area through which a sound wave of specific frequency propagates.

In general, there is a phase relation between the pressure and the particle velocity so complex acoustic impedance is consisting of two parts:

*Resistance* which is the real part of acoustic impedance Z and represents energy losses an acoustic wave takes due to various mechanisms involving the structure of propagation way of the wave and structure of surface area it meets.

*Reactance* which is the imaginary part of acoustic impedance Z and represents energy type changing mechanisms involving compression of the air which leads to potential energy building taken from kinetic energy of the air and energy release.

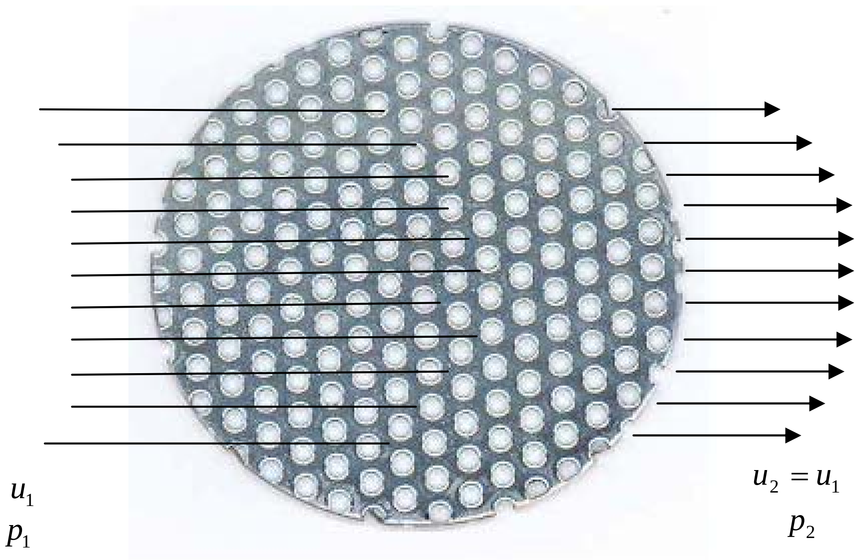


$$Z = {p}/{u} = \frac{p_1 - p_2}{u_1} \qquad \textbf{(2.2)}$$

**Figure 3. Acoustic impedance of perforates**

# 2.3 Nonlinearity

Previously described properties are frequency dependent parameters but should be constant for different sound levels. But this is not true for higher excitation levels when acoustic properties change with changing sound level and show non-linear behavior.

For the case of perforated samples these non-linear effects are mostly caused by flow separation in the pulsating flow through the holes and due to turbulence with vortex shedding occurring at the edge of the holes, which is changing with varying particle velocity inside the holes, so the result will depend on the time variation of the flow through the holes [Ref-2 BODEN (2005)] The conclusion is that nonlinear effects are depending on number of holes or so called porosity, which can be calculated as percentage open area, and diameter of holes as well as their depth which is the same as thickness of the sample.

The remaining realistic samples used in aircraft engine have complex unknown for us structure and it is difficult to predict the result of acoustic properties behavior for them. It will be shown that the results depend on thickness of the sample but it is unknown whether the structure for R2 sample, which is thicker, consists of additional material layers compared with thinner R1 sample.

## 2.4 Impedance tube

In this work the result of using ordinary impedance tube measurements for studying non-linear effects is investigated. And as for every impedance tube measurement the following assumptions must be made:

- Plane waves, measurements at rather low-frequency region where only one acoustic mode can propagate. The ideal case is taken where only perfectly plane wave fronts perpendicular to the duct axis build the mode.
- No propagation losses as wave attenuation, the duct is straight and hard-walled
- Microphones and PU-probe are point-liked objects, so that special averaging over the sensing area does not lead to any errors in measured properties.
- No flow for our case and constant acoustic particle velocity over the duct cross-section.

In practice, all this will not be true even for no flow case because of various mechanisms caused by such things as interaction between the sound and flow fields, heat conduction and viscosity.

# 3. Two-microphone method

This method is an old, well-known and reliable tool. Using the two-microphone method, acoustic properties in ducts, as, for example, reflection coefficient and acoustic impedance, can be calculated from a transfer function measurement between two microphones. The finite difference approximation of the pressure gradient will determine the particle velocity. The following calculations will present acoustic impedance as ratio between sound pressure and particle velocity.

The **Figure 4** shows three microphones which are making two microphone pairs and are used to make two different two-microphone measurements simultaneously.

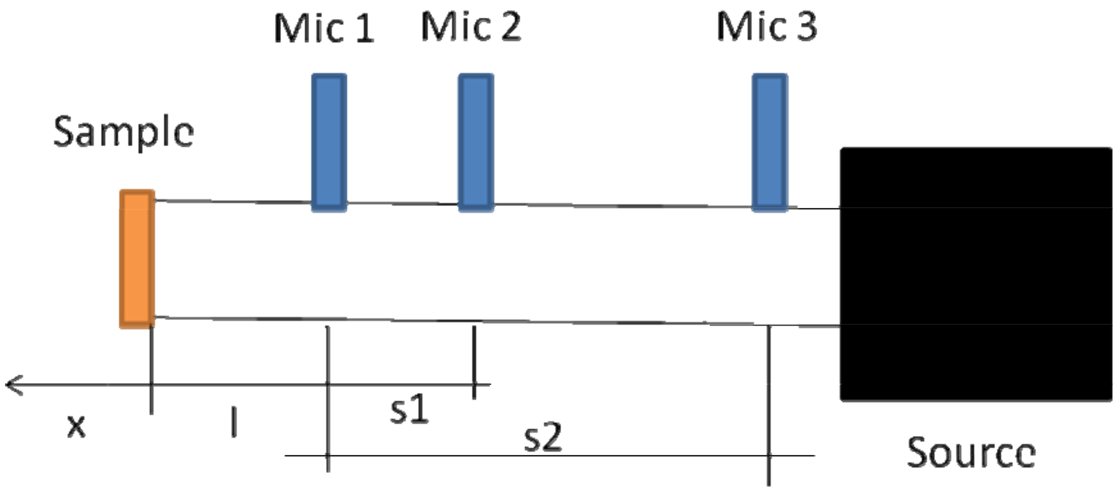


**Figure 4. Sketch of two-microphone method using impedance tube**

All microphones are assumed to be identical point-like objects which are flush mounted and have infinite input impedance with finely circular pressure sensing area. No real microphones are like this ideal case and will of course disturb the measured sound filed. But calibrations and compensations will be done to make them as ideal as possible. It is shown in [Ref-9 ÅBOM and BODEN (1988)] that the errors will be limited if we use this method in specific frequency range and with specific microphone separations.

$$0.1\pi(1-M^2) \leq ks \leq 0.8\pi(1-M^2) \qquad \textbf{(3.1)}$$

In the plane wave region of a duct, the sound field can be completely analyzed by decomposing into a left- and a right-running wave [Ref-4 BODEN H., CARLSSON U., GLAV R. WALLIN H.P. AND ÅBOM M. (2001)]

$$p(x,t) = p_+(t - x/c) + p_-(t + x/c) \tag{3.2}$$

The signals from microphones 1 and 3 (or 1 and 2 for another microphone separation and frequency range) are measured and transfer function between them is calculated by Siglab software

$$\begin{aligned} p_1 &= \hat{P}(f)(e^{jkl} + R_0(f)\cdot e^{-jkl}) \\ p_3 &= \hat{P}(f)(e^{jk(l+s)} + R_0(f)\cdot e^{-jk(l+s)}) \\ H_{13} &= \frac{p_3}{p_1} \end{aligned} \tag{3.3}$$

resulting in calculated acoustic properties [Ref-1 BODEN H. (2008)]

$$R_0(f) = e^{j2kl}\frac{e^{jks} - H_{13}}{H_{13} - e^{-jks}} \qquad Z_0(f) = \frac{1 + R_0(f)}{1 - R_0(f)} = \frac{p_0}{\rho_0 c \cdot u_0} \tag{3.4}$$

If we look at the ideal case with no flow and no losses etc., the pressure signals in a microphone pair will be the same every time $ks = n\pi$ , and n is an integer. The used spacing between microphones must be within a half wavelength of the highest frequency of interest, otherwise the method will produce poor results for the frequencies when multiples of half an acoustic wavelength is close to distance between the microphones.

Two pairs of microphones, Mic1-Mic2, Mic1-Mic3, with two separations are used in order cover our frequency range of interest 100-2000Hz and separations fulfill the equation

$$0.1\pi \le ks \le 0.8\pi \tag{3.5}$$

The equation does not include the Mach number because of no mean flow in our case.

Measurement error sensitivity grows with frequency, so we should use the method in previously mentioned frequency range to guarantee acceptable measurement accuracy with error magnification less than factor 10 [Ref-8 BODEN and ÅBOM (1986)].

# Microphone calibration

The presence of only plane waves in a duct theoretically results in that the sound pressure amplitude will be constant over the duct cross-section and the sound pressure measured by all microphones would give the same pressure amplitude with zero amplitude shift and phase shift. However there will in practice be a deviation from this ideal case because of different losses by measuring chain, amplifiers, cables and other, which introduce amplitude and phase shifts. Relative calibration of the microphones is therefore needed.

For ordinary sound pressure measurements, only amplitude calibration is enough which was done on microphone 1 with a known reference source, an acoustic calibrator. The received calibration factor was later added in calculations when the data was analyzed. For two-microphone method also a phase calibration is needed.

The calibration tube seen in **Figure 5** makes a relative calibration between the microphone channels. The speaker placed in the wooden box at the bottom of calibration tube sends plane waves with frequencies of interest, calibrations are made for each frequency. Three microphones are connected to the top of the tube and the fluctuating pressures measured at each position are corrected. The phase and amplitude relations between the three microphones are determined.

The calibration was made a number of times during the measurement period giving the same results.

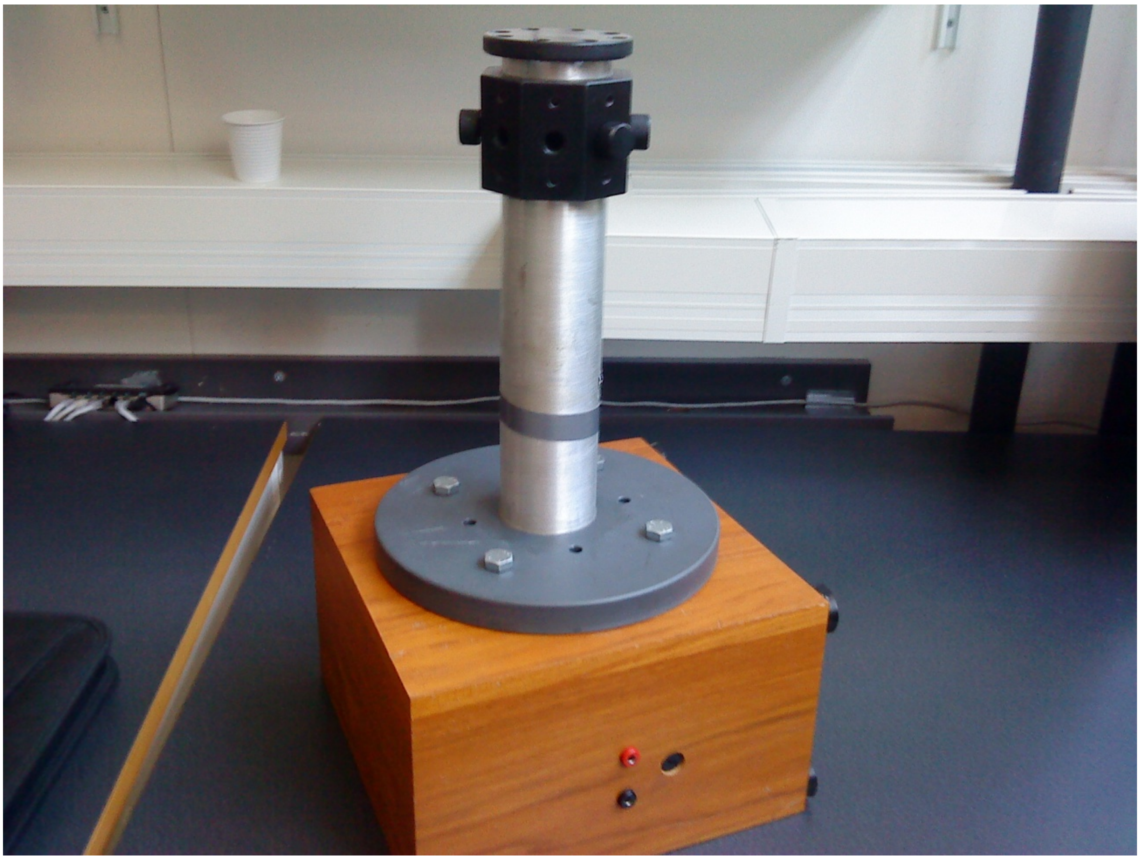

**Figure 5. Photo of calibration tube**

# 4. P-U method

For a few decades the so called “p-p method” based on two closely spaced pressure microphones has dominated sound intensity measurements. But some years ago a sound intensity measurement system was introduced by Microflown. It is a probe which combines two fundamentally different transducers: a pressure transducer and a particle velocity transducer.

The result is two signals, one for sound pressure and one for particle velocity. The frequency response function between them will be acoustic impedance, Z. Therefore the method is very useful for direct impedance measurements.

It is studied in [Ref-7 JACOBSEN F. AND DE BREE H.-E. (2005)] that strongly reactive sound fields increase the influence of p-u phase mismatch. In order to avoid such near-filed effects the probe is not placed at the sample but 15 cm away at the same position as Mic.1 used in two-microphone method for future comparison.

Two measured signals, one for sound pressure and one for particle velocity, are calculated by Siglab software to acoustic impedance at probe position as transfer function between signals

$$Z_s(f) = H_{12} \tag{4.1}$$

The measured acoustic impedance at this spot is used to calculate the reflection coefficient which can be easily moved to sample position where it is calculated back to impedance.

$$R_0(f) = e^{j2ks}\frac{H_{12}-1}{H_{12}+1} \qquad Z_0(f) = \frac{1+R_0(f)}{1-R_0(f)} \tag{4.2}$$

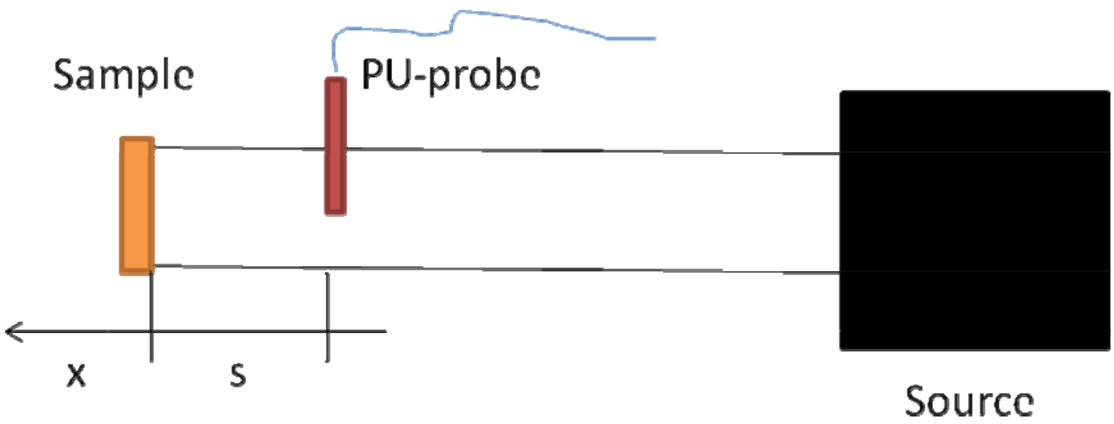


**Figure 6. Sketch of PU-method used in an impedance tube**

# Microflown sound intensity probe

The probe consists of a Microflown acoustical particle velocity sensor and miniature sound pressure transducer placed in a single spot with a cap with protective metal mesh which should always be kept on the probe.

The probe can be used for sound pressure measurements, particle velocity measurements, sound intensity measurements and impedance measurements.

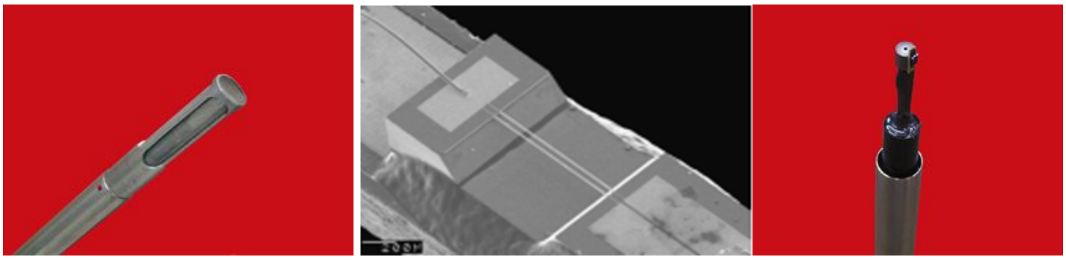

**Figure 7. Photos of Microflown sound intensity probe.**

# Working principle of Microflown sensor

The sensor measures velocity of air across two tiny, heated resistive strips of platinum.  When air flows the first wire cools down, the air gets hotter (picks up the heat) so the second wire cools down less. Temperature differences due to electrical resistances of the wires generates a voltage difference that is proportional to the particle velocity.

The probe is directivity dependent and has a red dot as a directivity mark which marks the positive side of the sensor. This side needs to be directed towards the sound source.

# Sound intensity probe calibration

Because of the probes presences in the duct some disturbances in the original sound field will occur. The probe should be calibrated in an anechoic room or in a standing wave tube with rigid termination [Ref-6 JACOBSEN F. AND DE BREE H.-E.  (2005)], but in this work the choice was to find a calibration factor by comparing with the two-microphone measurement method.

The same sample under the same conditions was measured with both methods. The results were compared and a calibration factor was calculated for future use when analyzing data received with the P-U method. The calibration factor was later applied on measurements with other samples and should be the same for different sound levels and samples.

In order to give the same conditions holes not used were blocked by microphones used in the two-microphone method.

# 5. Test Setups

## Two-microphone method setup

All experiments were made at room temperature. The setup consists of well-known impedance tube with a loudspeaker as the source of excitation of sound wave at one end and sample at second end, two signal amplifiers and a Siglab signal analyzing system connected to a PC with Siglab software as can be seen in **Figure 8**.

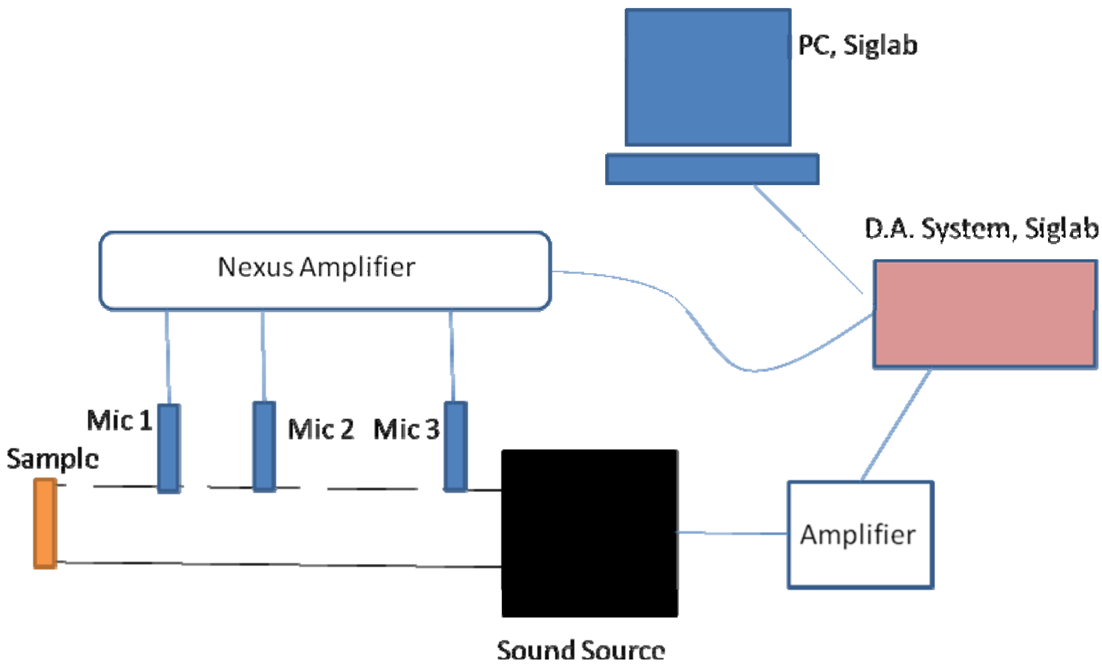


**Figure 8. Layout of two-microphone method measurements**

The pressures in the tube were measured using three quarter inch B&K condenser microphones. The distance between the microphones 1 and 3 was 30 cm, distance between microphones 1 and 2 was 5 cm and the distance from microphone 1 to the sample was 15 cm. The samples were mounted in a holder at the end of the measurement pipe as shown in **Figure 9**. The measurement pipe has an inner diameter of about 40 mm and the opening in the holder has a diameter of 38.5 mm. The realistic samples are wider than the pipe diameter therefore they were mounted outside the pipe and pressed against the impedance tube termination.

**Figure 9. Photo of layout of two-microphone method measurements**

The measurements were carried out using sine signal excitation at frequencies of interest with record length, frequency resolution, bandwidth, number of averages and other options according to **Figure 10.**

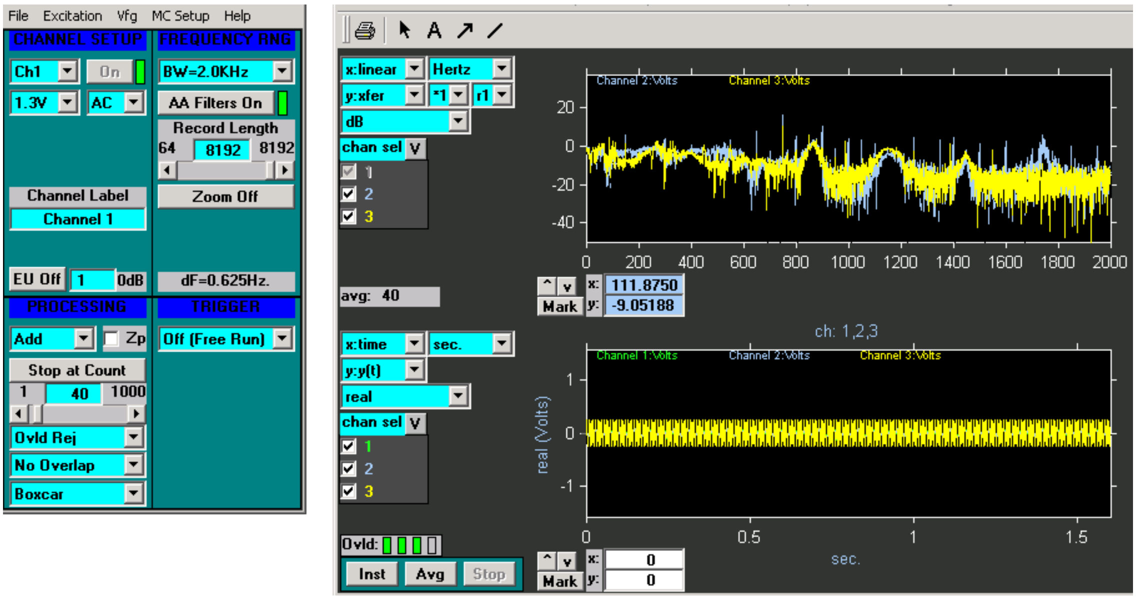


**Figure 10. Siglab software options used for two-microphone method**

# P-U probe method setup

All experiments were made at room temperature. The setup consists of well-known impedance tube with a loudspeaker as the source of excitation of sound wave at one end and sample at second end, and excitation signal amplifier, Microflown signal conditioner and a Siglab system connected to a PC with Siglab software as can be seen in **Figure 11**.

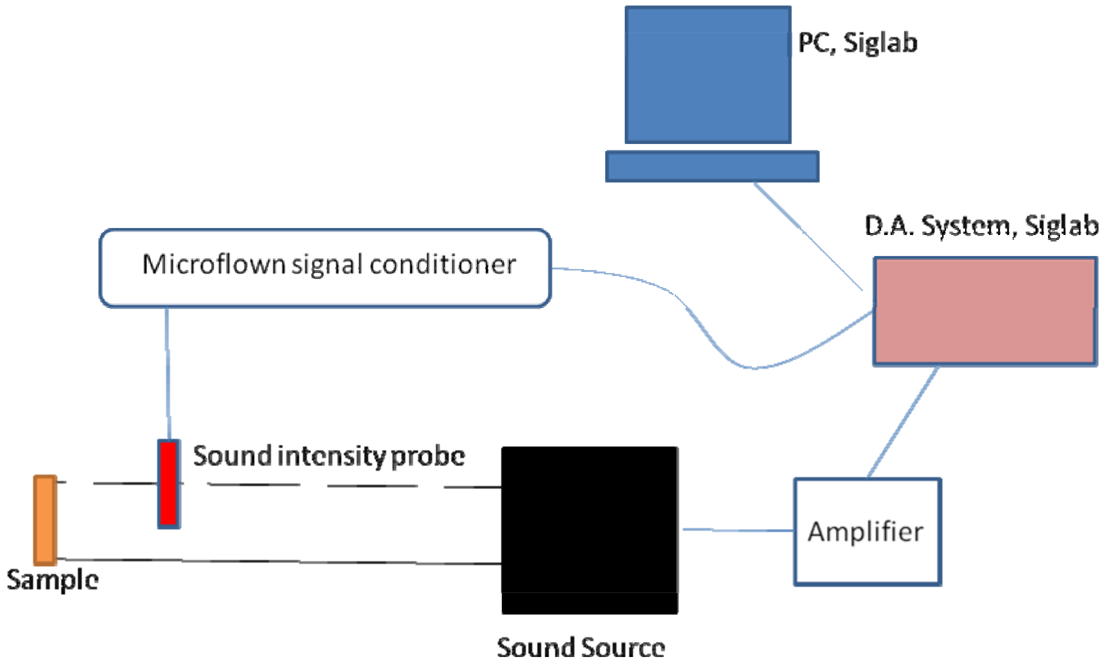


**Figure 11. Layout of PU-method measurements**

The distance between the probe and the sample was 15 cm. The samples were mounted in a holder at the end of the measurement pipe as shown in Figure 12. The measurement pipe has an inner diameter of about 40 mm and the opening in the holder has a diameter of 38.5 mm.

The realistic samples are wider than pipe diameter therefore they were mounted outside the pipe and pressed against the impedance tube termination.

The Microflown sound intensity probe was mounted halfway inside the pipe to place the transducers in the middle of the duct even if it is assumed that the pressure and particle velocity are constant over the duct cross-section due to the plane wave assumption.

The probe has smaller diameter than the hole in the duct wall and is treated with tape to hold it fixed. The red dot on the probe marking the directivity of the probe was turned towards the sound source.

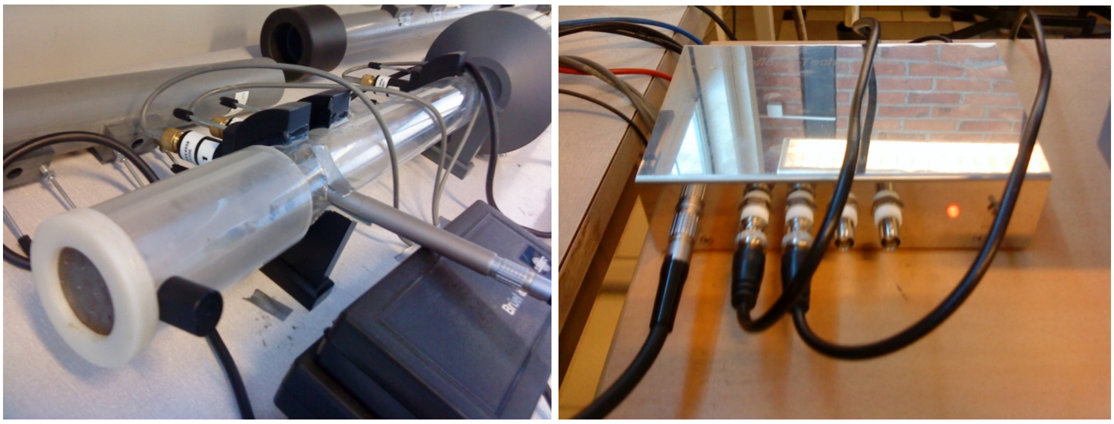

**Figure 12. Photo of layout of PU-method measurements**

The measurements were carried out using sine excitation at frequencies of interest with record length, frequency resolution, bandwidth and averages and other options according to **Figure 13**. The frequency response function between two signals was used to estimate components of acoustic impedance and reflection coefficient.

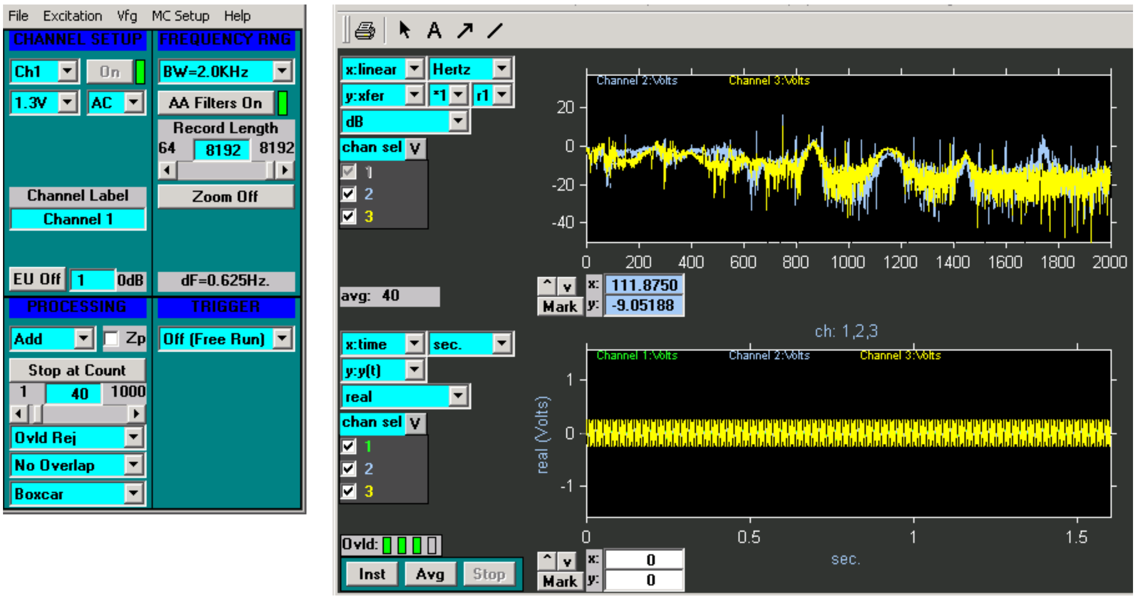


**Figure 13. Siglab software options used for PU-method**

# 6. Results and Discussion

Here the results are presented as plots of acoustic properties for the following measurements:

- Single pure tone excitation at 110Hz, 220Hz, 330Hz and 990Hz (for realistic samples)
- Two tone excitations with harmonics 110-220-330Hz and 990Hz (for realistic samples)
- Two tone excitations 330Hz and 100Hz or 110Hz or 120Hz
- Two tone excitation with shifted phase on varied signal, 110Hz and 330Hz
- PU-probe measurements (single pure tone excitation)

For single tone excitation the plots will include results for all five samples with the acoustic properties as functions of particle velocities at sample position and not inside the holes. This is because the realistic samples do not have any visible holes but we want to compare them with perforate plates. The remaining figures will separate the P2,P3 and P4 samples to present the acoustic properties plotted against peak amplitude of particle velocities inside the holes of perforates and realistic R1,R2 samples to present the acoustic properties as functions of particle velocities at the sample position.

## Single tone excitation with harmonics at 110Hz, 220 Hz and 330 Hz

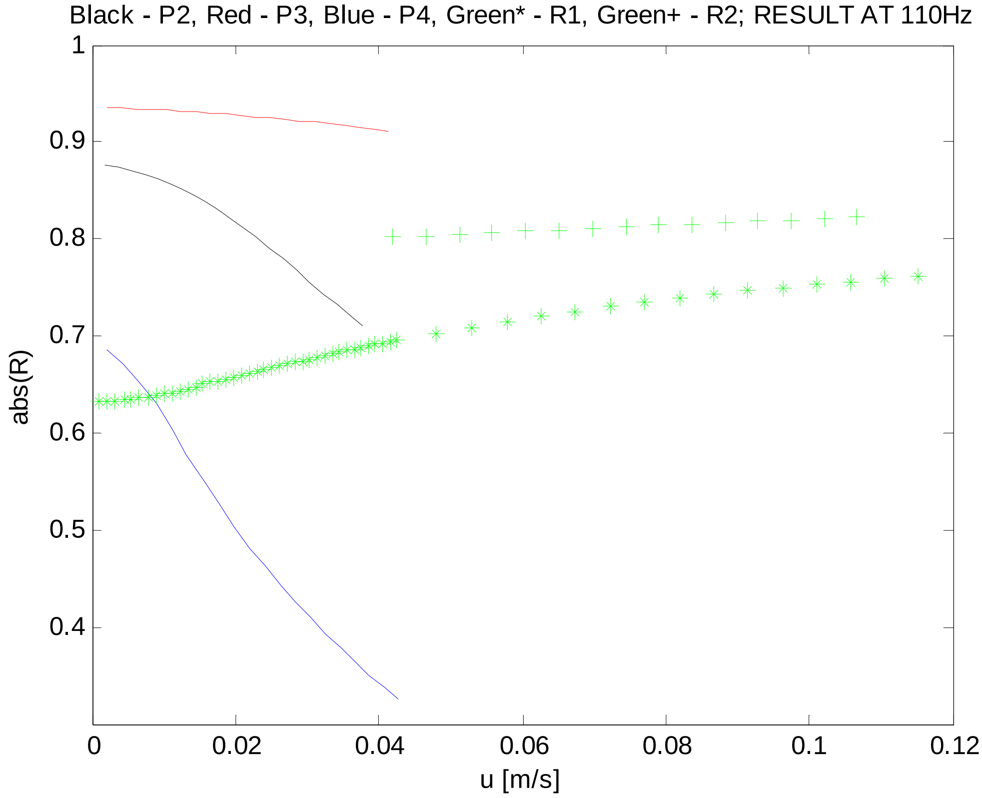


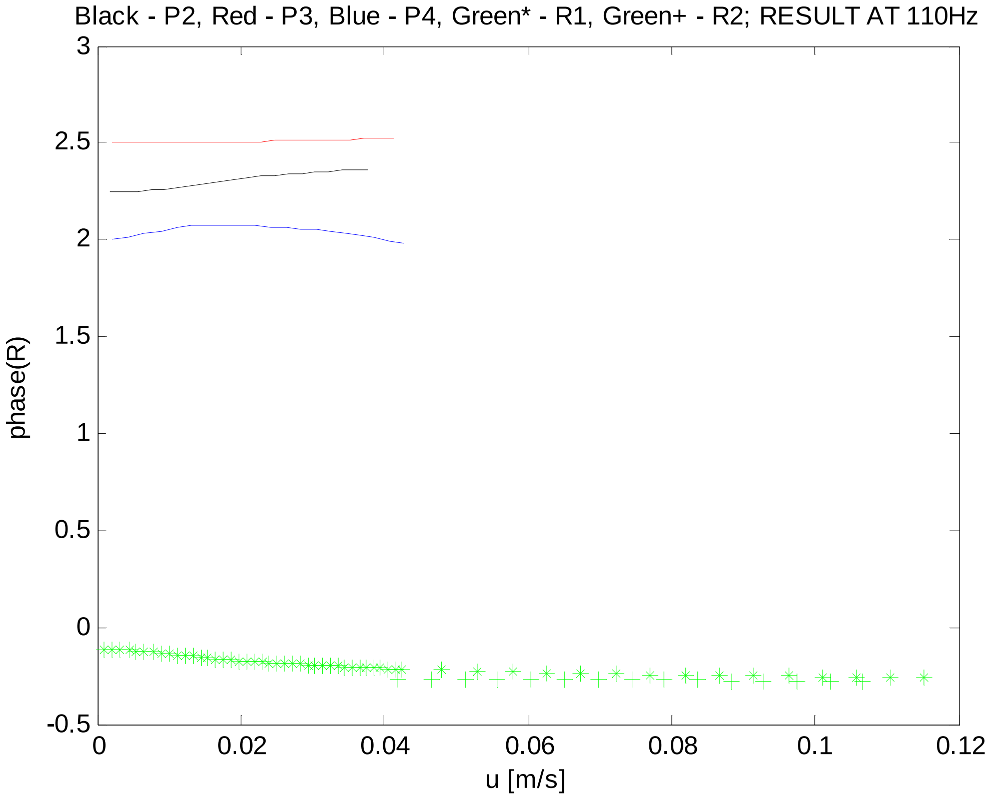

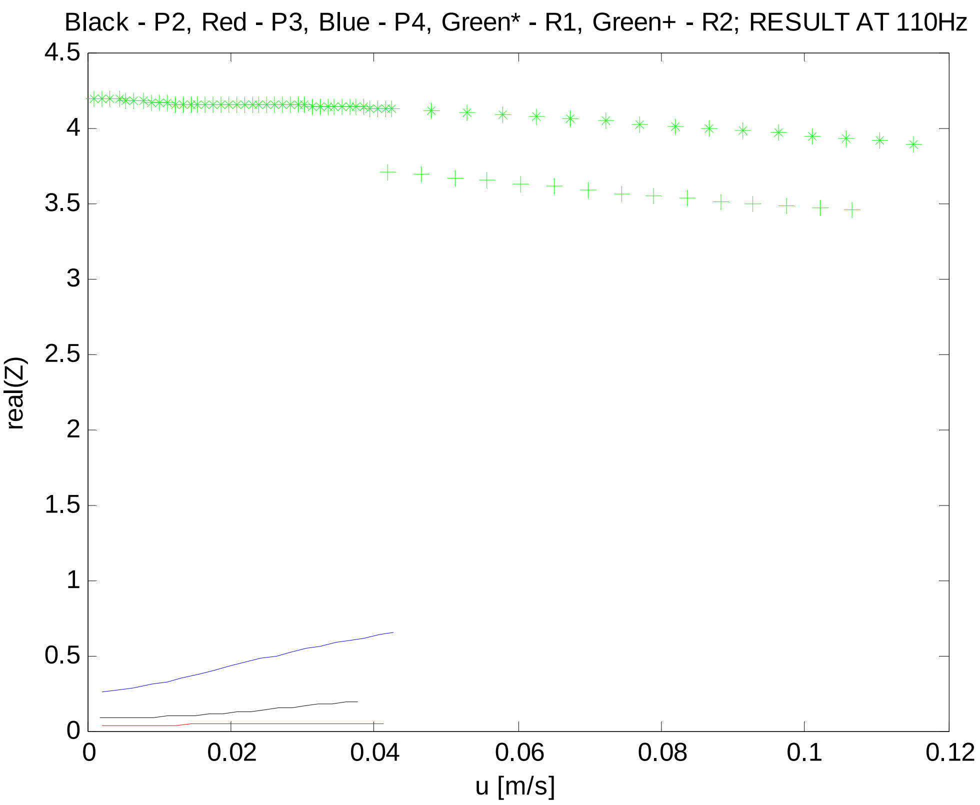
Black - P2, Red - P3, Blue - P4, Green* - R1, Green+ - R2; RESULT AT 110Hz
real(Z)
u [m/s]
4.5
4
3.5
3
2.5
2
1.5
1
0.5
0
0.02
0.04
0.06
0.08
0.1
0.12

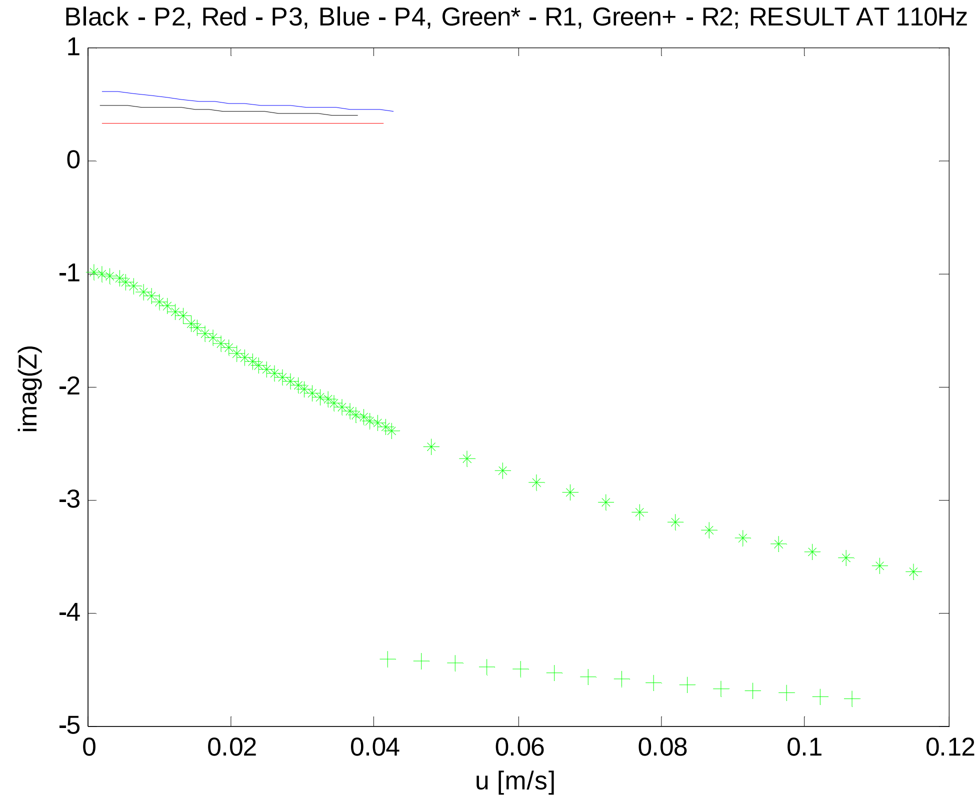
Black - P2, Red - P3, Blue - P4, Green* - R1, Green+ - R2; RESULT AT 110Hz
imag(Z)
u [m/s]
1
0
-1
-2
-3
-4
-5
0.02
0.04
0.06
0.08
0.1
0.12

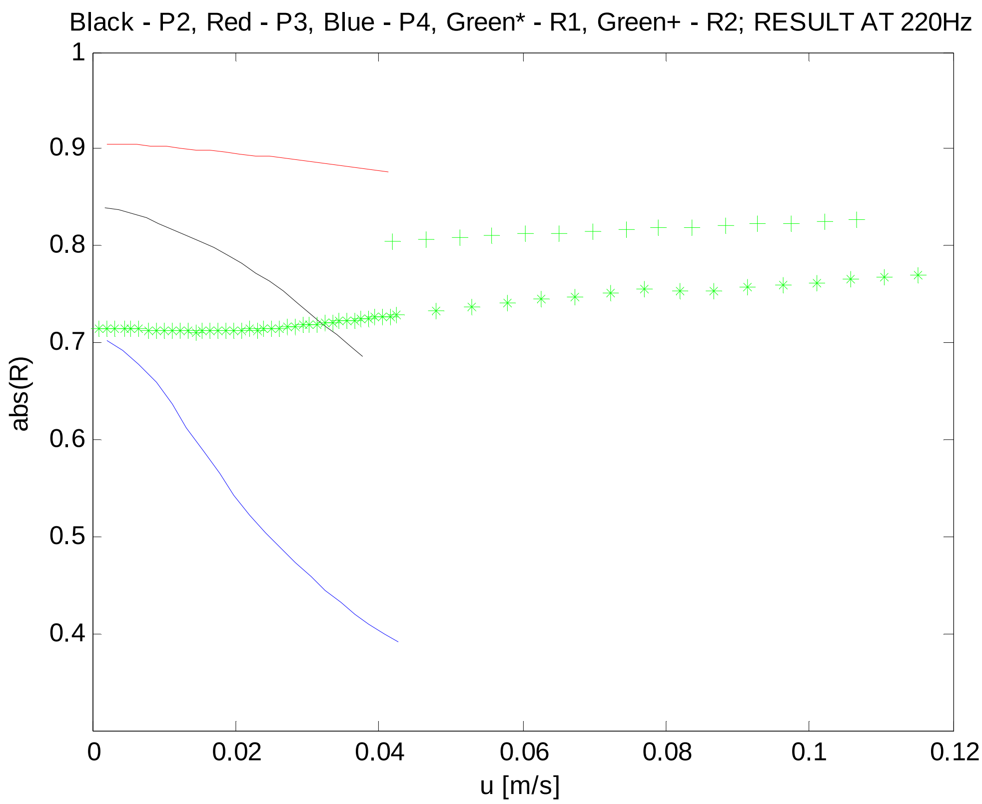

Black - P2, Red - P3, Blue - P4, Green* - R1, Green+ - R2; RESULT AT 220Hz
abs(R)
u [m/s]
1
0.9
0.8
0.7
0.6
0.5
0.4
0
0.02
0.04
0.06
0.08
0.1
0.12


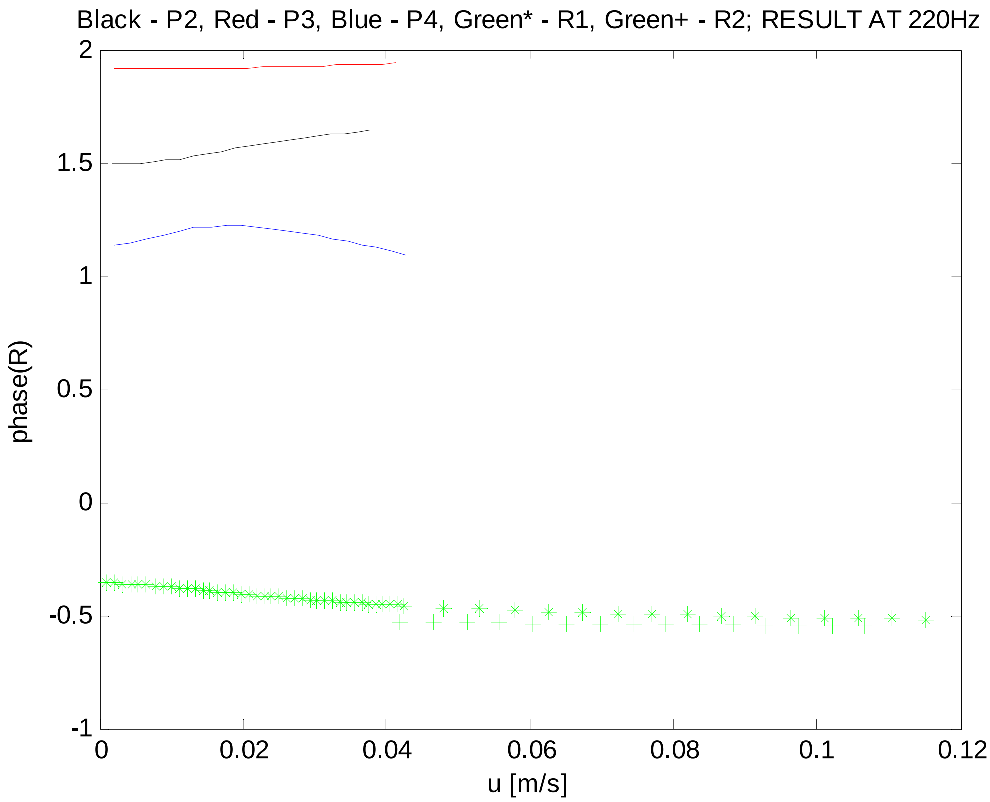

Black - P2, Red - P3, Blue - P4, Green* - R1, Green+ - R2; RESULT AT 220Hz
phase(R)
u [m/s]
2
1.5
1
0.5
0
-0.5
-1
0
0.02
0.04
0.06
0.08
0.1
0.12

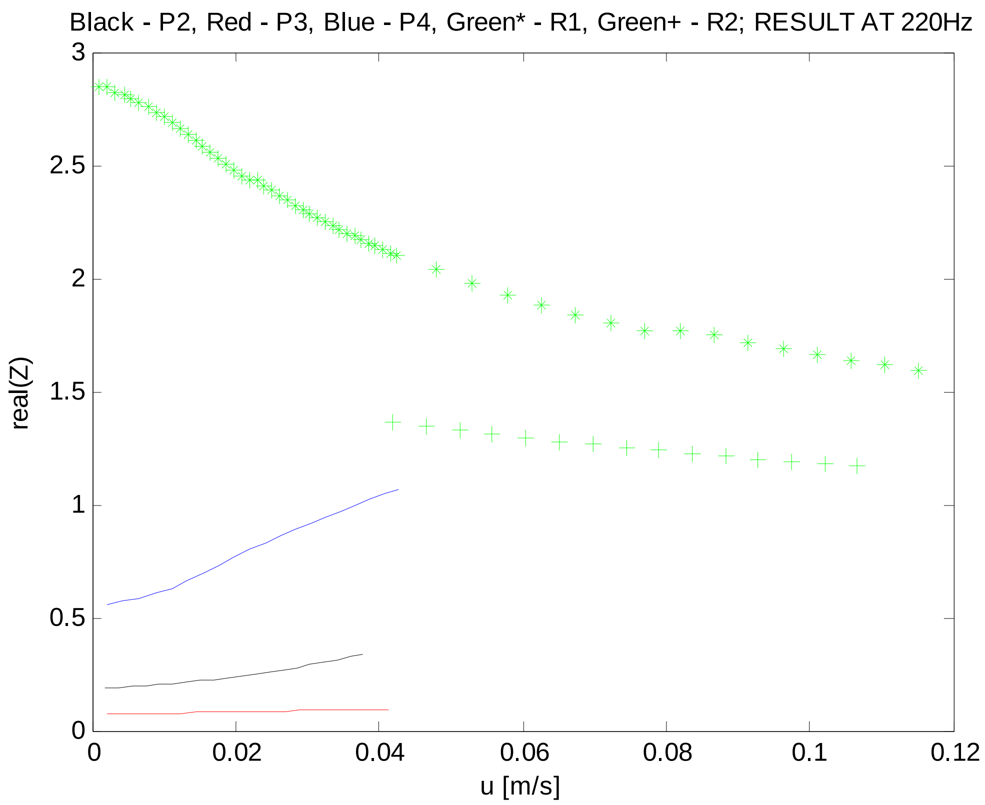
Black - P2, Red - P3, Blue - P4, Green* - R1, Green+ - R2; RESULT AT 220Hz
real(Z)
u [m/s]
3
2.5
2
1.5
1
0.5
0
0
0.02
0.04
0.06
0.08
0.1
0.12

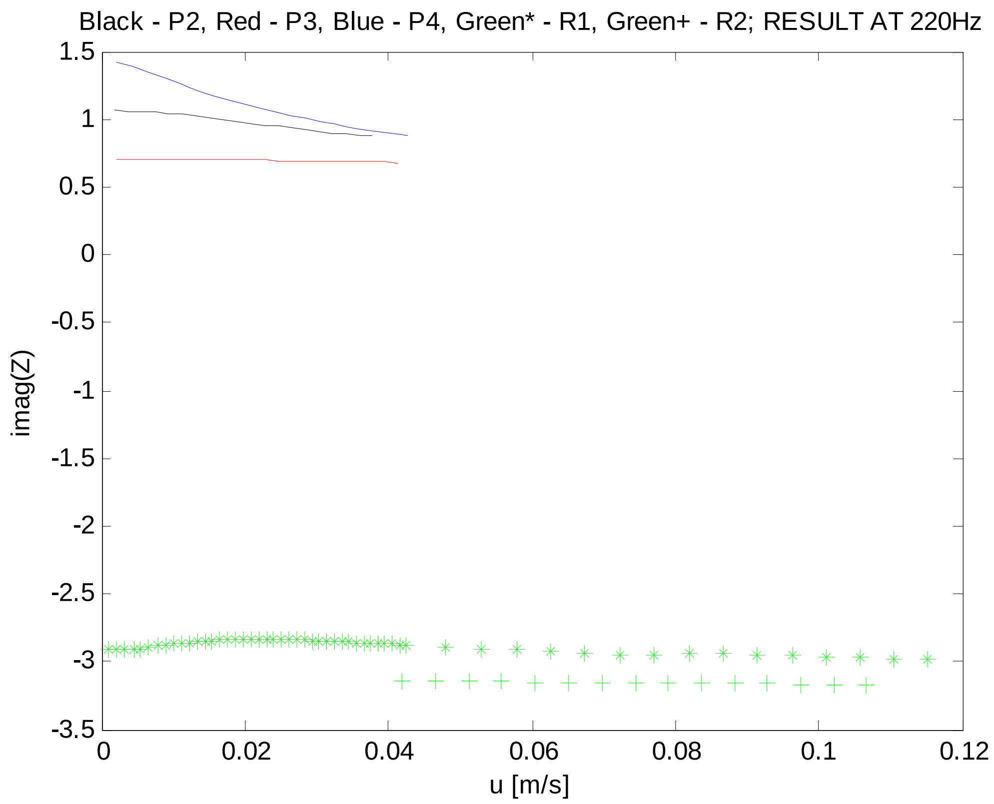
Black - P2, Red - P3, Blue - P4, Green* - R1, Green+ - R2; RESULT AT 220Hz
imag(Z)
u [m/s]
1.5
1
0.5
0
-0.5
-1
-1.5
-2
-2.5
-3
-3.5
0
0.02
0.04
0.06
0.08
0.1
0.12

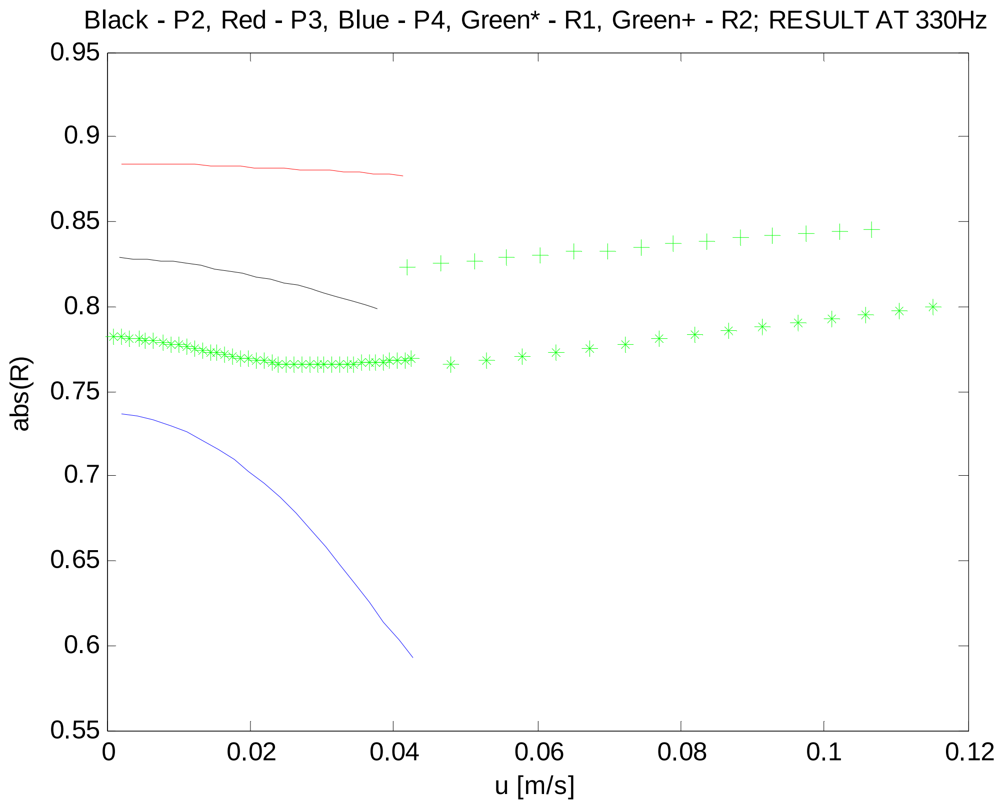
Black - P2, Red - P3, Blue - P4, Green* - R1, Green+ - R2; RESULT AT 330Hz
abs(R)
u [m/s]
0.95
0.9
0.85
0.8
0.75
0.7
0.65
0.6
0.55
0
0.02
0.04
0.06
0.08
0.1
0.12

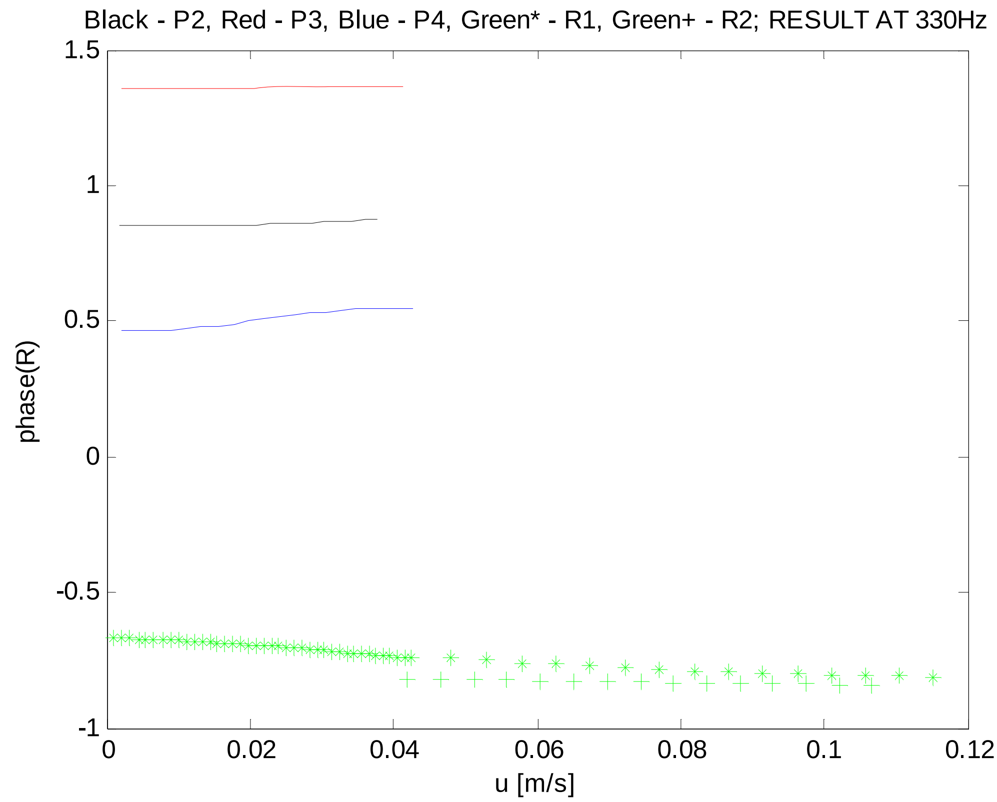
Black - P2, Red - P3, Blue - P4, Green* - R1, Green+ - R2; RESULT AT 330Hz
phase(R)
u [m/s]
1.5
1
0.5
0
-0.5
-1
0
0.02
0.04
0.06
0.08
0.1
0.12

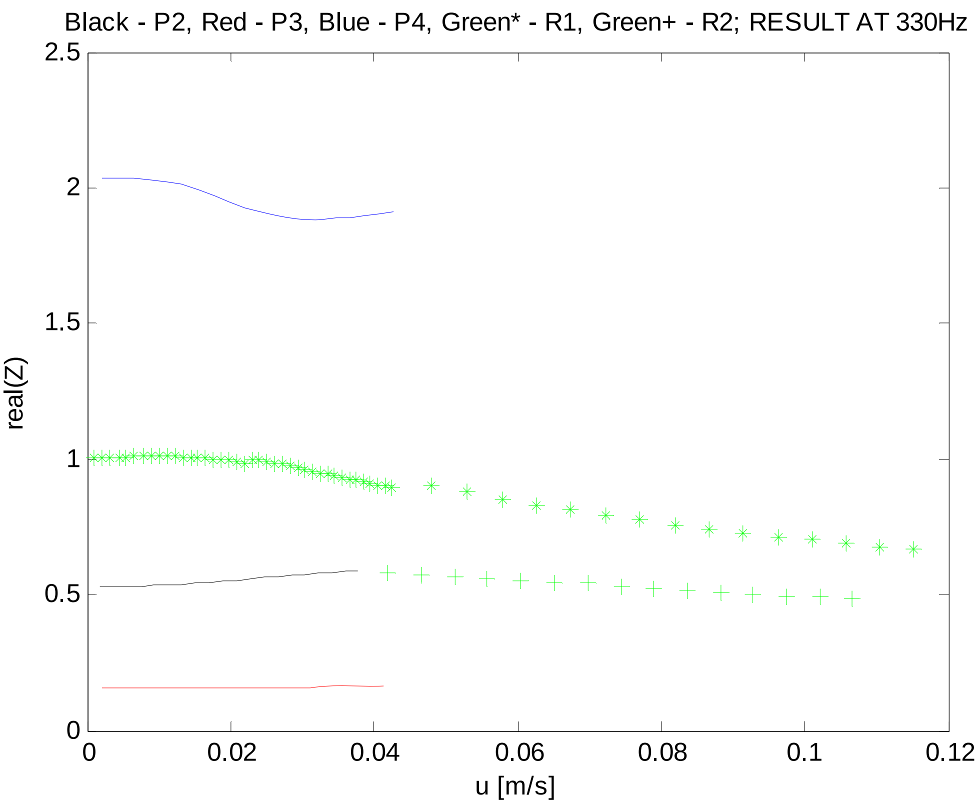
Black - P2, Red - P3, Blue - P4, Green* - R1, Green+ - R2; RESULT AT 330Hz
real(Z)
2.5
2
1.5
1
0.5
0
0
0.02
0.04
0.06
0.08
0.1
0.12
u [m/s]

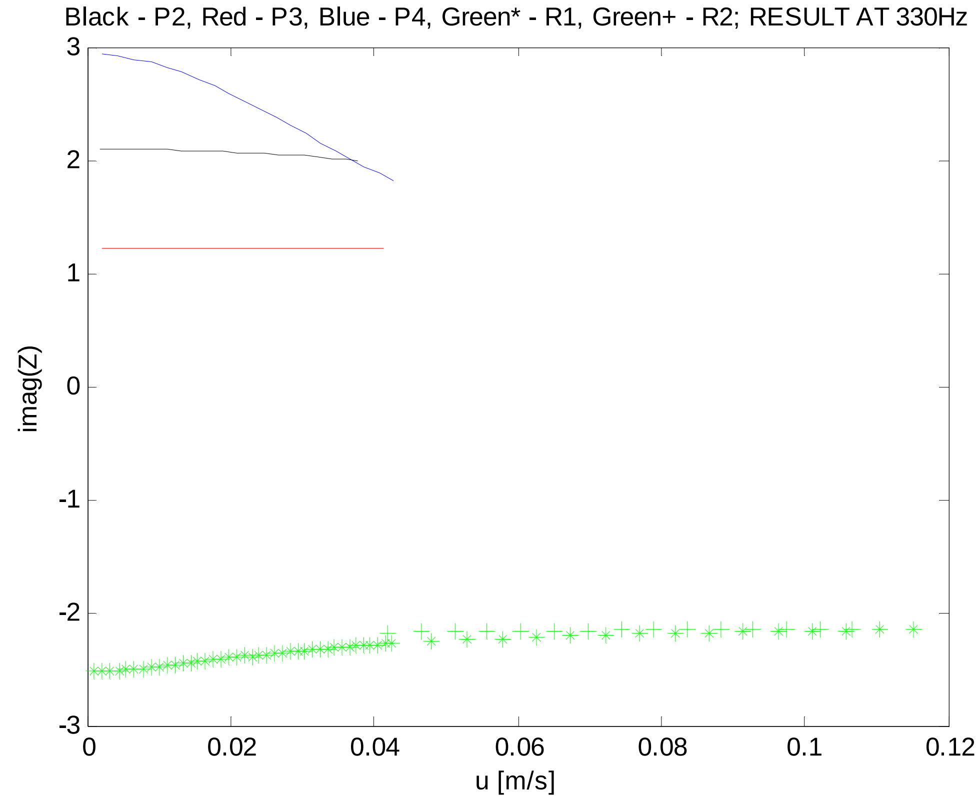
Black - P2, Red - P3, Blue - P4, Green* - R1, Green+ - R2; RESULT AT 330Hz
imag(Z)
3
2
1
0
-1
-2
-3
0
0.02
0.04
0.06
0.08
0.1
0.12
u [m/s]

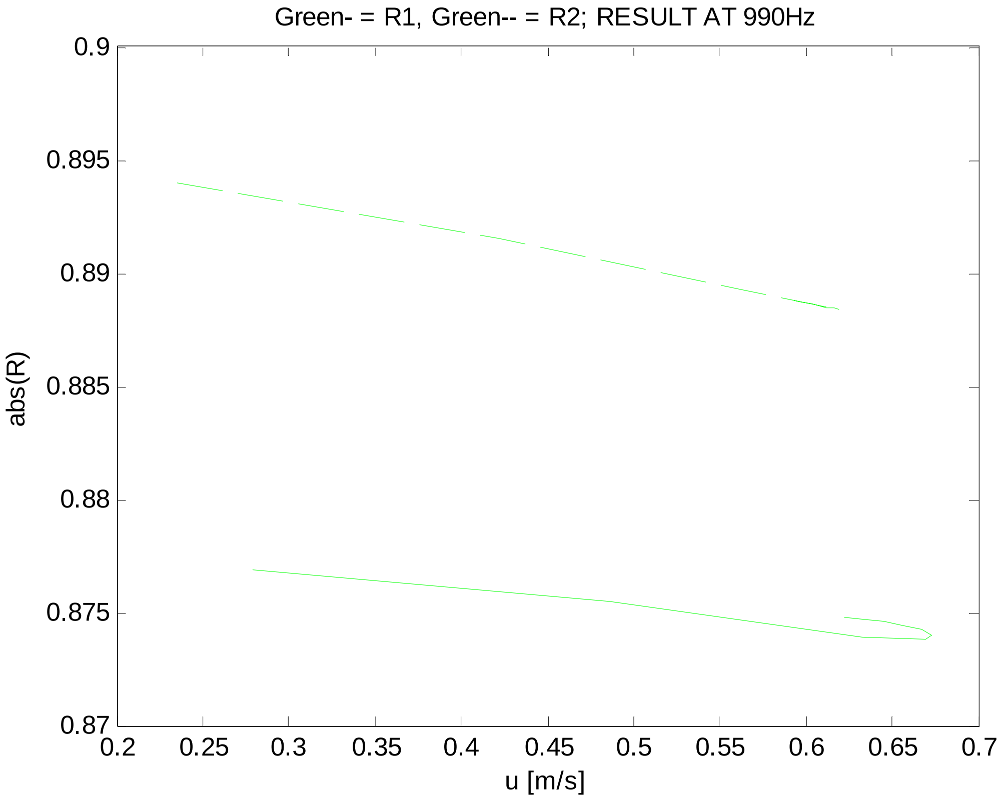
Green- = R1, Green-- = R2; RESULT AT 990Hz
abs(R)
u [m/s]
0.9
0.895
0.89
0.885
0.88
0.875
0.87
0.2
0.25
0.3
0.35
0.4
0.45
0.5
0.55
0.6
0.65
0.7

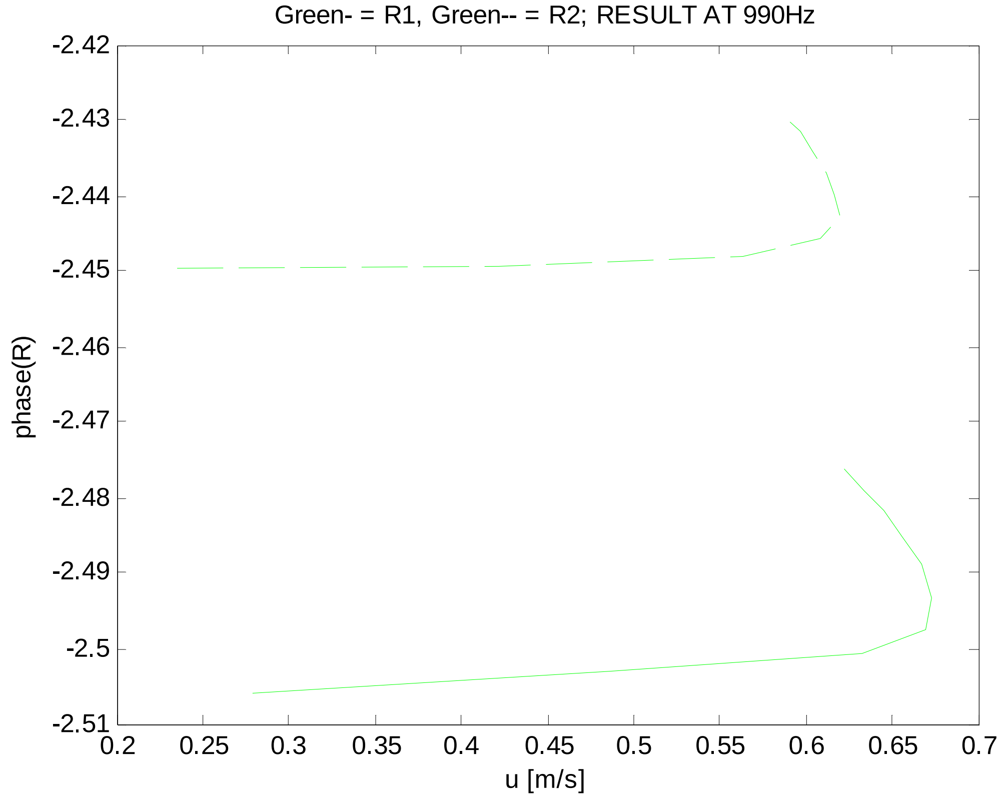
Green- = R1, Green-- = R2; RESULT AT 990Hz
phase(R)
u [m/s]
-2.42
-2.43
-2.44
-2.45
-2.46
-2.47
-2.48
-2.49
-2.5
-2.51
0.2
0.25
0.3
0.35
0.4
0.45
0.5
0.55
0.6
0.65
0.7

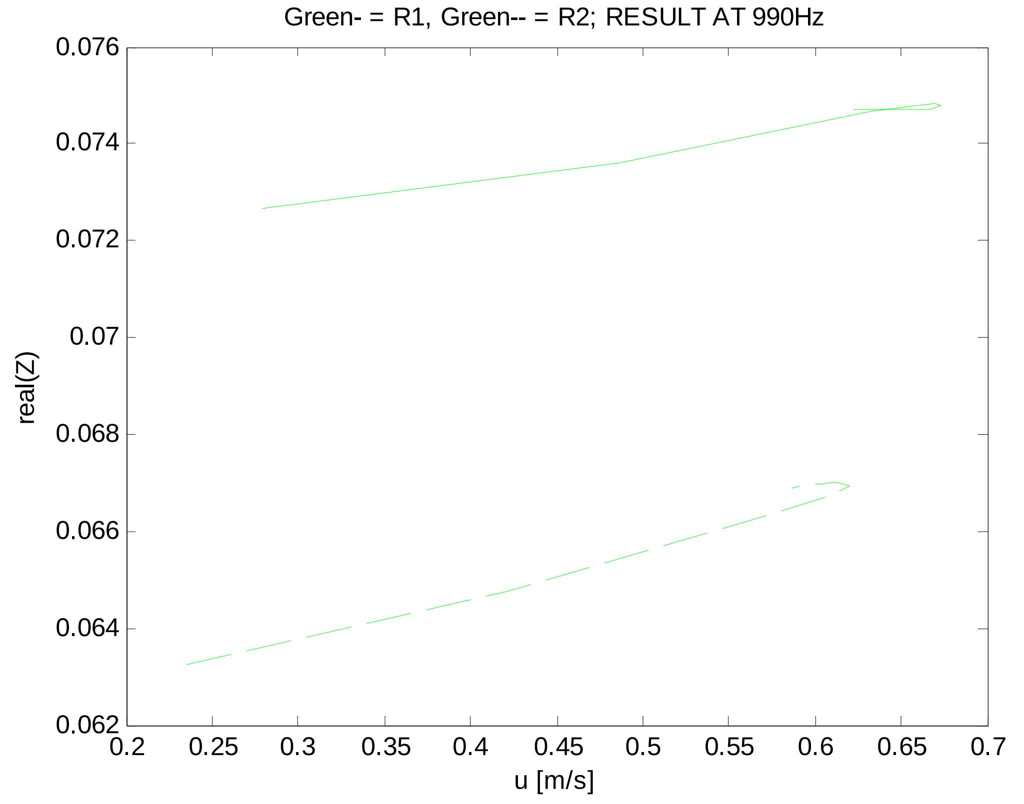
Green- = R1, Green-- = R2; RESULT AT 990Hz
0.076
0.074
0.072
0.07
0.068
0.066
0.064
0.062
real(Z)
0.2
0.25
0.3
0.35
0.4
0.45
0.5
0.55
0.6
0.65
0.7
u [m/s]

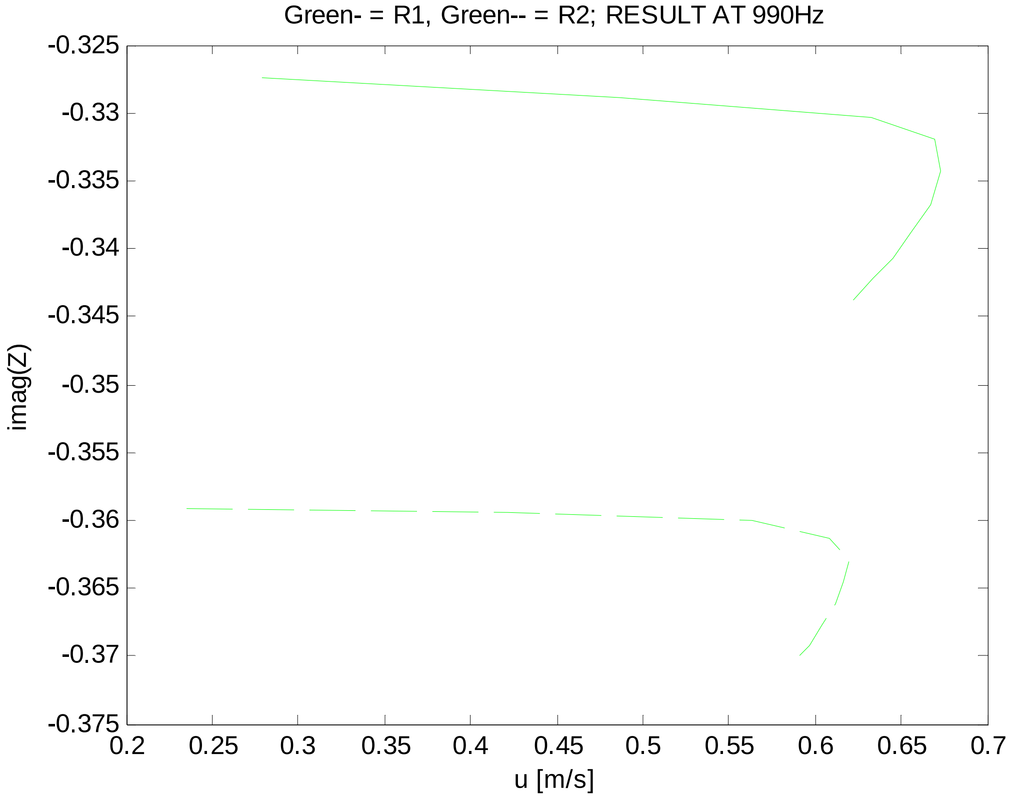
Green- = R1, Green-- = R2; RESULT AT 990Hz
-0.325
-0.33
-0.335
-0.34
-0.345
-0.35
-0.355
-0.36
-0.365
-0.37
-0.375
imag(Z)
0.2
0.25
0.3
0.35
0.4
0.45
0.5
0.55
0.6
0.65
0.7
u [m/s]

## Two-tone excitation with harmonics;P2,P3 and P4

The green lines represent the case with single tone excitation at same frequency as the constant signal. It can be seen that even a low signal at varied frequency contributes to a shift in result compared with single pure tone excitation at studied frequency.

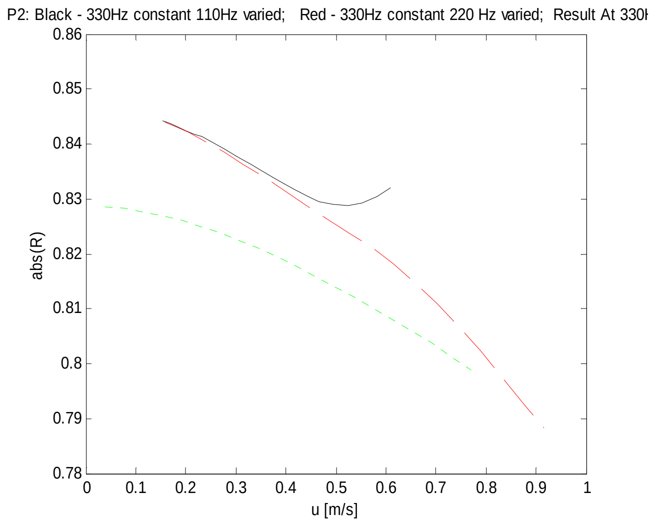


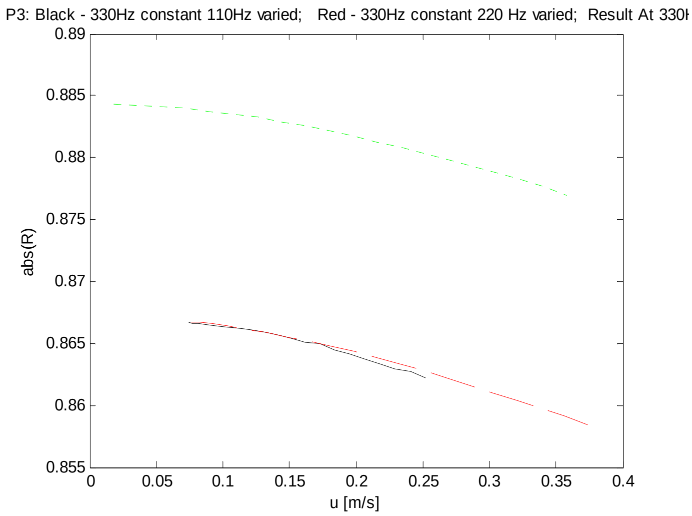


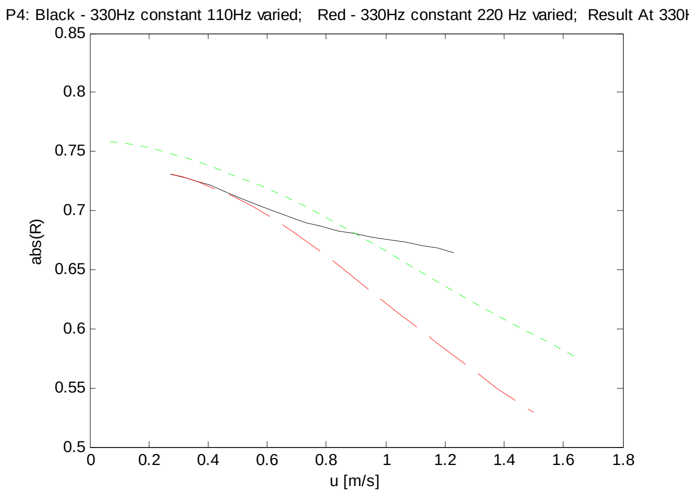

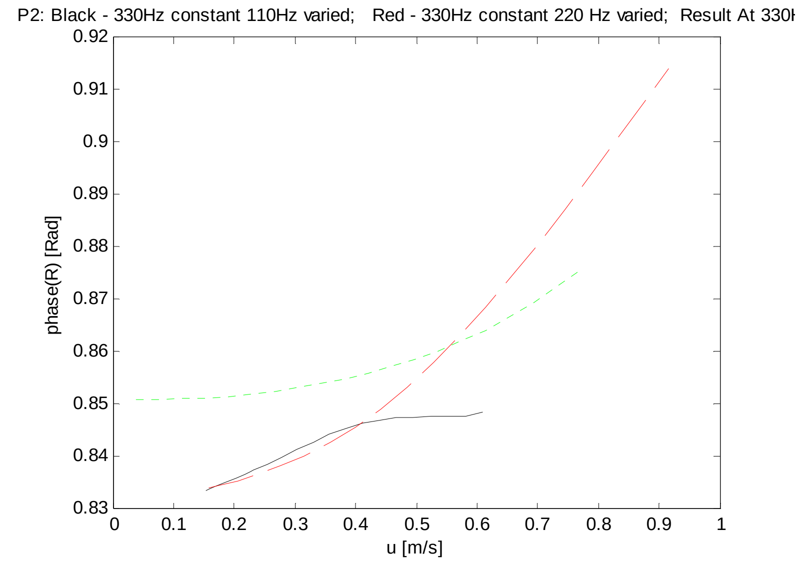

P2: Black - 330Hz constant 110Hz varied; Red - 330Hz constant 220 Hz varied; Result At 330H
phase(R) [Rad]
u [m/s]


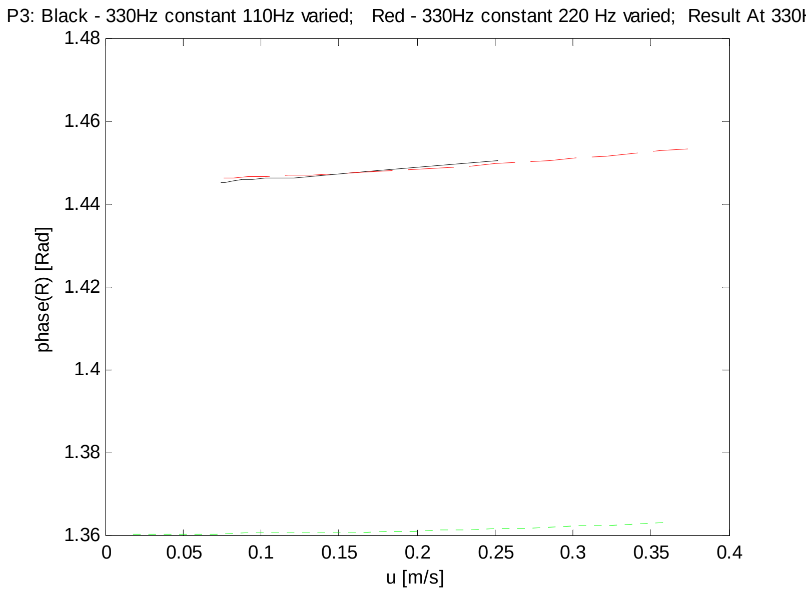

P3: Black - 330Hz constant 110Hz varied; Red - 330Hz constant 220 Hz varied; Result At 330H
phase(R) [Rad]
u [m/s]


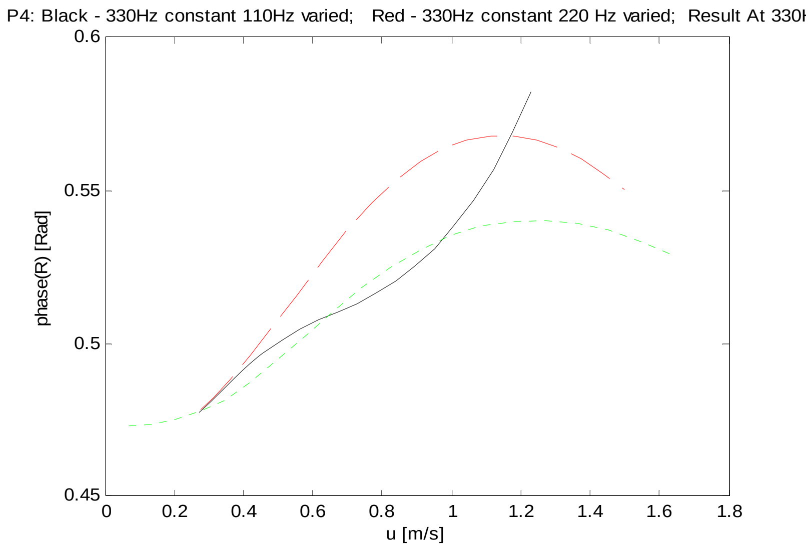

P4: Black - 330Hz constant 110Hz varied; Red - 330Hz constant 220 Hz varied; Result At 330H
phase(R) [Rad]
u [m/s]

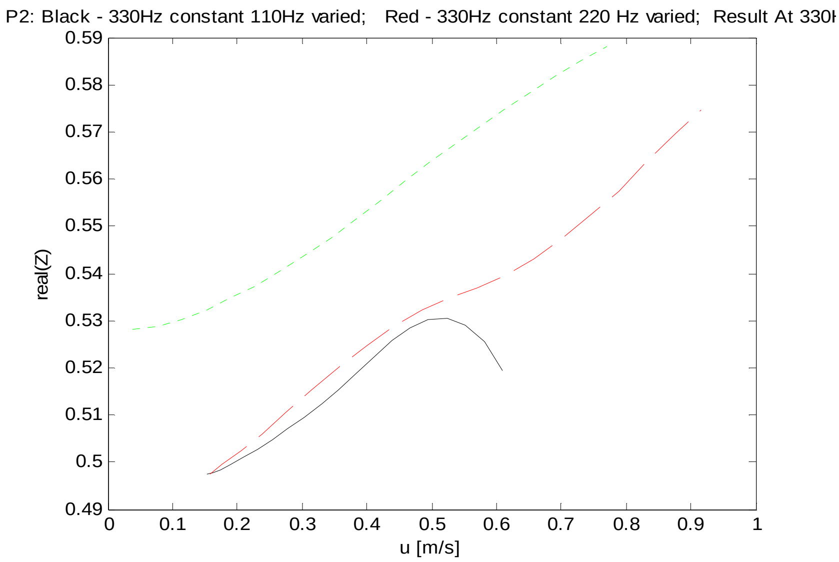
P2: Black - 330Hz constant 110Hz varied; Red - 330Hz constant 220 Hz varied; Result At 330H
real(Z)
u [m/s]
0.59
0.58
0.57
0.56
0.55
0.54
0.53
0.52
0.51
0.5
0.49
0
0.1
0.2
0.3
0.4
0.5
0.6
0.7
0.8
0.9
1

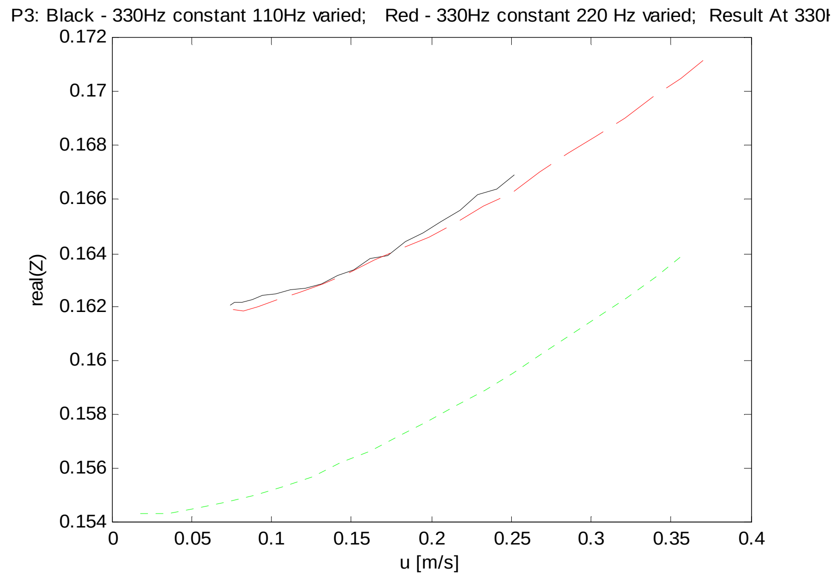
P3: Black - 330Hz constant 110Hz varied; Red - 330Hz constant 220 Hz varied; Result At 330H
real(Z)
u [m/s]
0.172
0.17
0.168
0.166
0.164
0.162
0.16
0.158
0.156
0.154
0
0.05
0.1
0.15
0.2
0.25
0.3
0.35
0.4

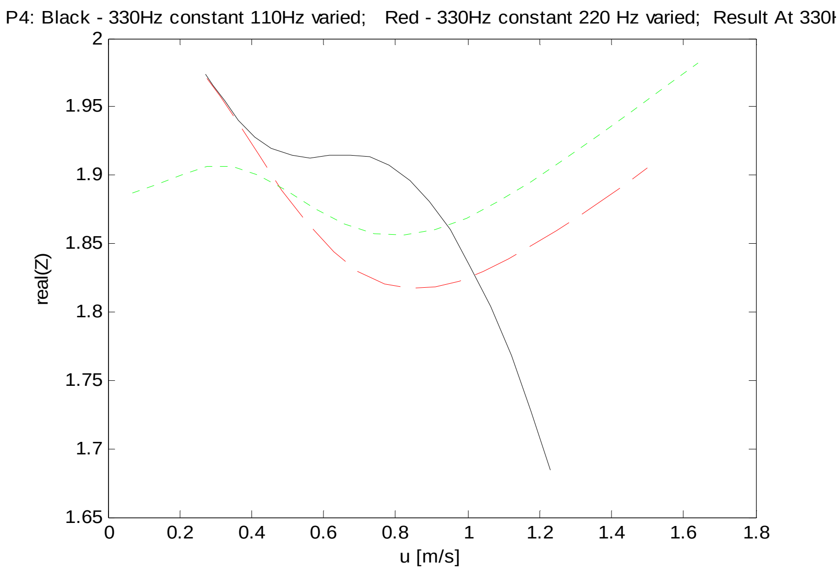
P4: Black - 330Hz constant 110Hz varied; Red - 330Hz constant 220 Hz varied; Result At 330H
real(Z)
u [m/s]
2
1.95
1.9
1.85
1.8
1.75
1.7
1.65
0
0.2
0.4
0.6
0.8
1
1.2
1.4
1.6
1.8

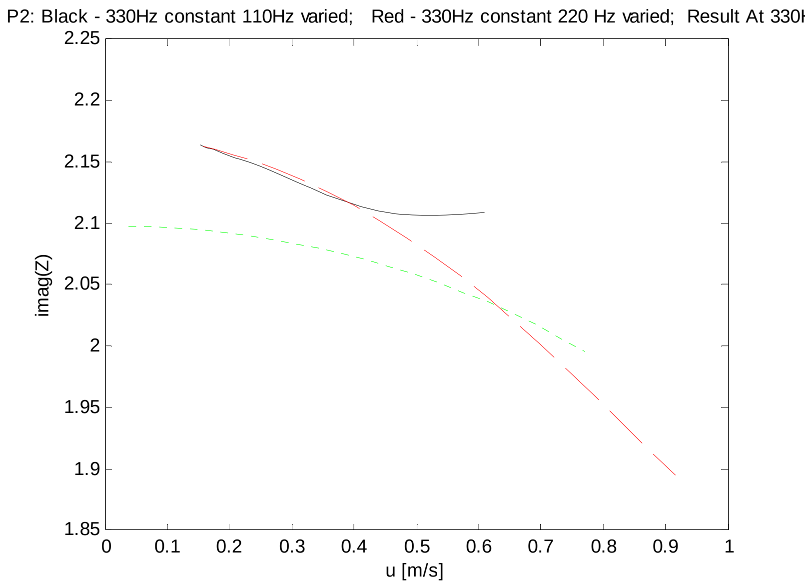
P2: Black - 330Hz constant 110Hz varied; Red - 330Hz constant 220 Hz varied; Result At 330I
imag(Z)
u [m/s]
2.25
2.2
2.15
2.1
2.05
2
1.95
1.9
1.85
0
0.1
0.2
0.3
0.4
0.5
0.6
0.7
0.8
0.9
1

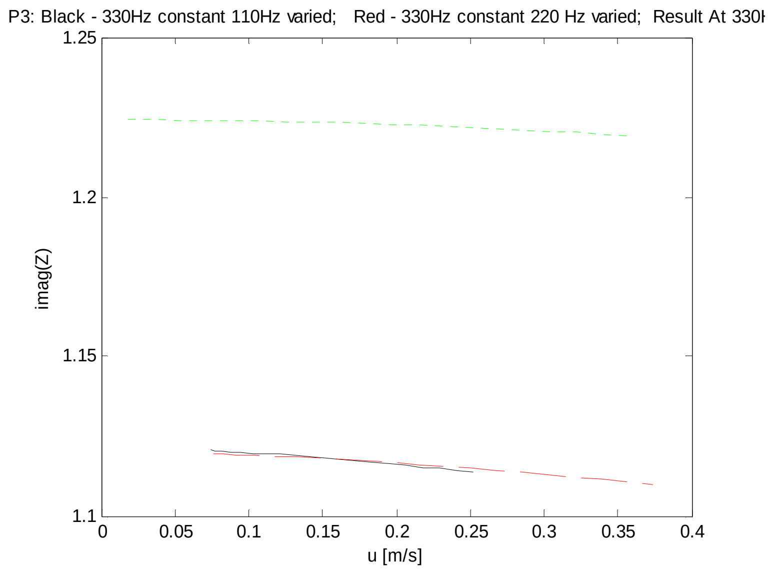
P3: Black - 330Hz constant 110Hz varied; Red - 330Hz constant 220 Hz varied; Result At 330I
imag(Z)
u [m/s]
1.25
1.2
1.15
1.1
0
0.05
0.1
0.15
0.2
0.25
0.3
0.35
0.4

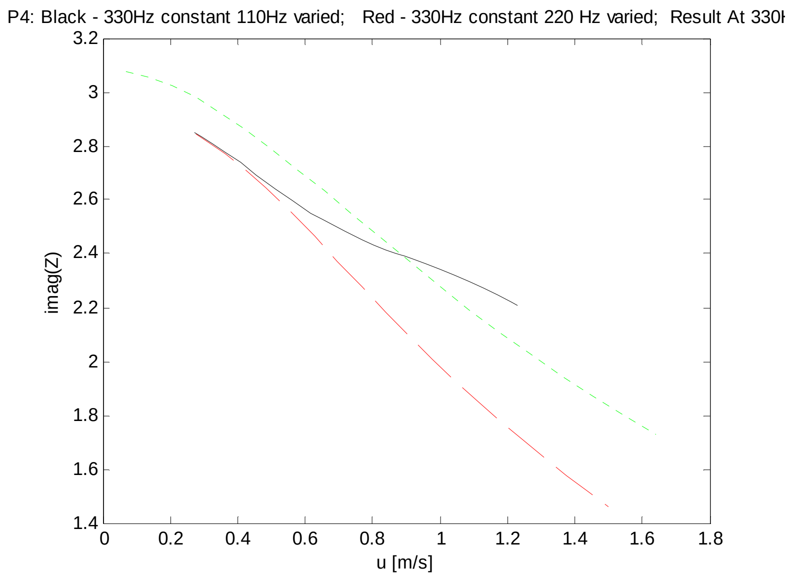
P4: Black - 330Hz constant 110Hz varied; Red - 330Hz constant 220 Hz varied; Result At 330I
imag(Z)
u [m/s]
3.2
3
2.8
2.6
2.4
2.2
2
1.8
1.6
1.4
0
0.2
0.4
0.6
0.8
1
1.2
1.4
1.6
1.8

P2: Black - 220Hz constant 110Hz varied;   Red - 220Hz constant 330 Hz varied;  Result At 220H

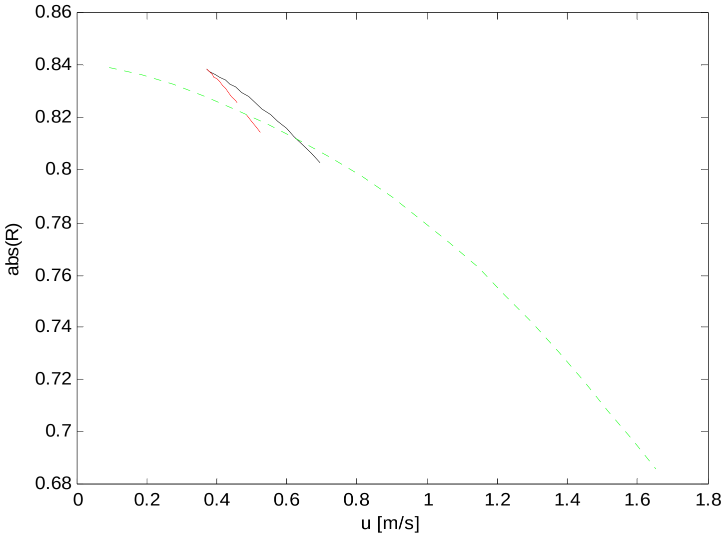


P3: Black - 220Hz constant 110Hz varied;   Red - 220Hz constant 330 Hz varied;  Result At 220H

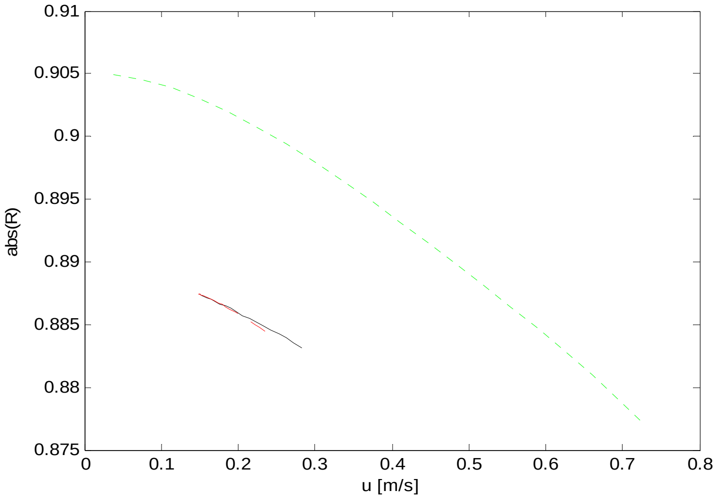


P4: Black - 220Hz constant 110Hz varied;   Red - 220Hz constant 330 Hz varied;  Result At 220H

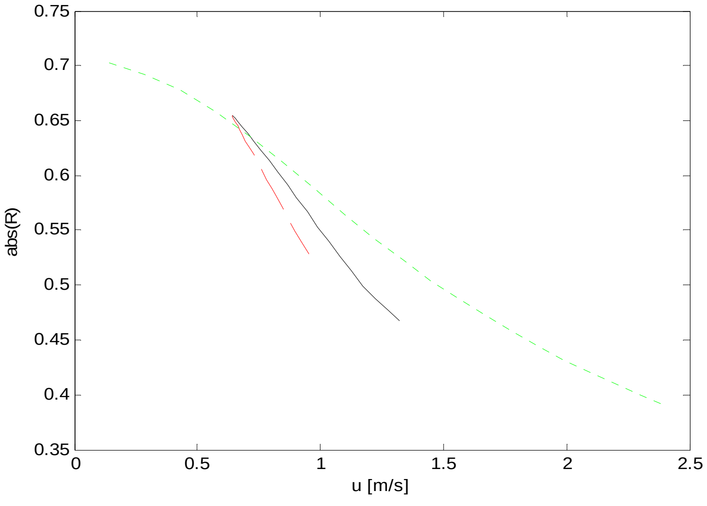

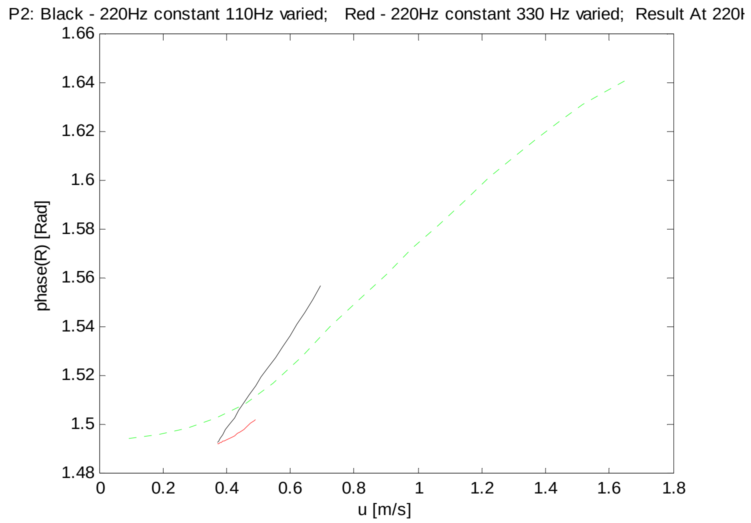
P2: Black - 220Hz constant 110Hz varied; Red - 220Hz constant 330 Hz varied; Result At 220H
phase(R) [Rad]
u [m/s]
1.66
1.64
1.62
1.6
1.58
1.56
1.54
1.52
1.5
1.48
0
0.2
0.4
0.6
0.8
1
1.2
1.4
1.6
1.8

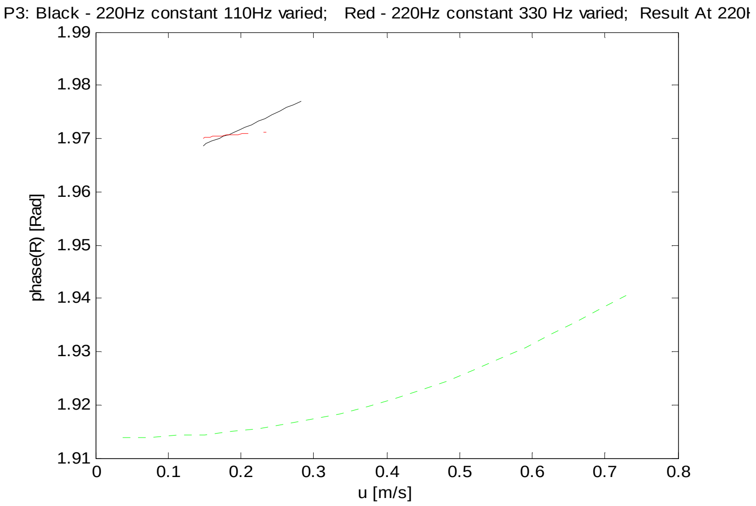
P3: Black - 220Hz constant 110Hz varied; Red - 220Hz constant 330 Hz varied; Result At 220H
phase(R) [Rad]
u [m/s]
1.99
1.98
1.97
1.96
1.95
1.94
1.93
1.92
1.91
0
0.1
0.2
0.3
0.4
0.5
0.6
0.7
0.8

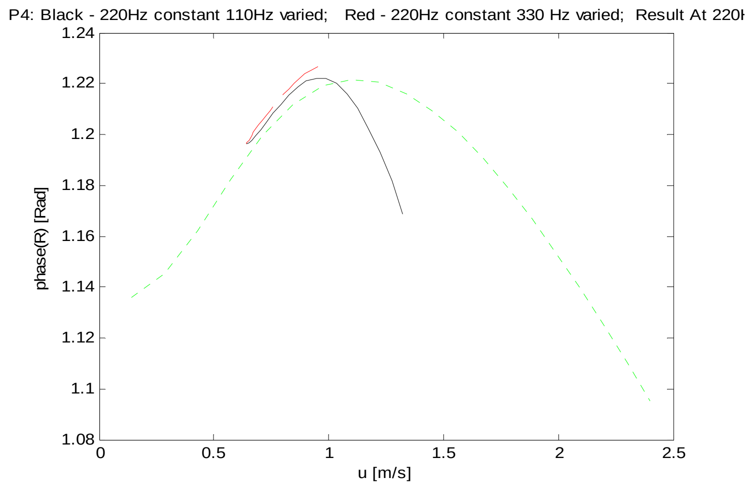
P4: Black - 220Hz constant 110Hz varied; Red - 220Hz constant 330 Hz varied; Result At 220H
phase(R) [Rad]
u [m/s]
1.24
1.22
1.2
1.18
1.16
1.14
1.12
1.1
1.08
0
0.5
1
1.5
2
2.5

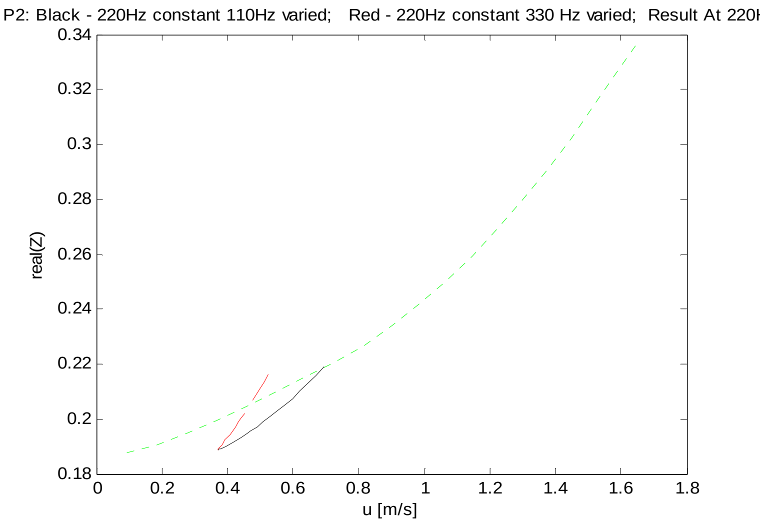
P2: Black - 220Hz constant 110Hz varied; Red - 220Hz constant 330 Hz varied; Result At 220H
real(Z)
u [m/s]
0.34
0.32
0.3
0.28
0.26
0.24
0.22
0.2
0.18
0
0.2
0.4
0.6
0.8
1
1.2
1.4
1.6
1.8

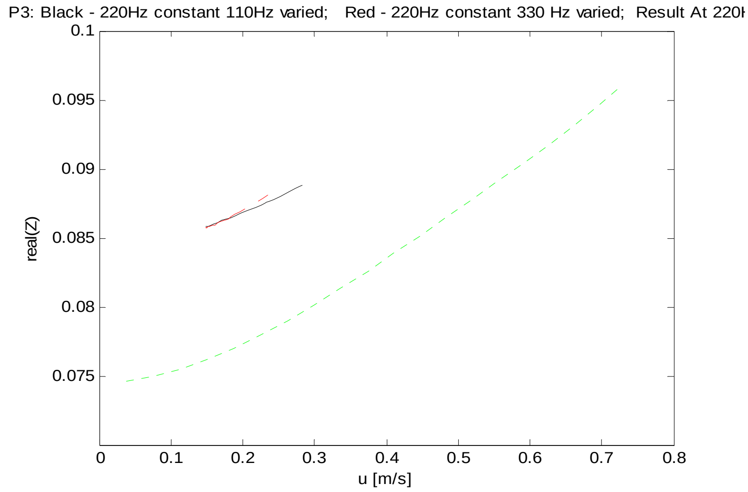
P3: Black - 220Hz constant 110Hz varied; Red - 220Hz constant 330 Hz varied; Result At 220H
real(Z)
u [m/s]
0.1
0.095
0.09
0.085
0.08
0.075
0
0.1
0.2
0.3
0.4
0.5
0.6
0.7
0.8

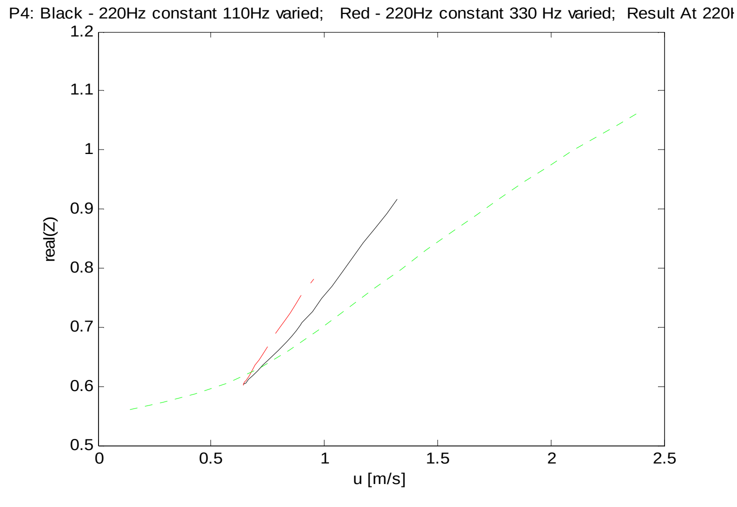
P4: Black - 220Hz constant 110Hz varied; Red - 220Hz constant 330 Hz varied; Result At 220H
real(Z)
u [m/s]
1.2
1.1
1
0.9
0.8
0.7
0.6
0.5
0
0.5
1
1.5
2
2.5

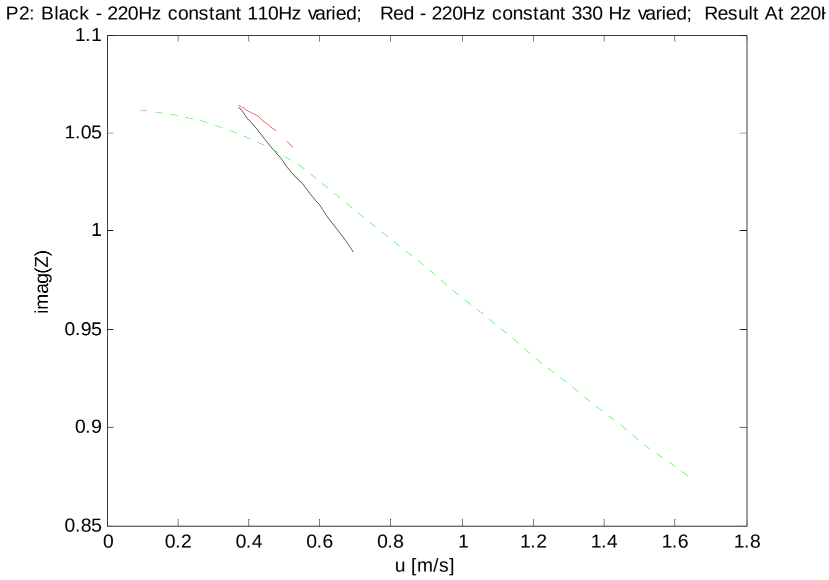

P2: Black - 220Hz constant 110Hz varied; Red - 220Hz constant 330 Hz varied; Result At 220I
imag(Z)
u [m/s]


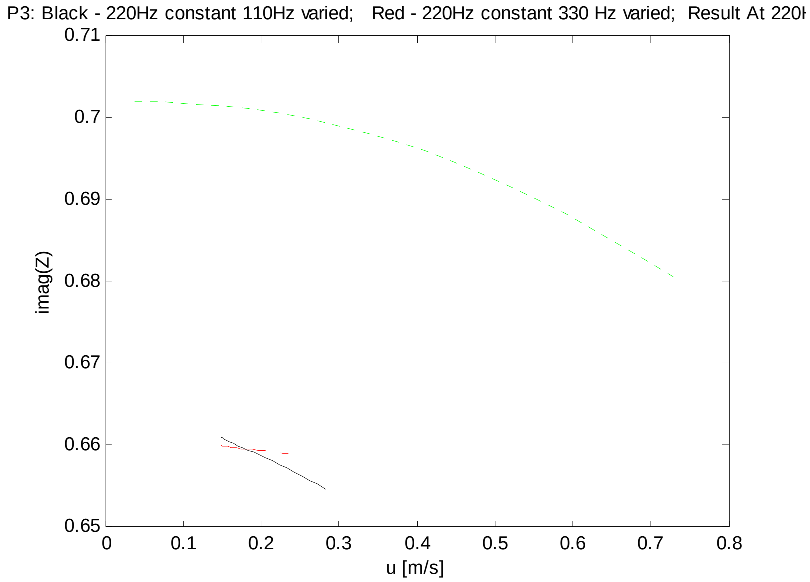

P3: Black - 220Hz constant 110Hz varied; Red - 220Hz constant 330 Hz varied; Result At 220I
imag(Z)
u [m/s]


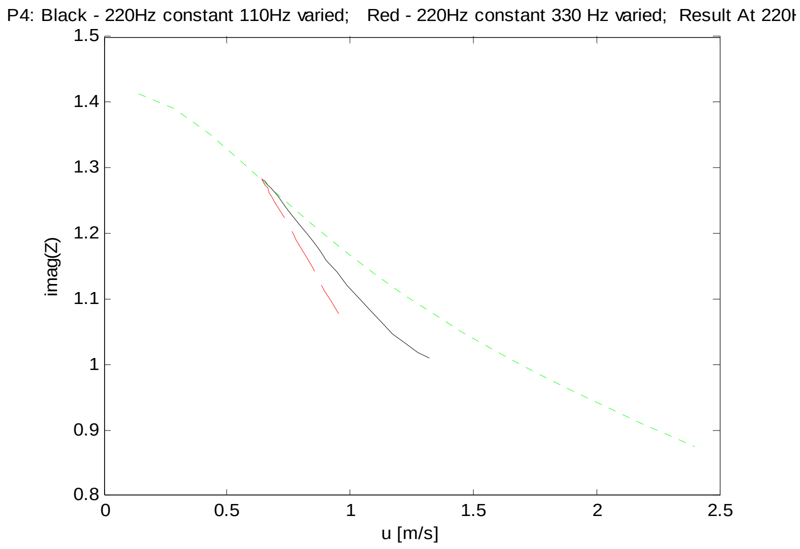

P4: Black - 220Hz constant 110Hz varied; Red - 220Hz constant 330 Hz varied; Result At 220I
imag(Z)
u [m/s]

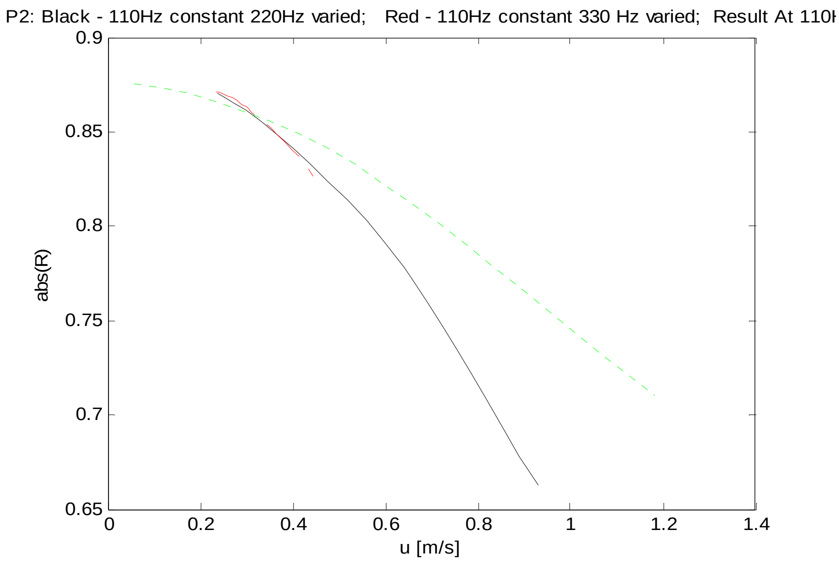
P2: Black - 110Hz constant 220Hz varied; Red - 110Hz constant 330 Hz varied; Result At 110H
abs(R)
u [m/s]

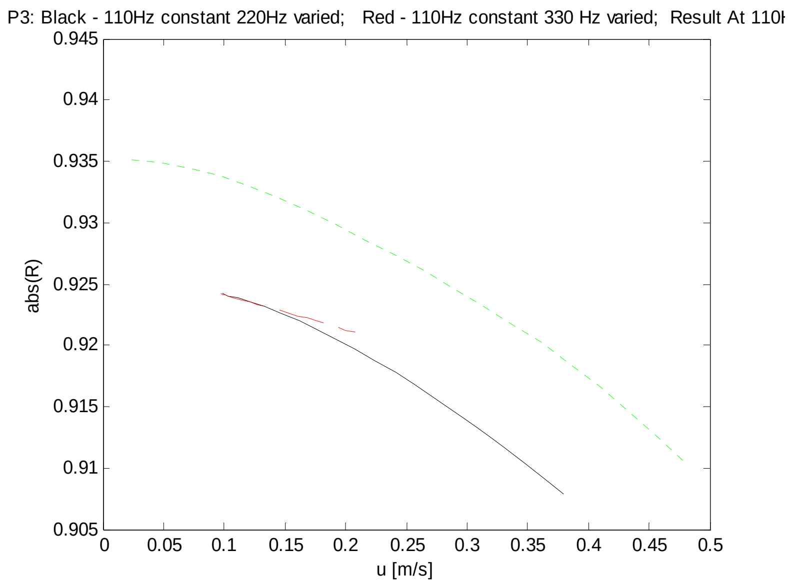
P3: Black - 110Hz constant 220Hz varied; Red - 110Hz constant 330 Hz varied; Result At 110H
abs(R)
u [m/s]

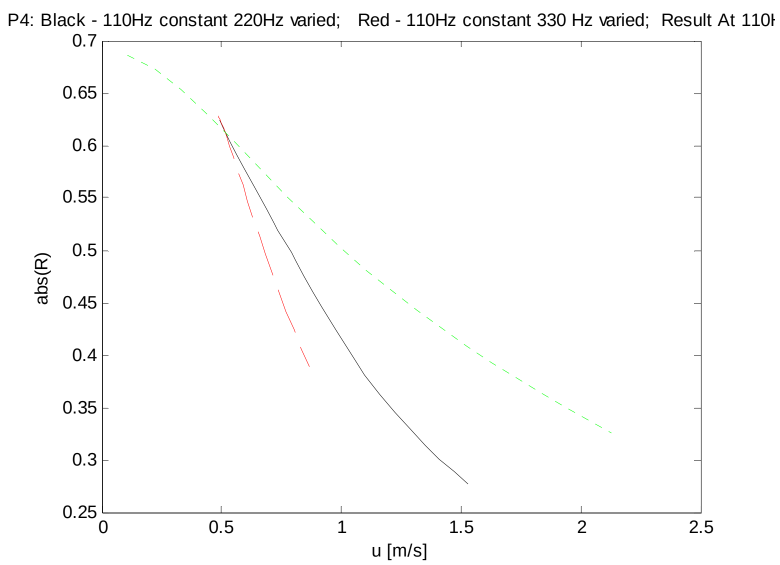
P4: Black - 110Hz constant 220Hz varied; Red - 110Hz constant 330 Hz varied; Result At 110H
abs(R)
u [m/s]

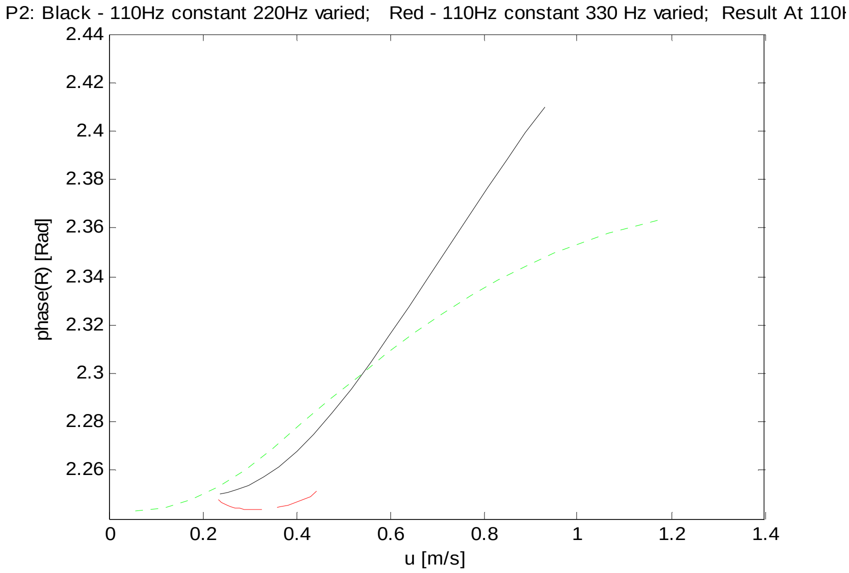
P2: Black - 110Hz constant 220Hz varied; Red - 110Hz constant 330 Hz varied; Result At 110H
phase(R) [Rad]
u [m/s]

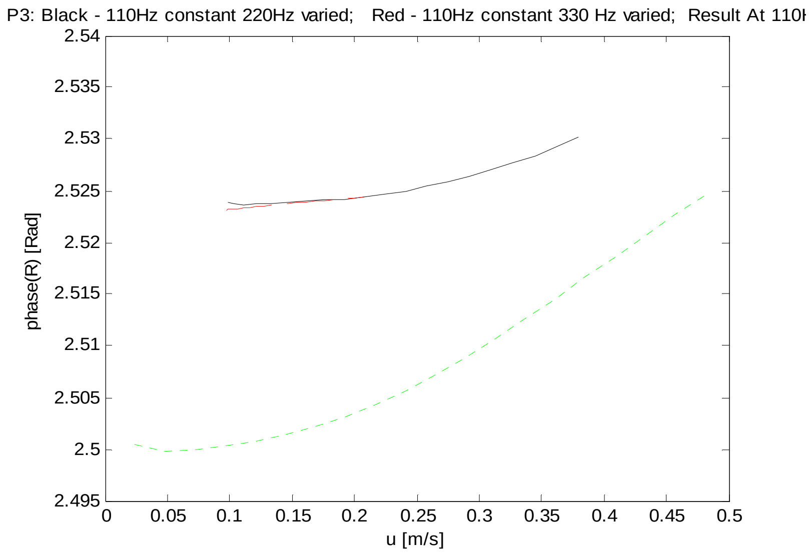
P3: Black - 110Hz constant 220Hz varied; Red - 110Hz constant 330 Hz varied; Result At 110H
phase(R) [Rad]
u [m/s]

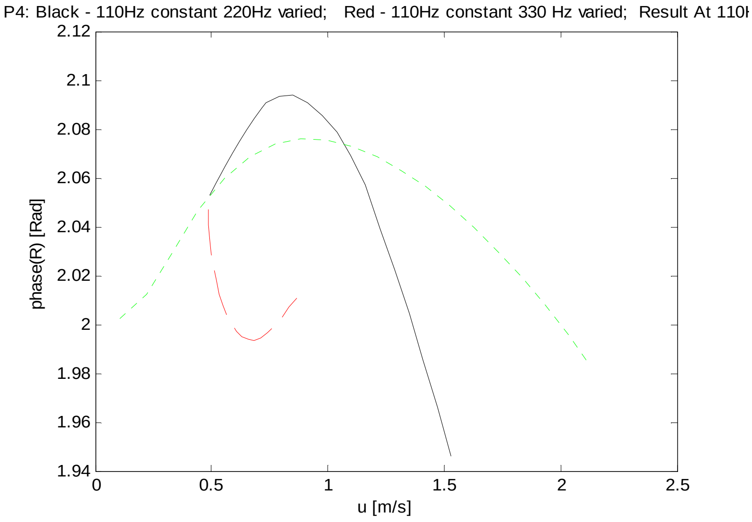
P4: Black - 110Hz constant 220Hz varied; Red - 110Hz constant 330 Hz varied; Result At 110H
phase(R) [Rad]
u [m/s]

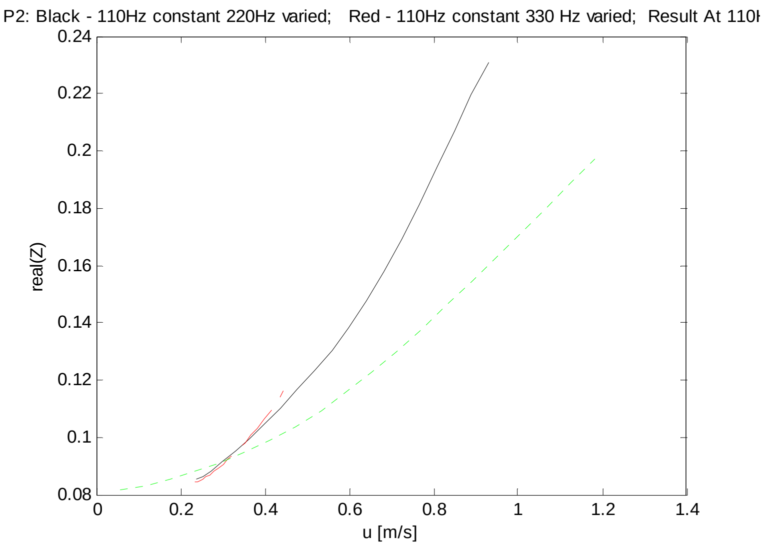
P2: Black - 110Hz constant 220Hz varied; Red - 110Hz constant 330 Hz varied; Result At 110H
real(Z)
u [m/s]
0.24
0.22
0.2
0.18
0.16
0.14
0.12
0.1
0.08
0
0.2
0.4
0.6
0.8
1
1.2
1.4

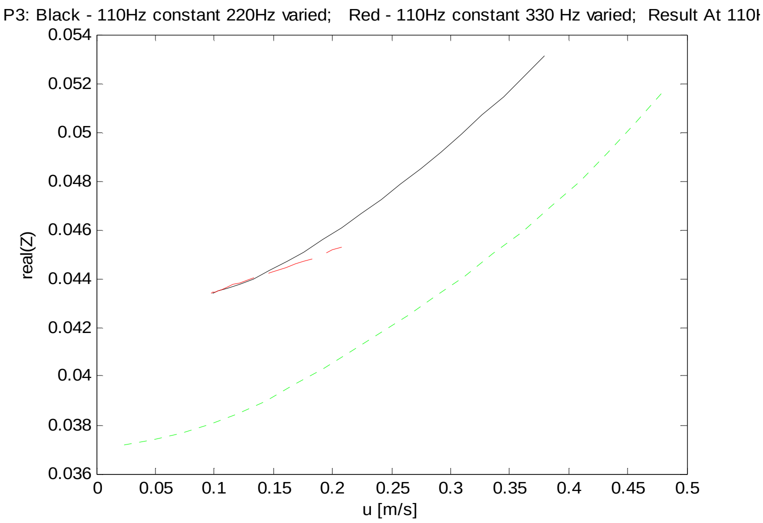
P3: Black - 110Hz constant 220Hz varied; Red - 110Hz constant 330 Hz varied; Result At 110H
real(Z)
u [m/s]
0.054
0.052
0.05
0.048
0.046
0.044
0.042
0.04
0.038
0.036
0
0.05
0.1
0.15
0.2
0.25
0.3
0.35
0.4
0.45
0.5

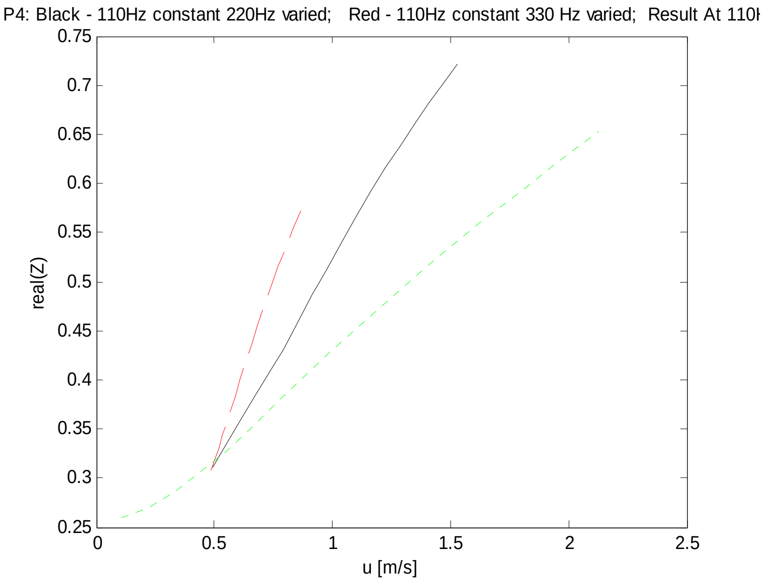
P4: Black - 110Hz constant 220Hz varied; Red - 110Hz constant 330 Hz varied; Result At 110H
real(Z)
u [m/s]
0.75
0.7
0.65
0.6
0.55
0.5
0.45
0.4
0.35
0.3
0.25
0
0.5
1
1.5
2
2.5

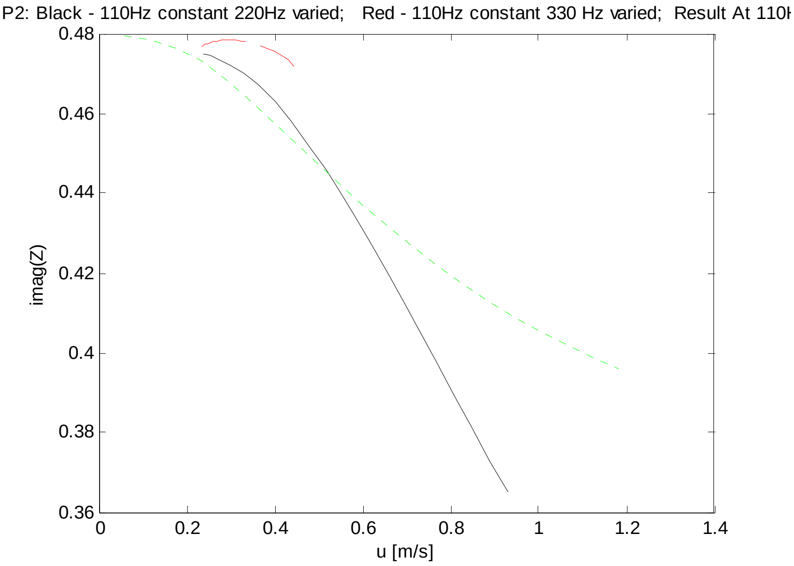
P2: Black - 110Hz constant 220Hz varied; Red - 110Hz constant 330 Hz varied; Result At 110H
imag(Z)
u [m/s]

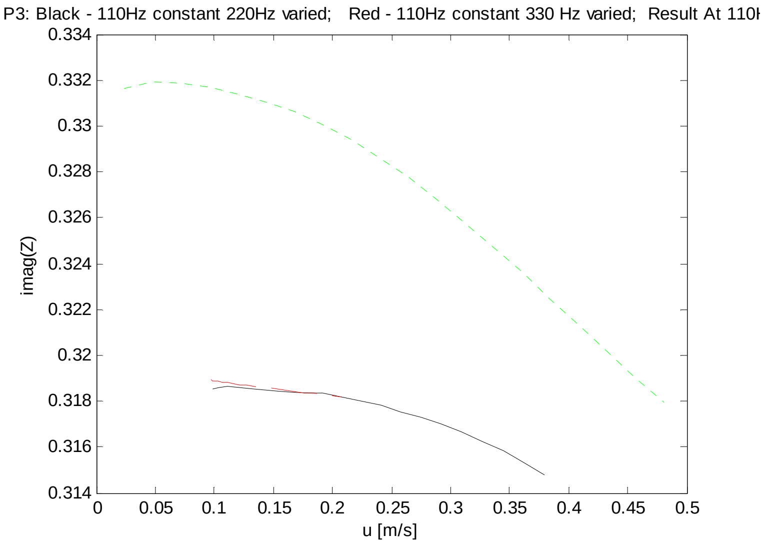
P3: Black - 110Hz constant 220Hz varied; Red - 110Hz constant 330 Hz varied; Result At 110H
imag(Z)
u [m/s]

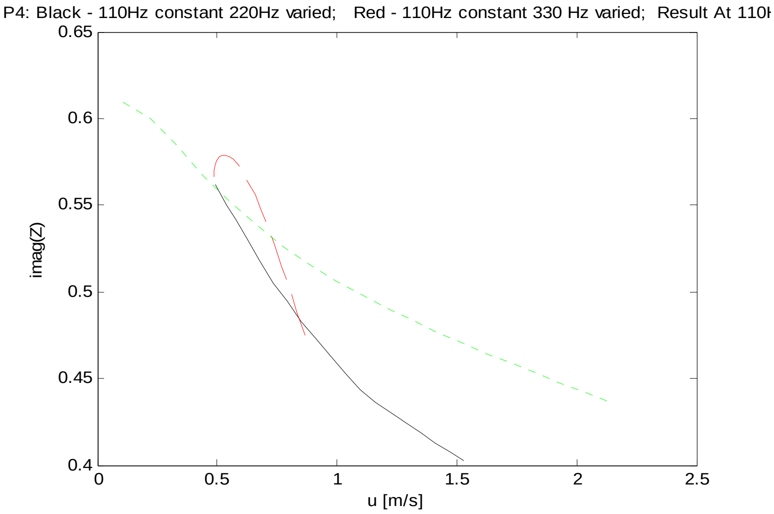
P4: Black - 110Hz constant 220Hz varied; Red - 110Hz constant 330 Hz varied; Result At 110H
imag(Z)
u [m/s]

# Two-tone excitation with harmonics at 110Hz, 220Hz, 330Hz for realistic samples R1 and R2

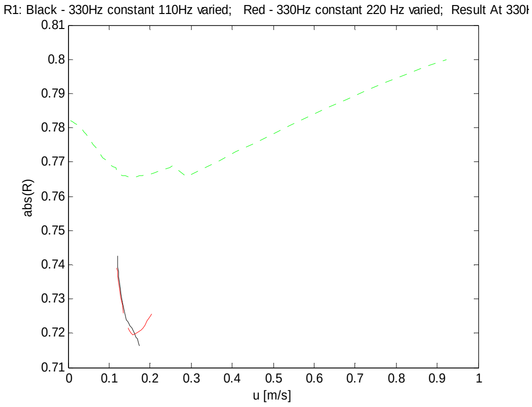


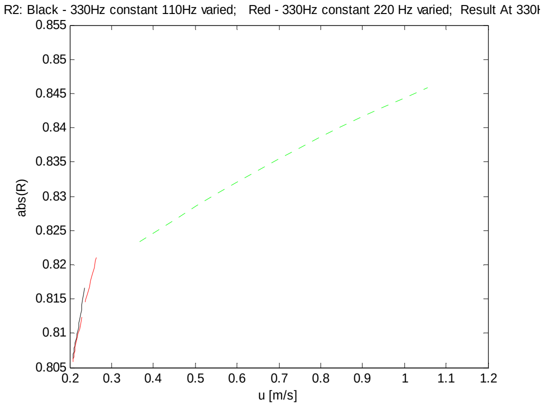


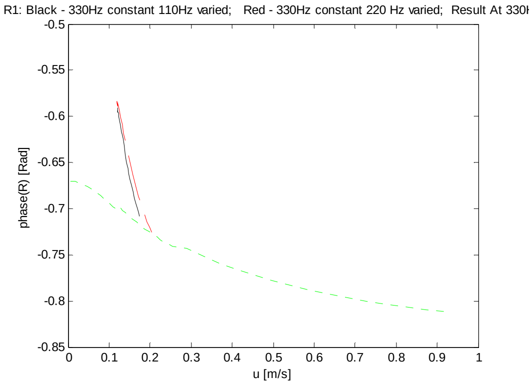


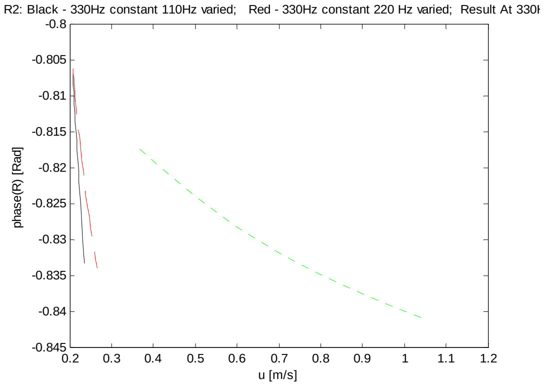


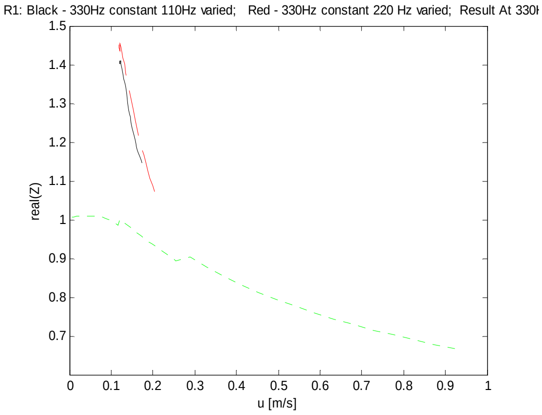


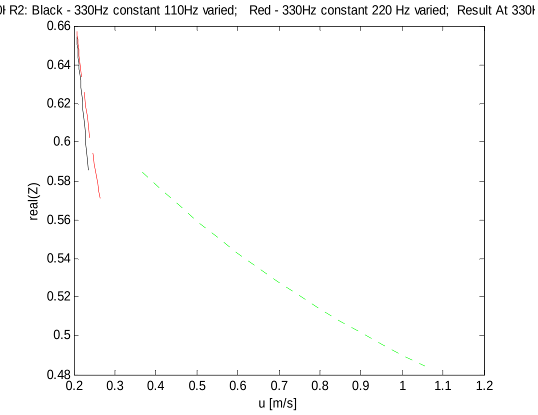


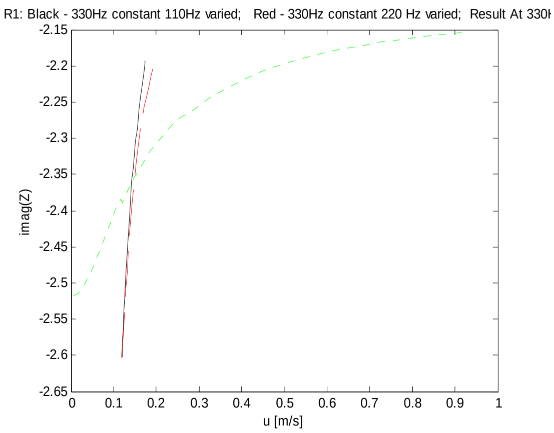


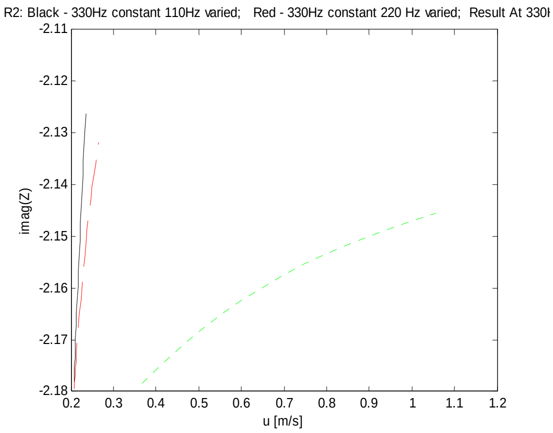

The green lines represent the case with single tone excitation at same frequency as the constant signal.  Even here It can be seen that even a low signal at varied frequency contributes to a shift in result compared with single pure tone excitation at studied frequency.

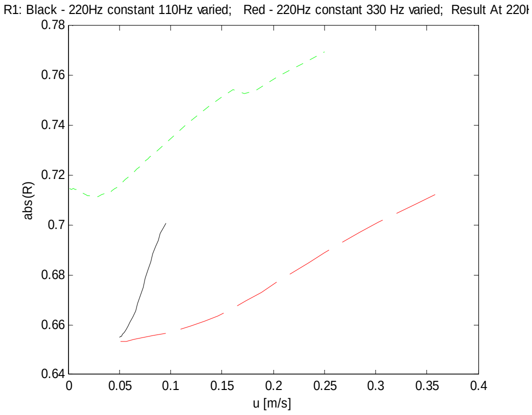


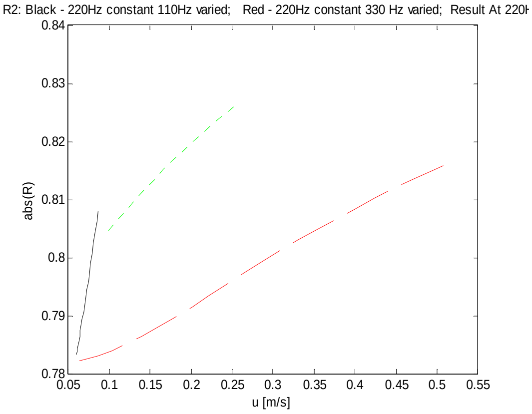


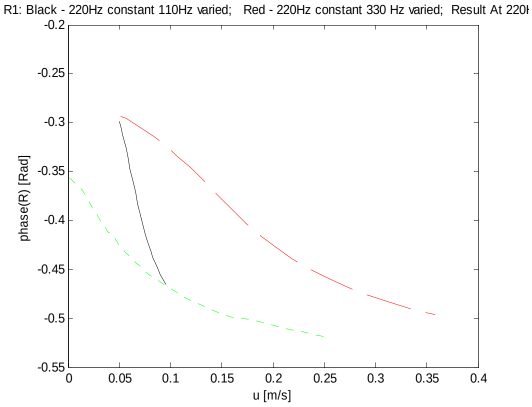


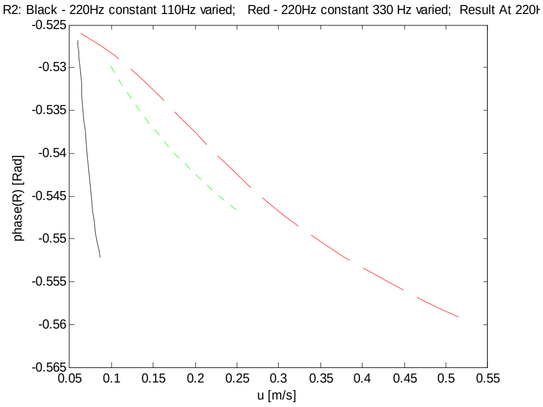


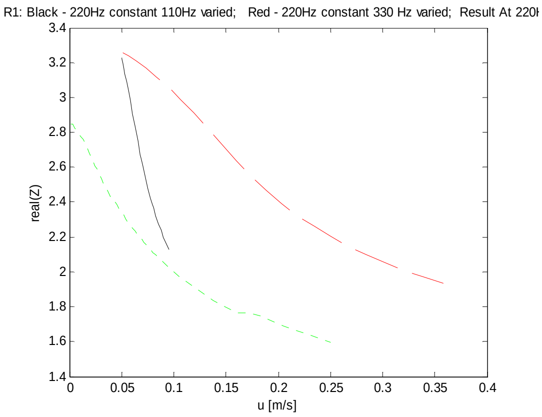


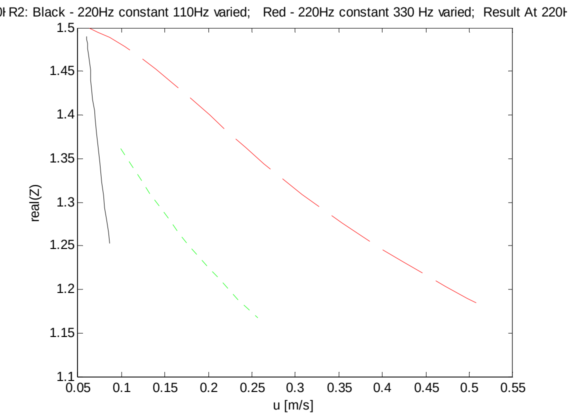


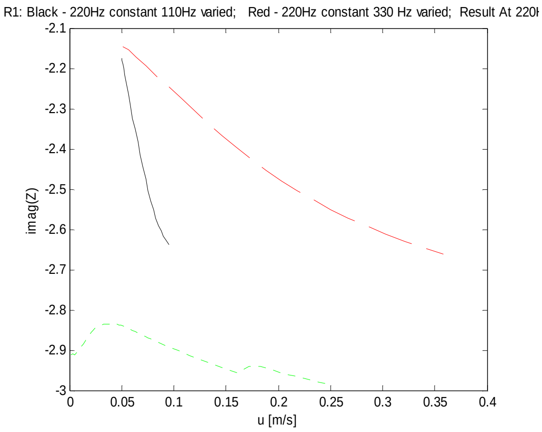


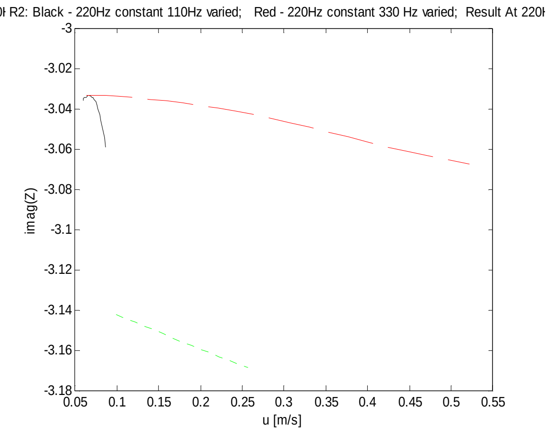

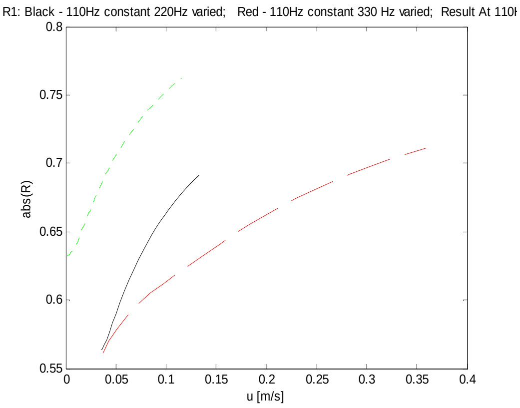
R1: Black - 110Hz constant 220Hz varied; Red - 110Hz constant 330 Hz varied; Result At 110I
abs(R)
u [m/s]

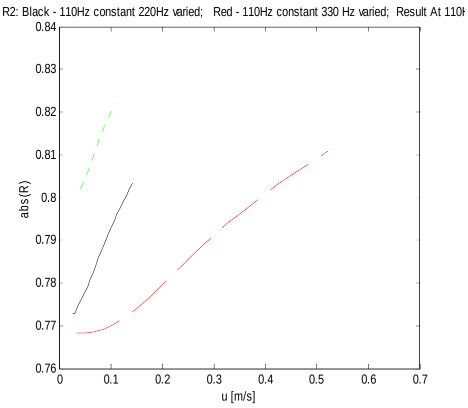
R2: Black - 110Hz constant 220Hz varied; Red - 110Hz constant 330 Hz varied; Result At 110I
abs(R)
u [m/s]

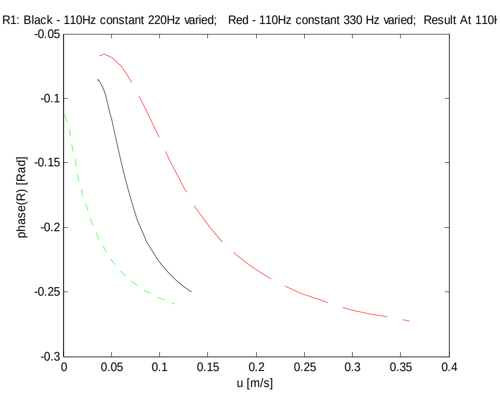
R1: Black - 110Hz constant 220Hz varied; Red - 110Hz constant 330 Hz varied; Result At 110I
phase(R) [Rad]
u [m/s]

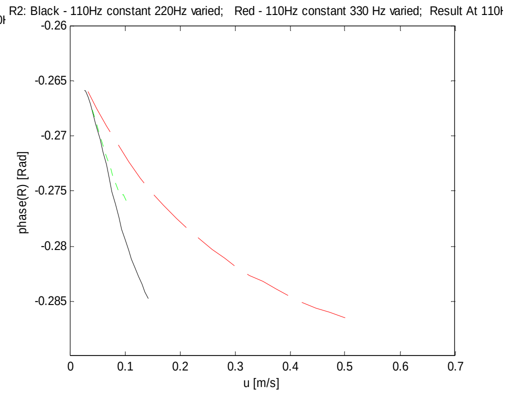
R2: Black - 110Hz constant 220Hz varied; Red - 110Hz constant 330 Hz varied; Result At 110I
phase(R) [Rad]
u [m/s]

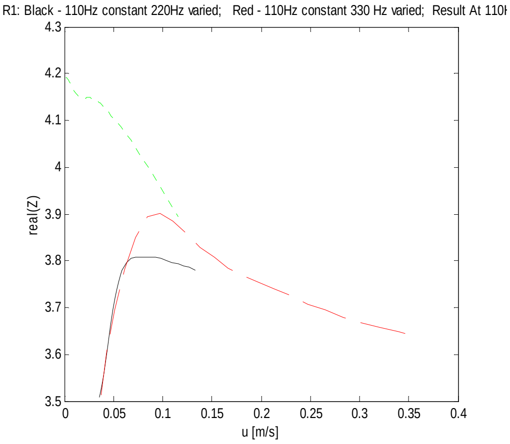
R1: Black - 110Hz constant 220Hz varied; Red - 110Hz constant 330 Hz varied; Result At 110I
real(Z)
u [m/s]

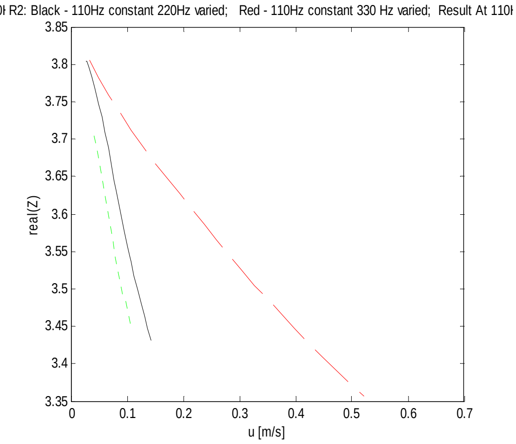
R2: Black - 110Hz constant 220Hz varied; Red - 110Hz constant 330 Hz varied; Result At 110I
real(Z)
u [m/s]

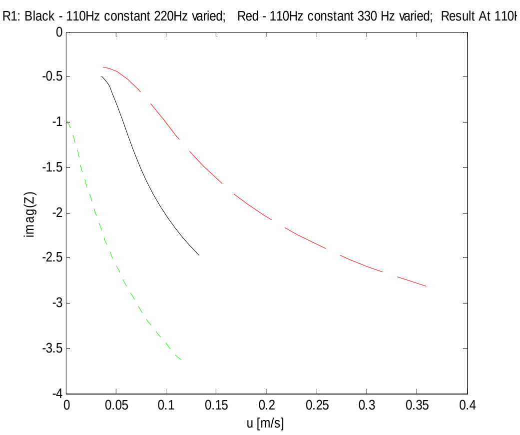
R1: Black - 110Hz constant 220Hz varied; Red - 110Hz constant 330 Hz varied; Result At 110I
imag(Z)
u [m/s]

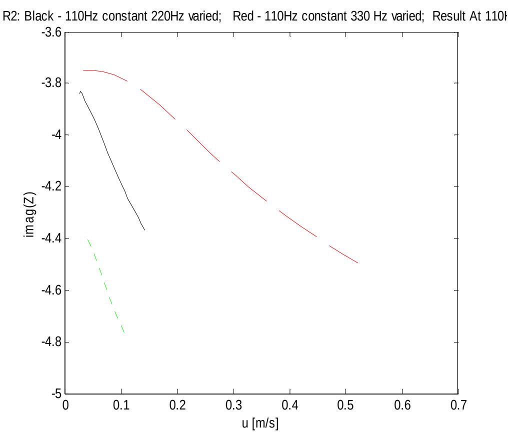
R2: Black - 110Hz constant 220Hz varied; Red - 110Hz constant 330 Hz varied; Result At 110I
imag(Z)
u [m/s]

# Two-tone excitation with harmonics at 110Hz, 330Hz, 990Hz for realistic samples R1 and R2

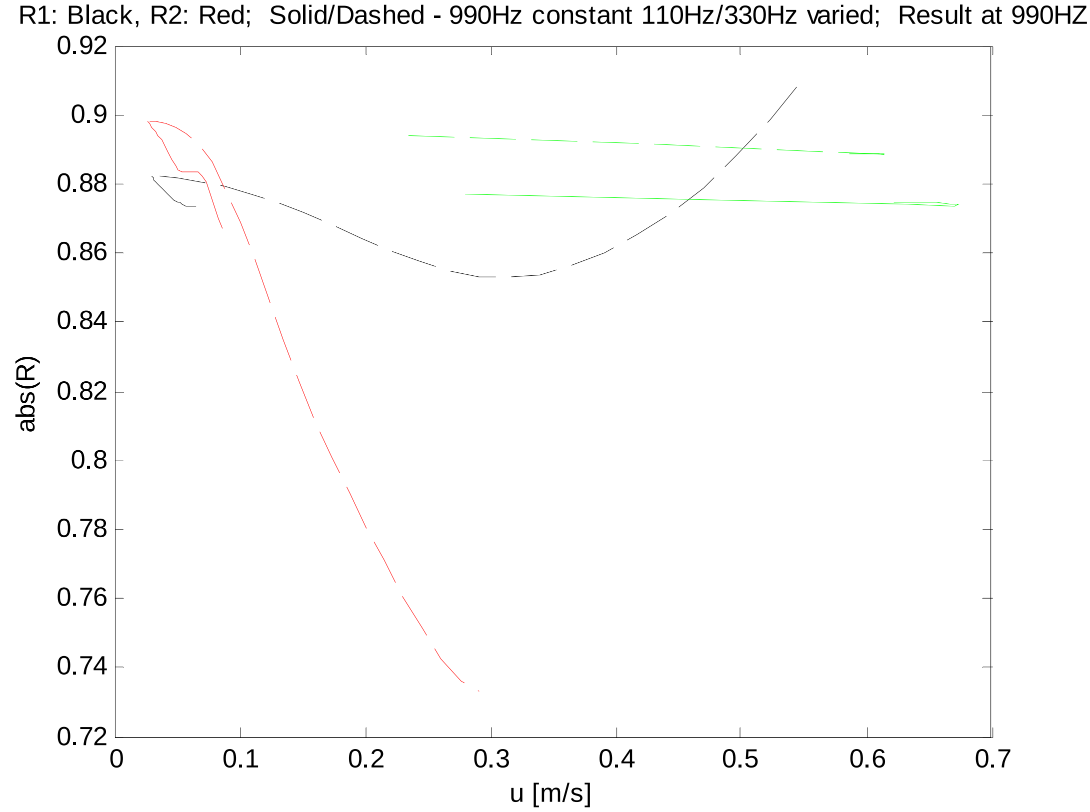


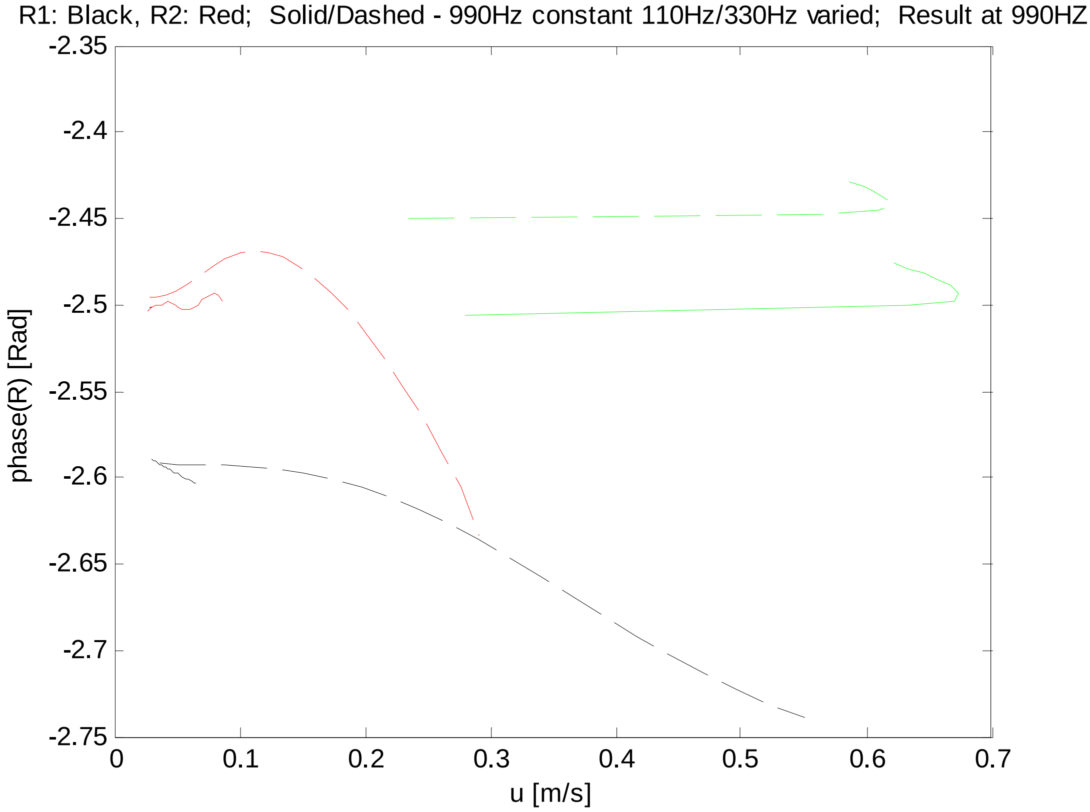

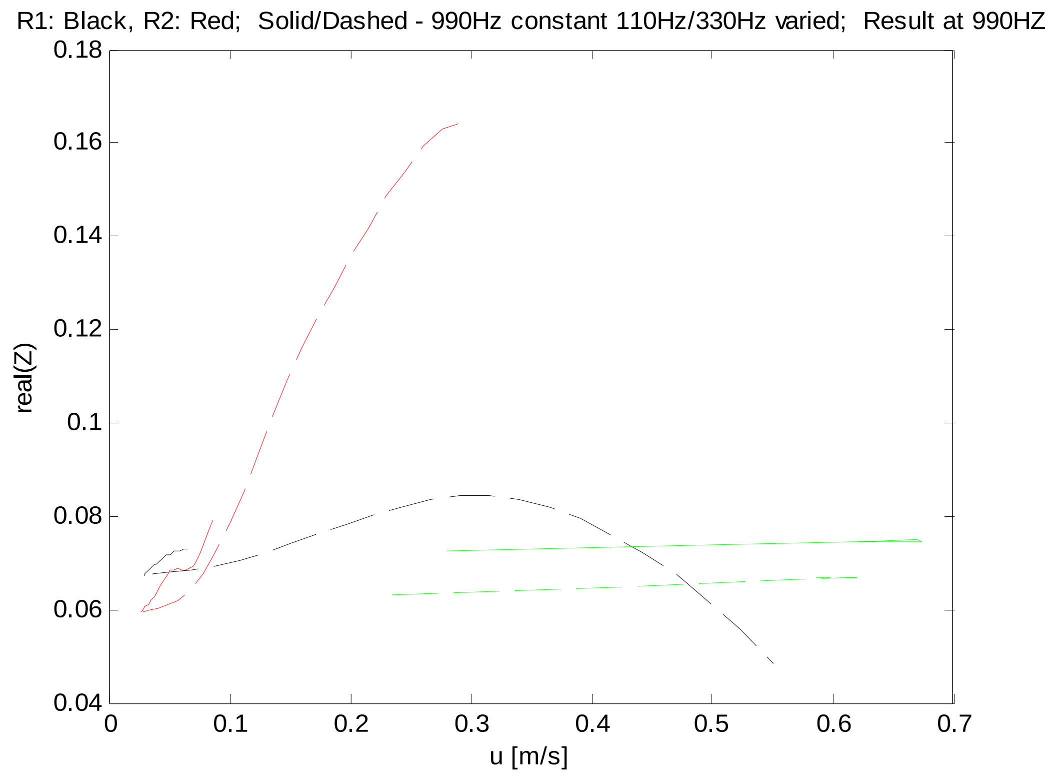


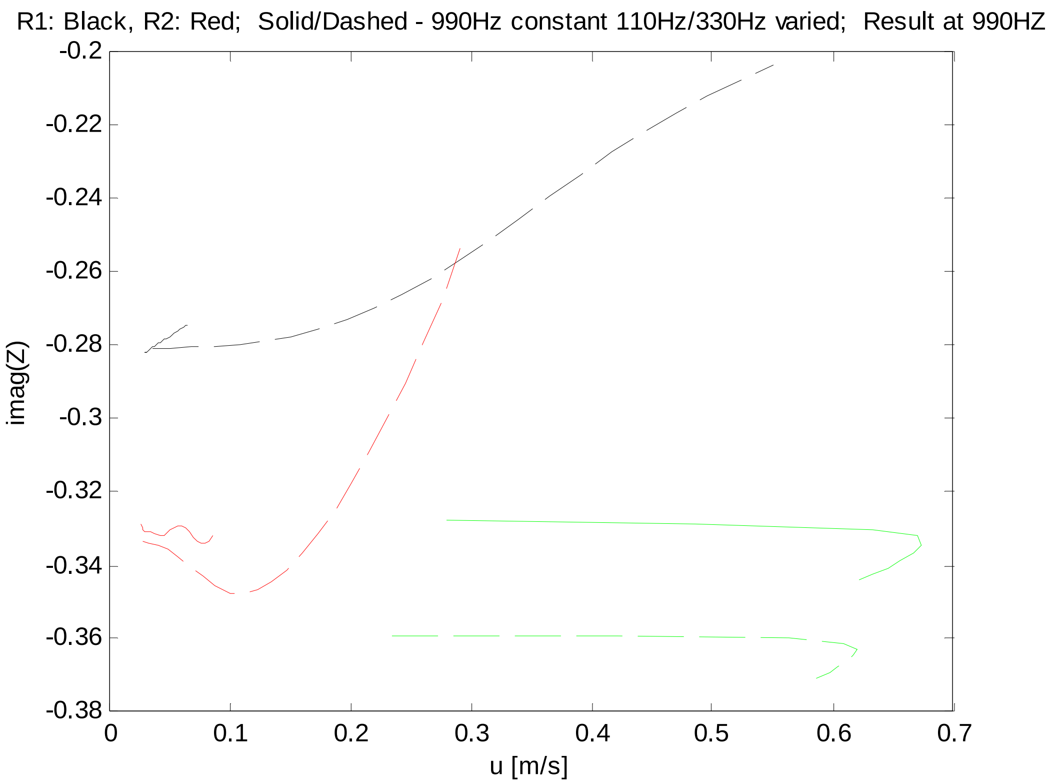


What is known about the realistic samples is that they are designed to have as linear behavior as possible for higher sound levels and mostly at frequencies higher than 1000 Hz. In previous four plots the green lines represent result at 990Hz with single pure tone excitation at that frequency. It can be clearly seen that the result is showing quite linear behavior compared with the cases when the excitation signals are at 110Hz and 330Hz.

# Two-tone excitation with not exact harmonics at 330 Hz and 100Hz or 110Hz or 120 Hz, P4

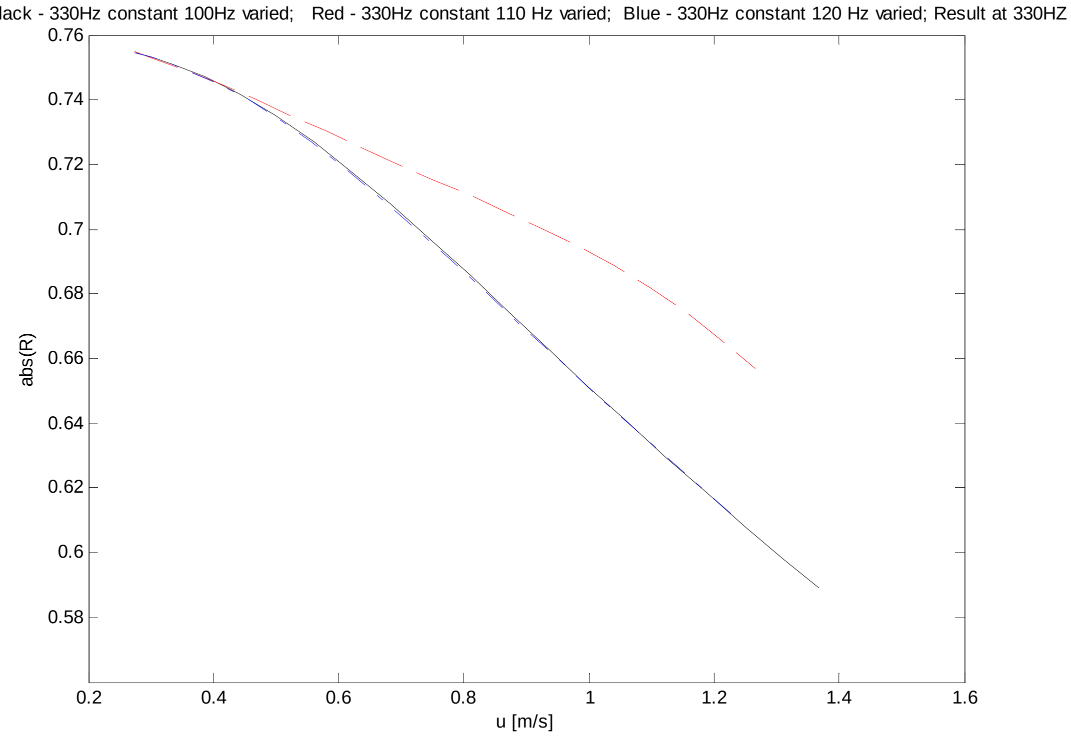


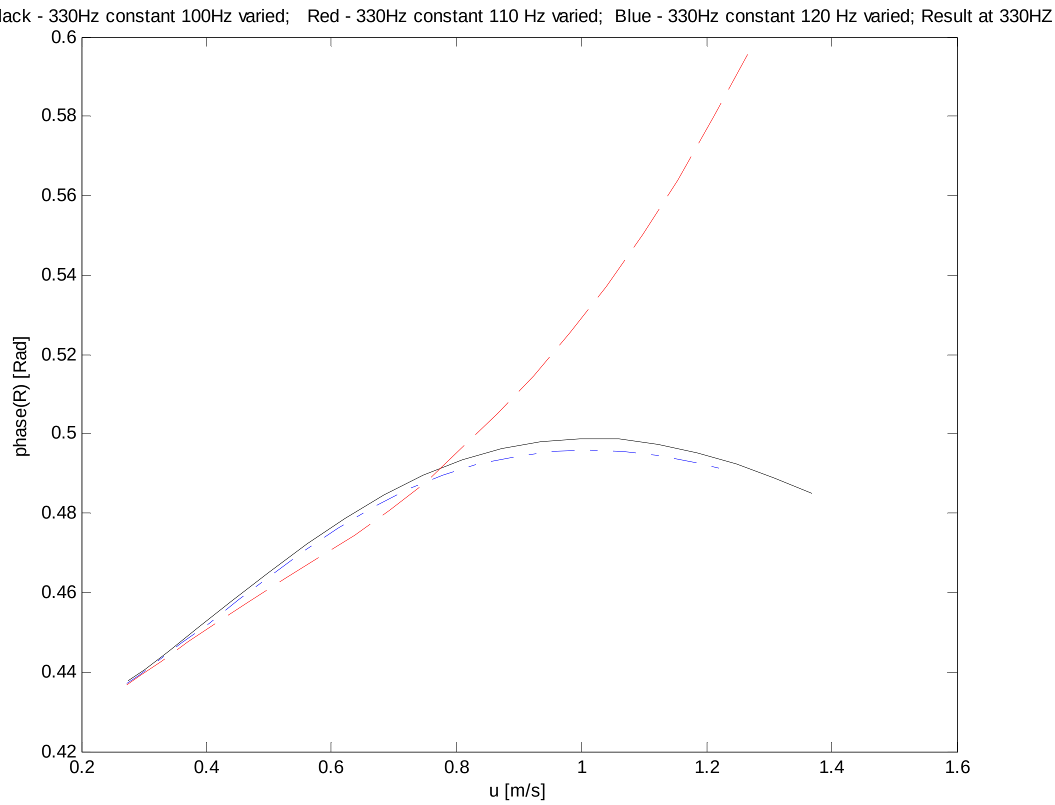

The plots are showing the results only for the P4 sample just to show whether there is a difference in the result at studied frequency when the varied excitation is made at not exactly three times lower frequency. It can be seen that a shift of 10Hz upwards or downwards at frequency is giving quite the same result which is different from the result when exact harmonics at 110Hz and 330Hz are studied..

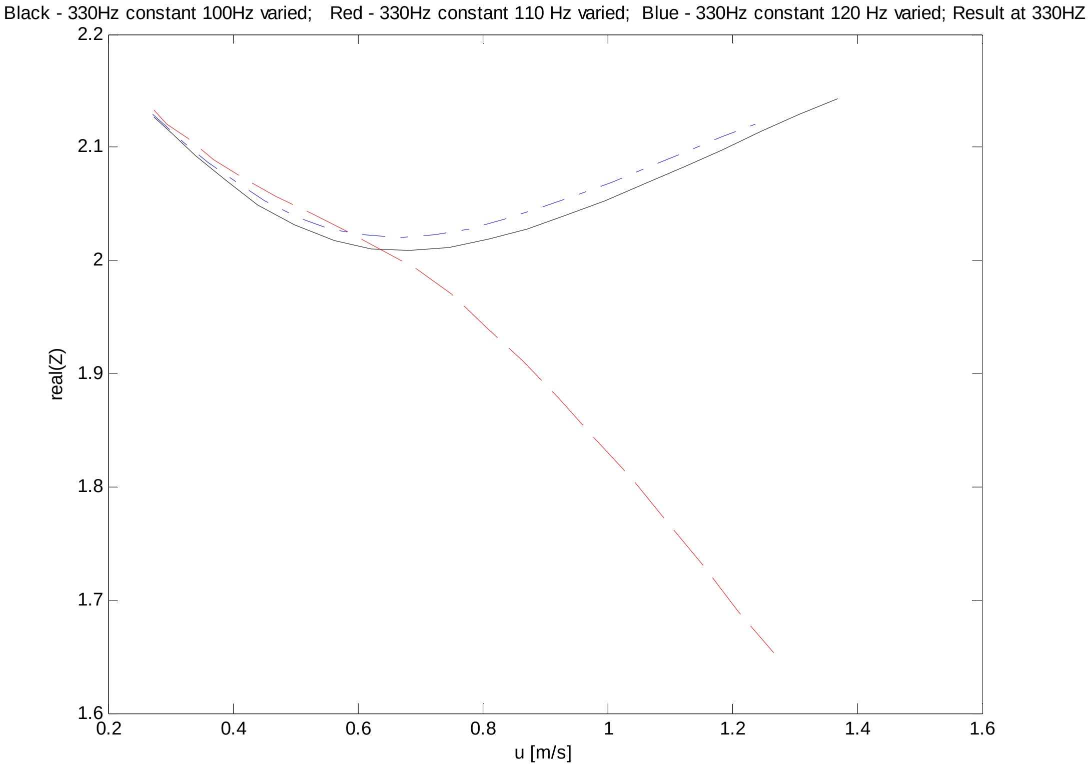


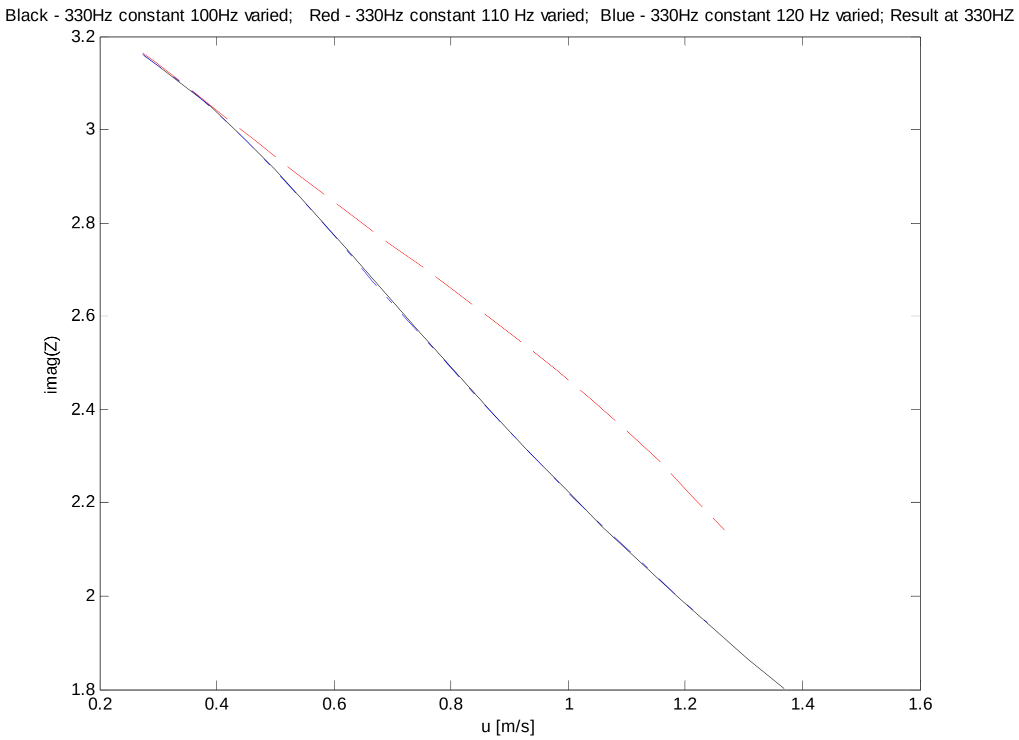

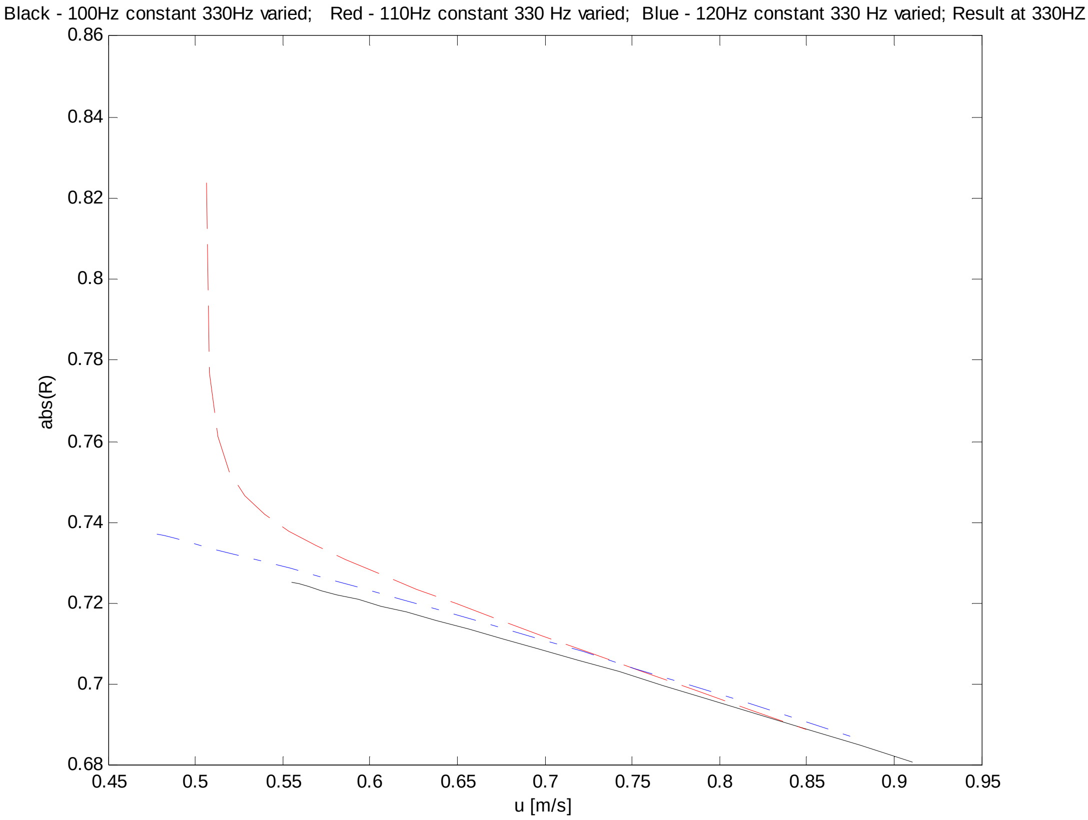
Black - 100Hz constant 330Hz varied;   Red - 110Hz constant 330 Hz varied;  Blue - 120Hz constant 330 Hz varied; Result at 330HZ
abs(R)
u [m/s]
0.86
0.84
0.82
0.8
0.78
0.76
0.74
0.72
0.7
0.68
0.45
0.5
0.55
0.6
0.65
0.7
0.75
0.8
0.85
0.9
0.95

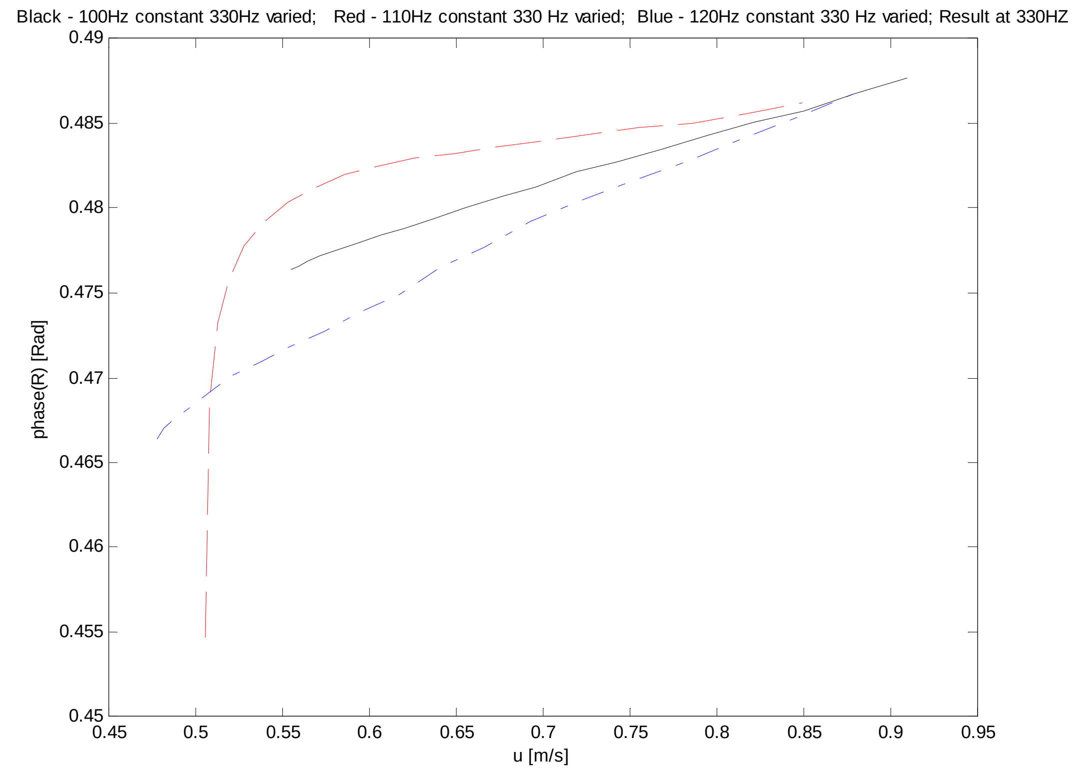
Black - 100Hz constant 330Hz varied;   Red - 110Hz constant 330 Hz varied;  Blue - 120Hz constant 330 Hz varied; Result at 330HZ
phase(R) [Rad]
u [m/s]
0.49
0.485
0.48
0.475
0.47
0.465
0.46
0.455
0.45
0.45
0.5
0.55
0.6
0.65
0.7
0.75
0.8
0.85
0.9
0.95

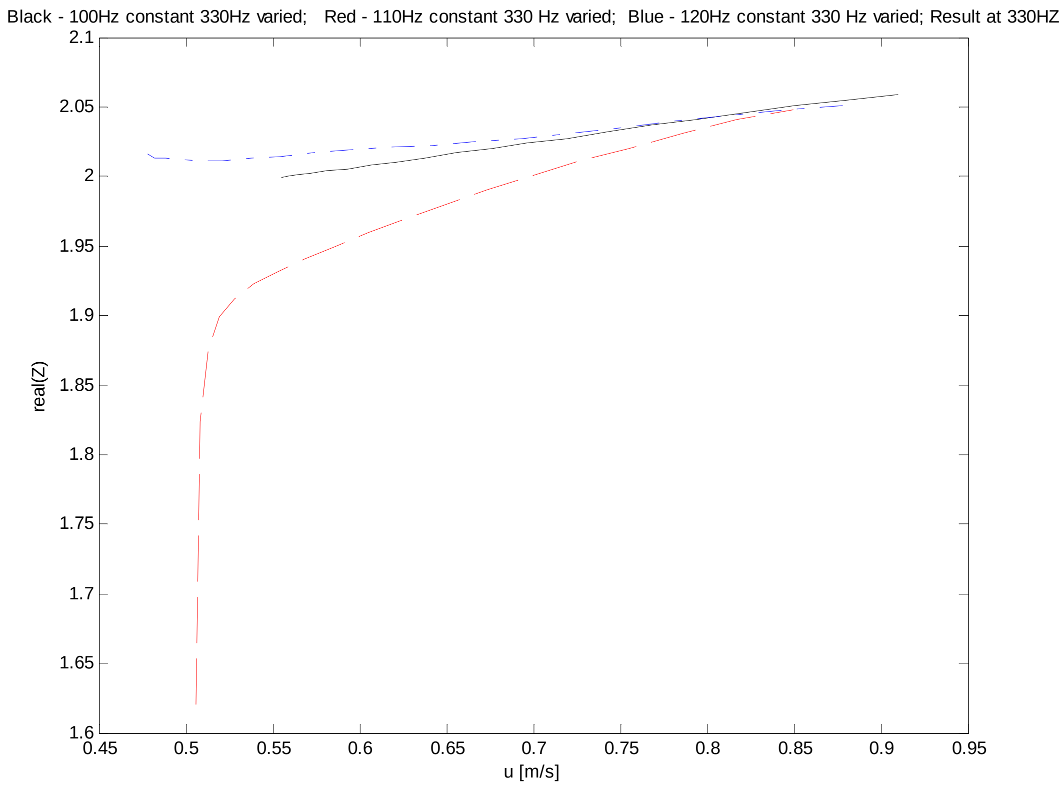
Black - 100Hz constant 330Hz varied; Red - 110Hz constant 330 Hz varied; Blue - 120Hz constant 330 Hz varied; Result at 330HZ
real(Z)
u [m/s]
2.1
2.05
2
1.95
1.9
1.85
1.8
1.75
1.7
1.65
1.6
0.45
0.5
0.55
0.6
0.65
0.7
0.75
0.8
0.85
0.9
0.95

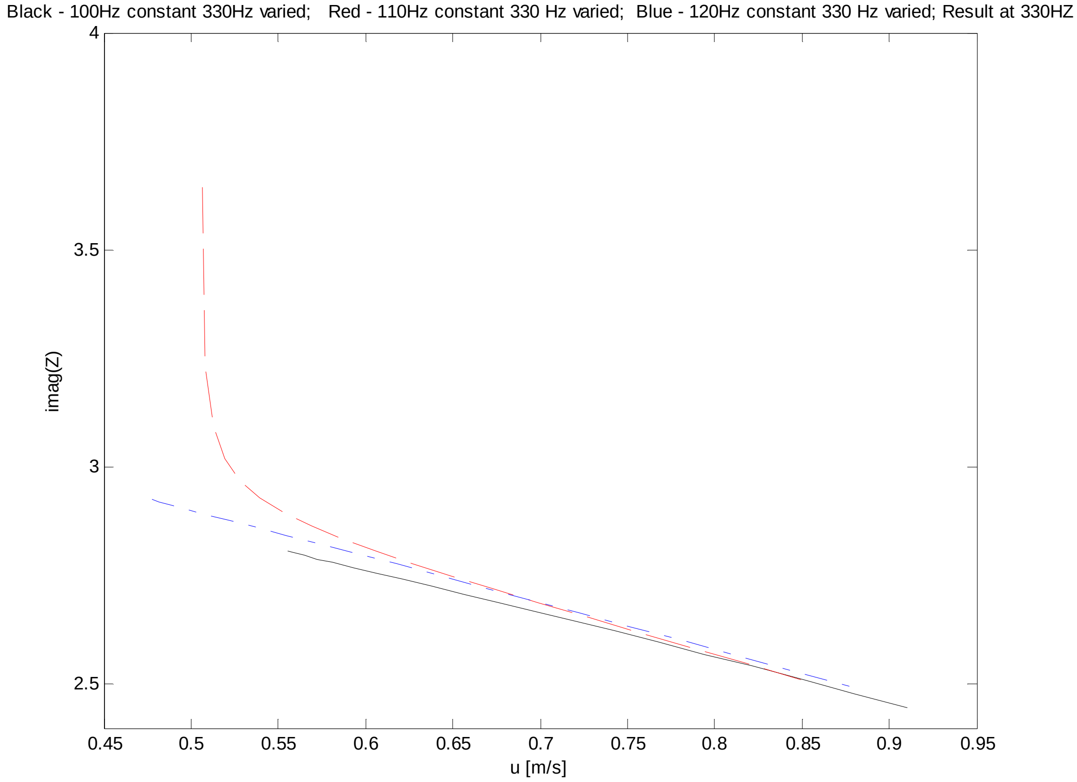
Black - 100Hz constant 330Hz varied; Red - 110Hz constant 330 Hz varied; Blue - 120Hz constant 330 Hz varied; Result at 330HZ
imag(Z)
u [m/s]
4
3.5
3
2.5
0.45
0.5
0.55
0.6
0.65
0.7
0.75
0.8
0.85
0.9
0.95

## Two-tone harmonic excitation, effect of shifting the phase of varied signal on acoustic properties measurement, P4 sample

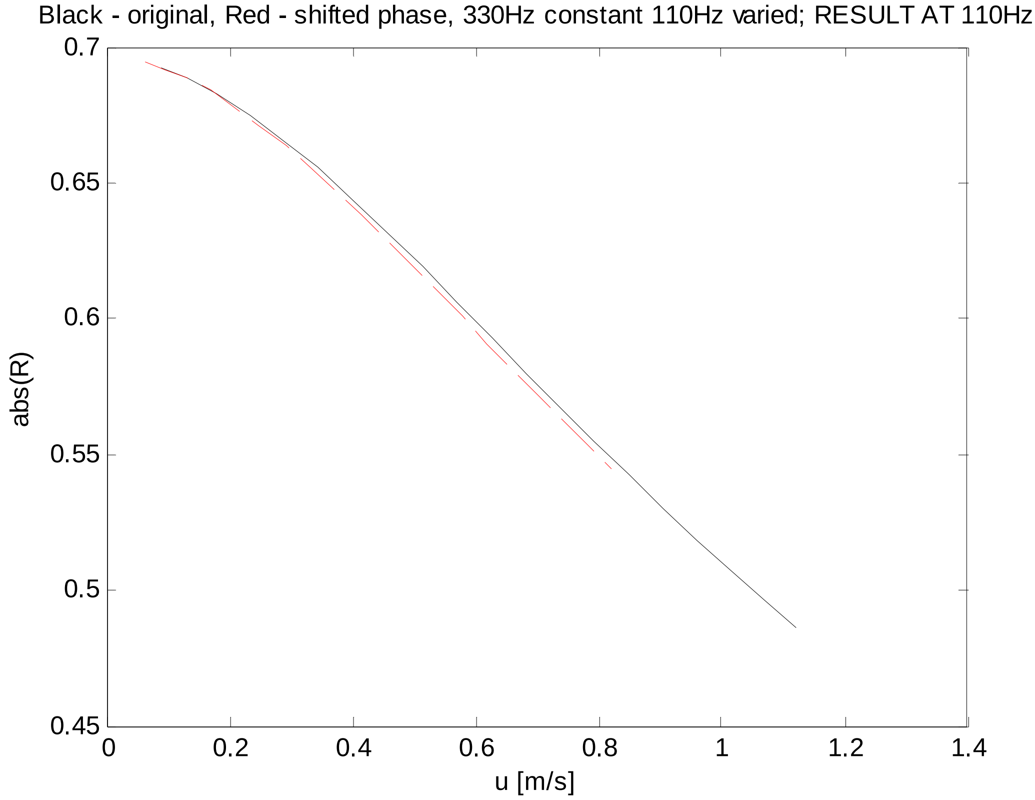


The varied signal on these plots had its phase shifted but the results are showing that there is not much difference at the same frequency as the frequency of the signal with shifted phase; however the result at frequency which is three times higher is different.

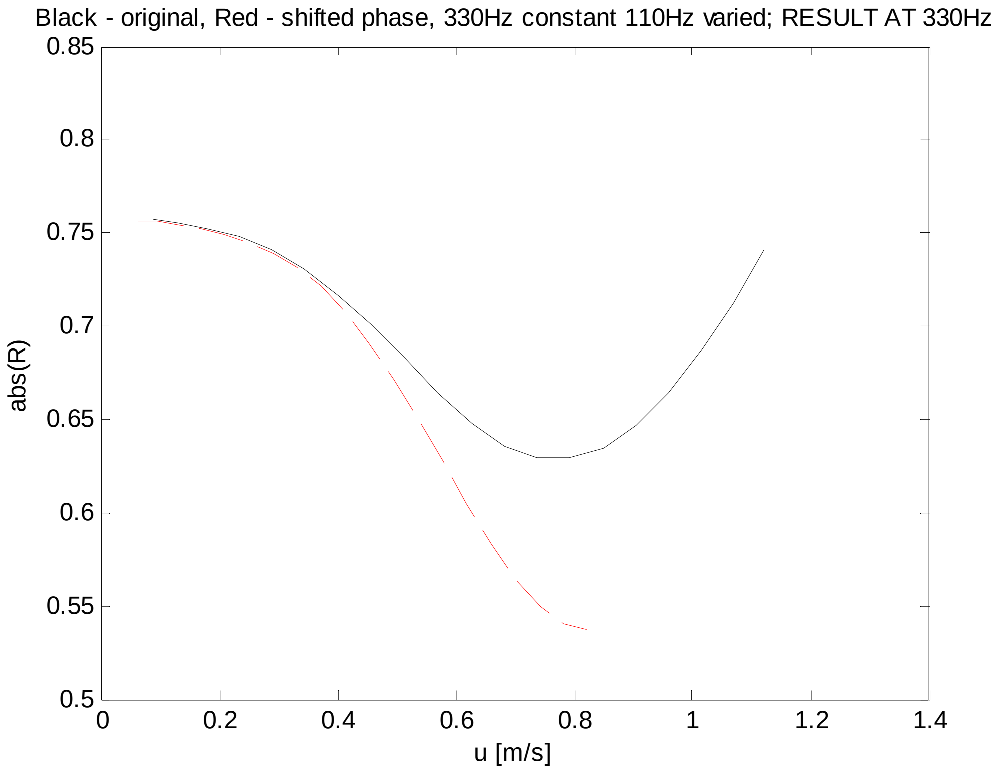

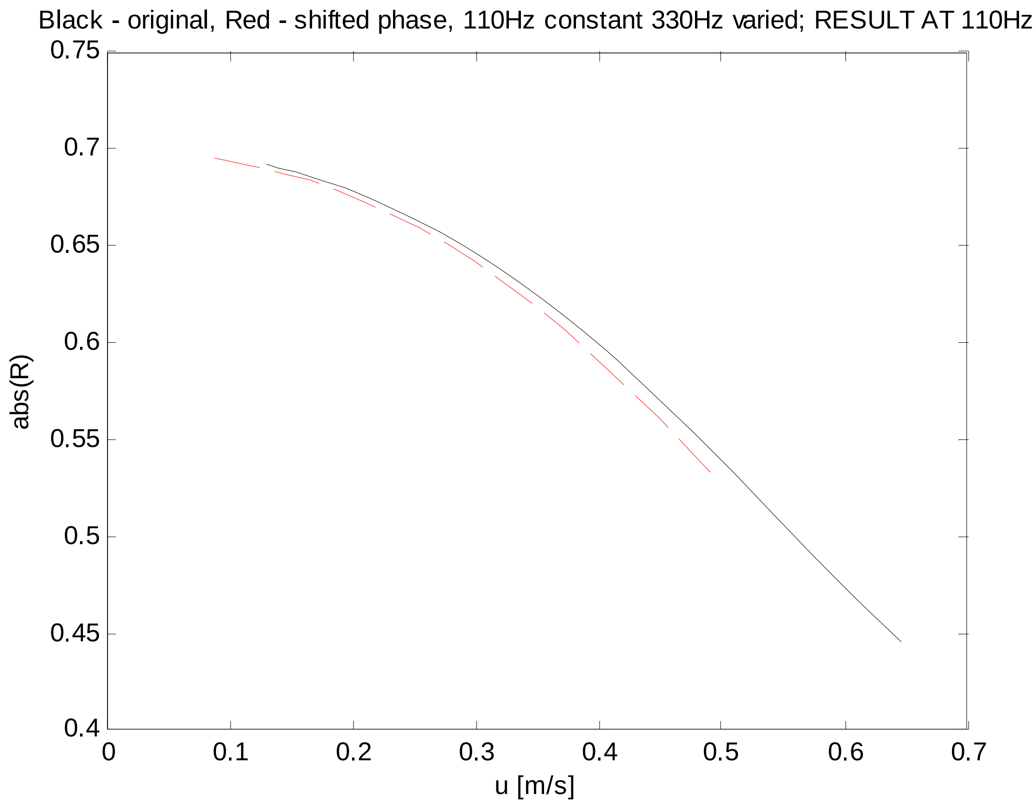
Black - original, Red - shifted phase, 110Hz constant 330Hz varied; RESULT AT 110Hz
abs(R)
u [m/s]
0.75
0.7
0.65
0.6
0.55
0.5
0.45
0.4
0
0.1
0.2
0.3
0.4
0.5
0.6
0.7

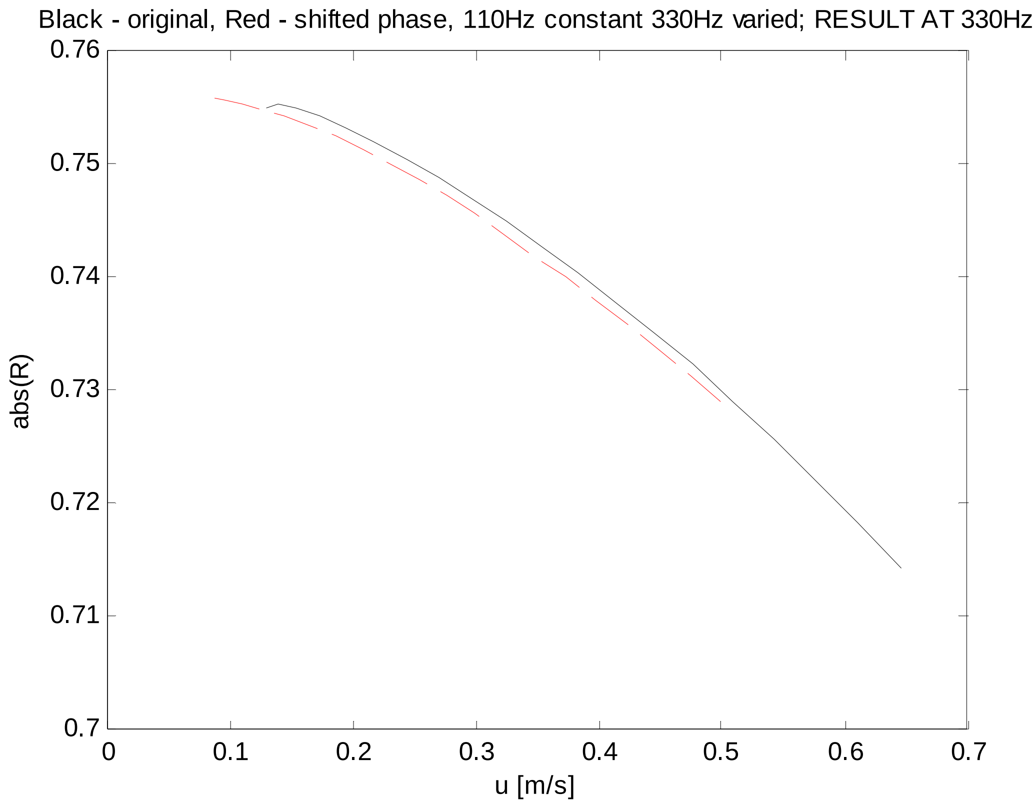
Black - original, Red - shifted phase, 110Hz constant 330Hz varied; RESULT AT 330Hz
abs(R)
u [m/s]
0.76
0.75
0.74
0.73
0.72
0.71
0.7
0
0.1
0.2
0.3
0.4
0.5
0.6
0.7

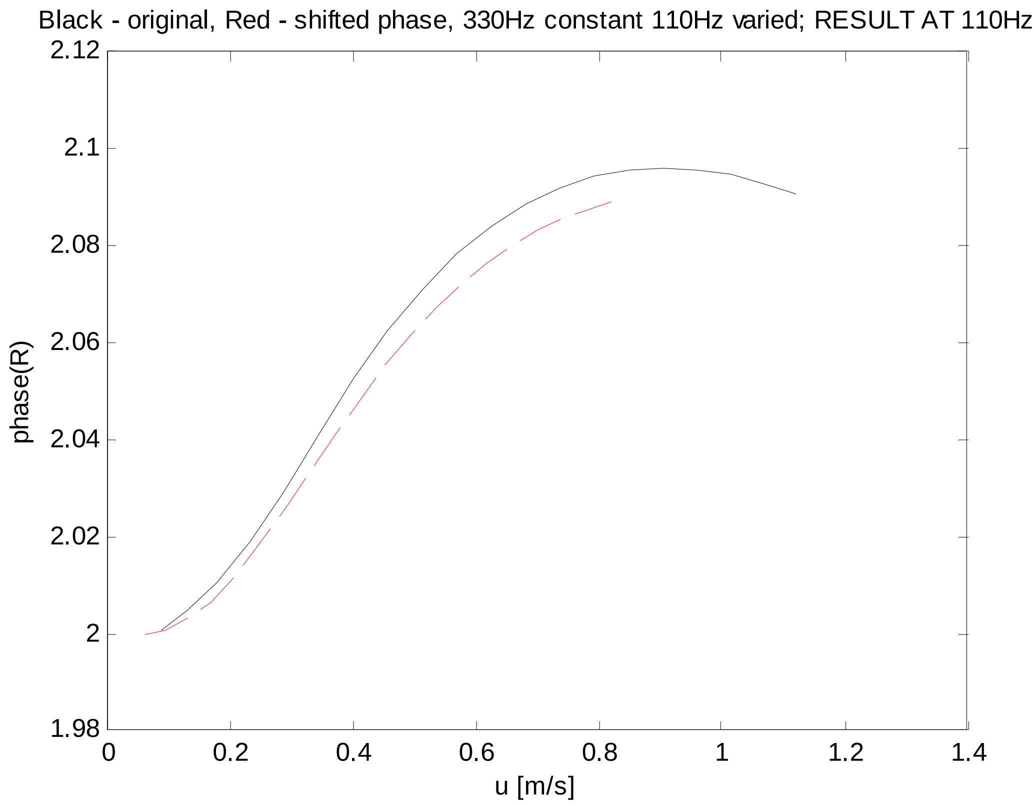
Black - original, Red - shifted phase, 330Hz constant 110Hz varied; RESULT AT 110Hz
phase(R)
u [m/s]
2.12
2.1
2.08
2.06
2.04
2.02
2
1.98
0
0.2
0.4
0.6
0.8
1
1.2
1.4

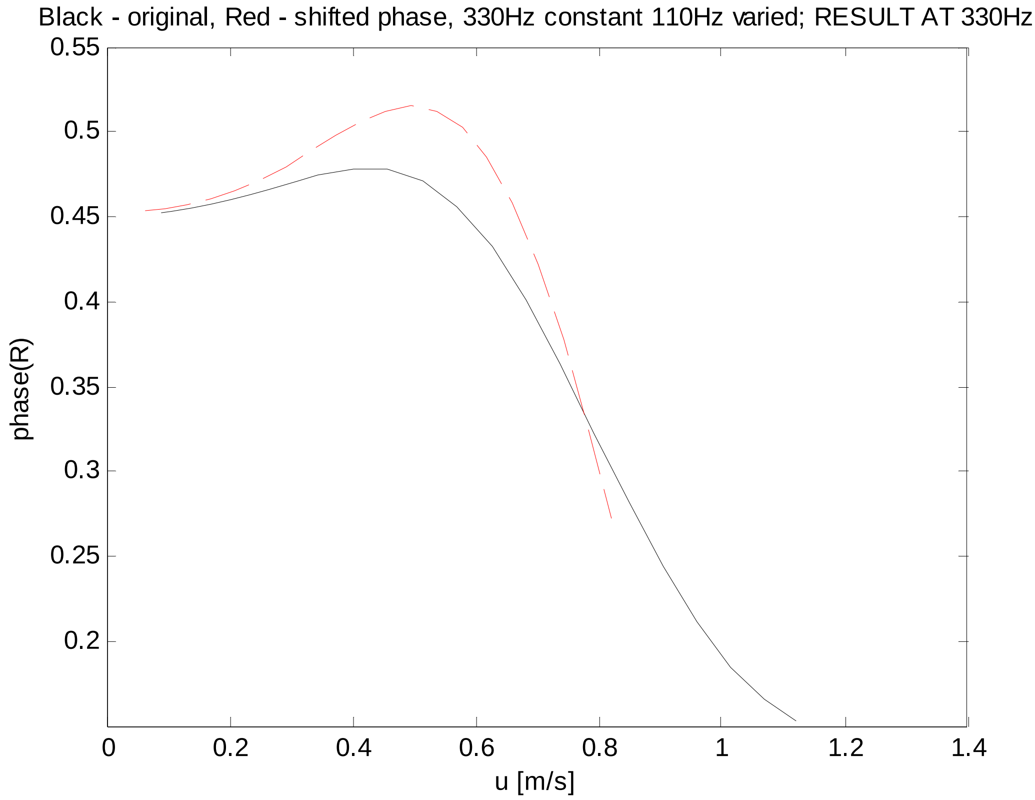
Black - original, Red - shifted phase, 330Hz constant 110Hz varied; RESULT AT 330Hz
phase(R)
u [m/s]
0.55
0.5
0.45
0.4
0.35
0.3
0.25
0.2
0
0.2
0.4
0.6
0.8
1
1.2
1.4

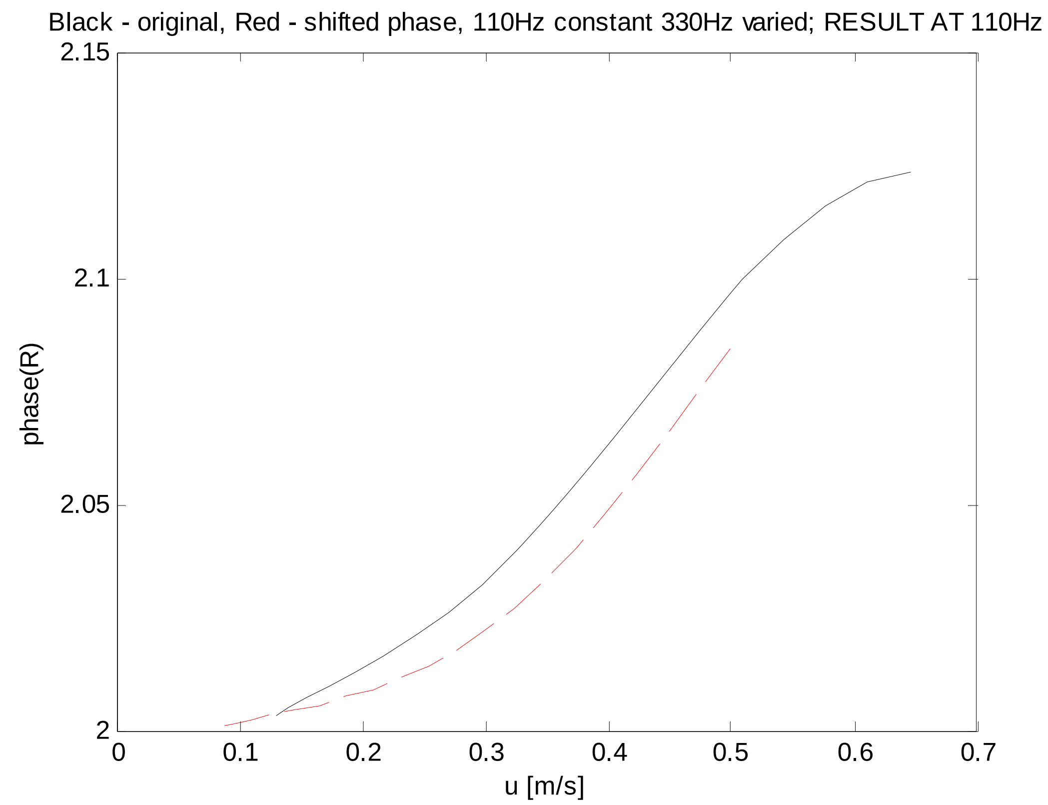

Black - original, Red - shifted phase, 110Hz constant 330Hz varied; RESULT AT 110Hz
phase(R)
u [m/s]
2.15
2.1
2.05
2
0
0.1
0.2
0.3
0.4
0.5
0.6
0.7


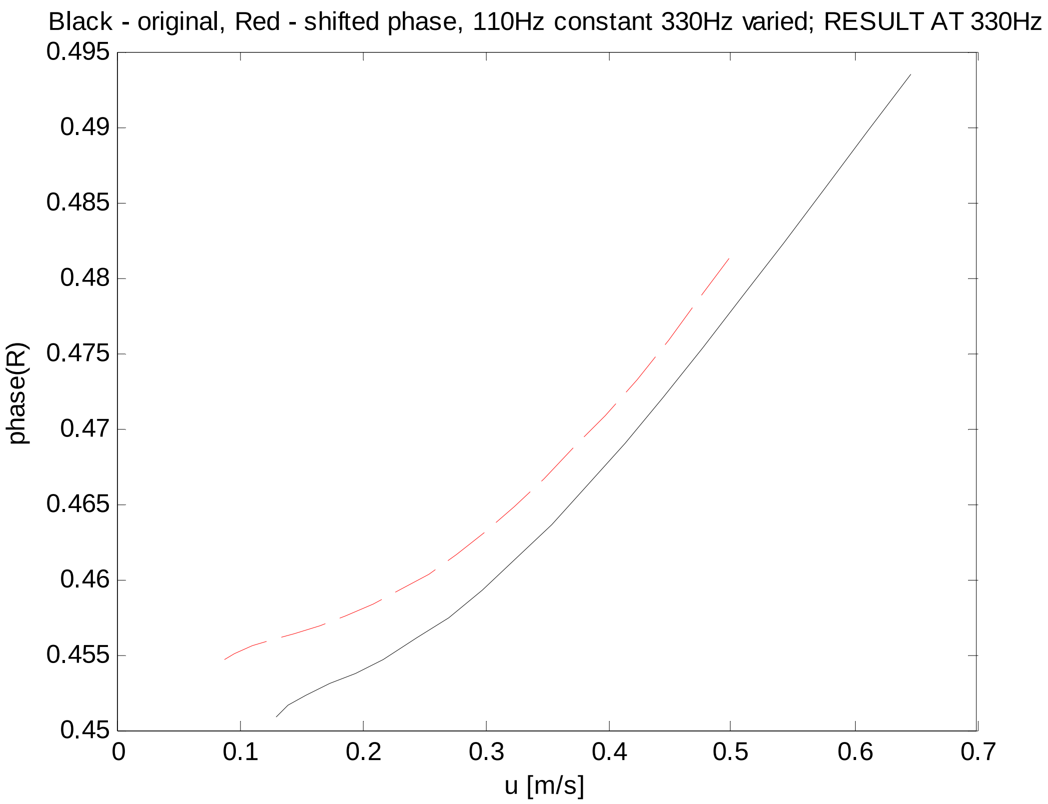

Black - original, Red - shifted phase, 110Hz constant 330Hz varied; RESULT AT 330Hz
phase(R)
u [m/s]
0.495
0.49
0.485
0.48
0.475
0.47
0.465
0.46
0.455
0.45
0
0.1
0.2
0.3
0.4
0.5
0.6
0.7

Black - original, Red - shifted phase, 330Hz constant 110Hz varied; RESULT AT 110Hz

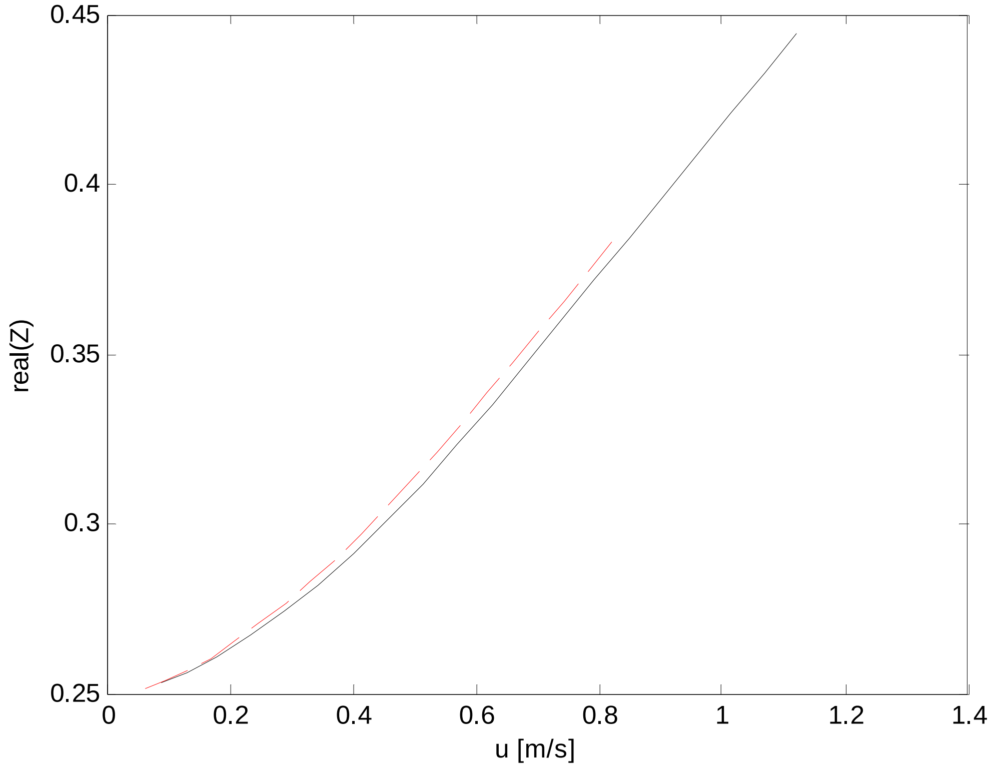


Black - original, Red - shifted phase, 330Hz constant 110Hz varied; RESULT AT 330Hz

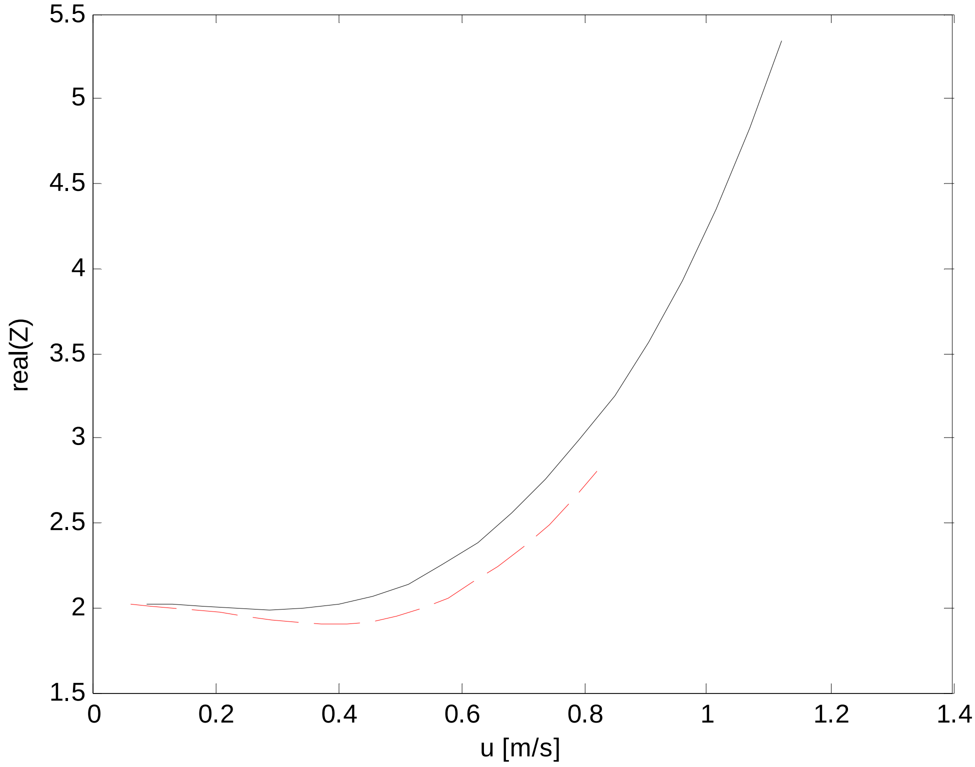

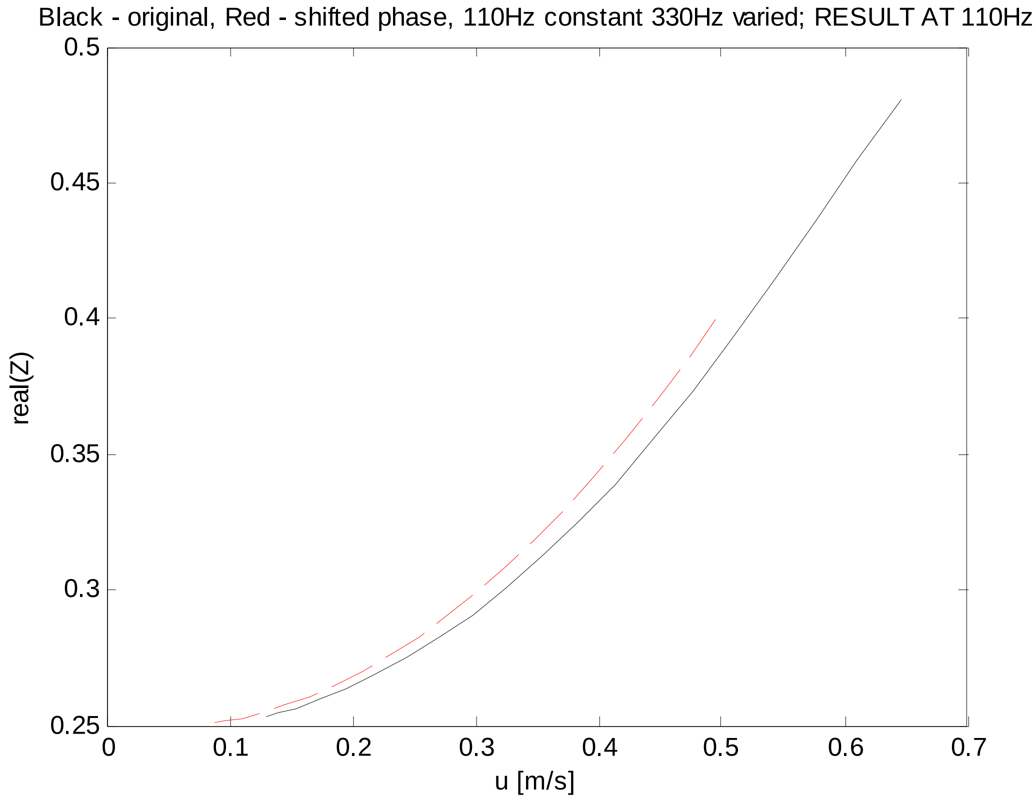
Black - original, Red - shifted phase, 110Hz constant 330Hz varied; RESULT AT 110Hz
real(Z)
u [m/s]
0.5
0.45
0.4
0.35
0.3
0.25
0
0.1
0.2
0.3
0.4
0.5
0.6
0.7

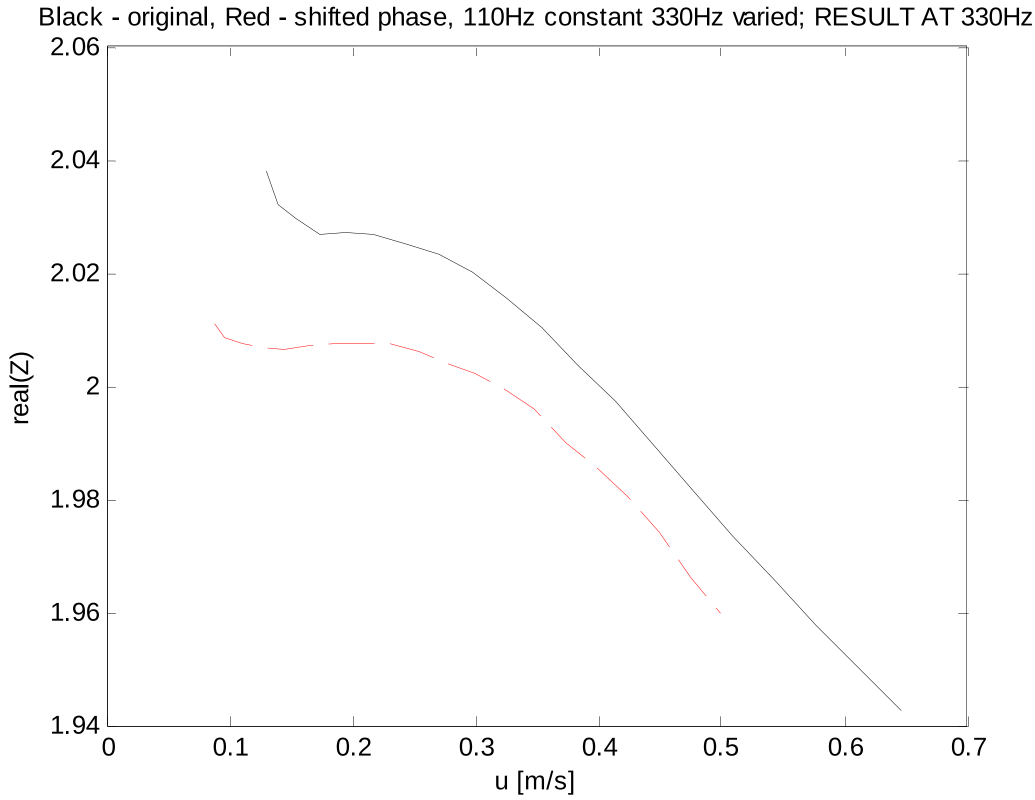
Black - original, Red - shifted phase, 110Hz constant 330Hz varied; RESULT AT 330Hz
real(Z)
u [m/s]
2.06
2.04
2.02
2
1.98
1.96
1.94
0
0.1
0.2
0.3
0.4
0.5
0.6
0.7

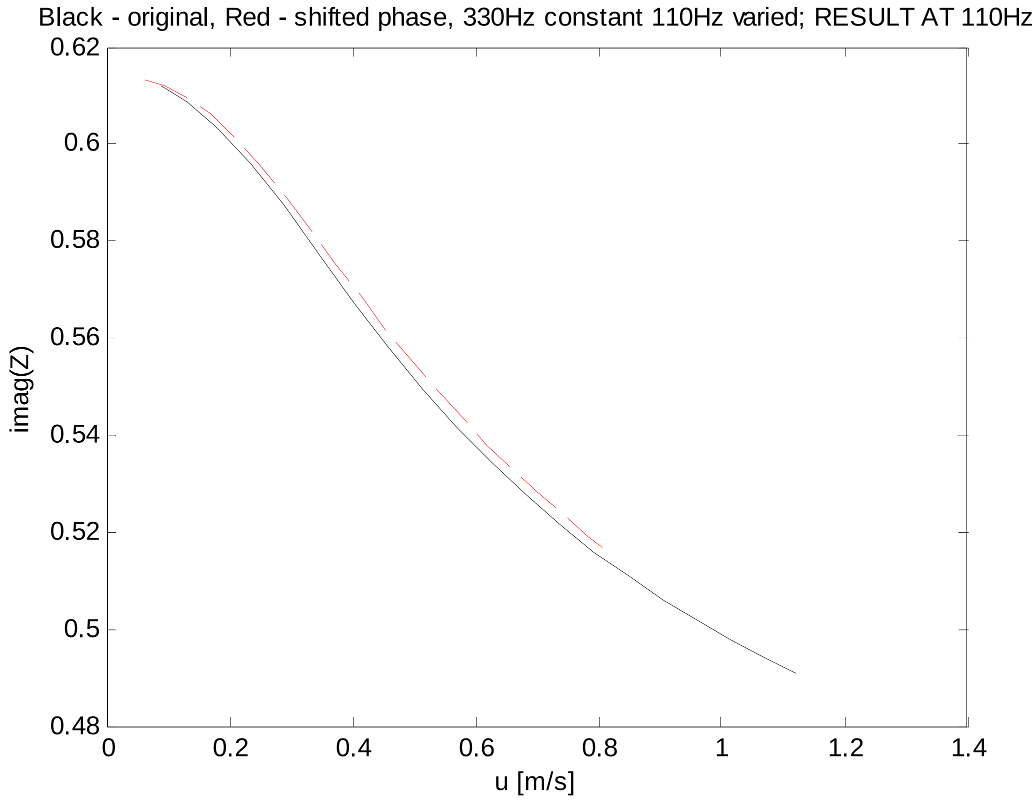
Black - original, Red - shifted phase, 330Hz constant 110Hz varied; RESULT AT 110Hz
imag(Z)
u [m/s]
0.62
0.6
0.58
0.56
0.54
0.52
0.5
0.48
0
0.2
0.4
0.6
0.8
1
1.2
1.4

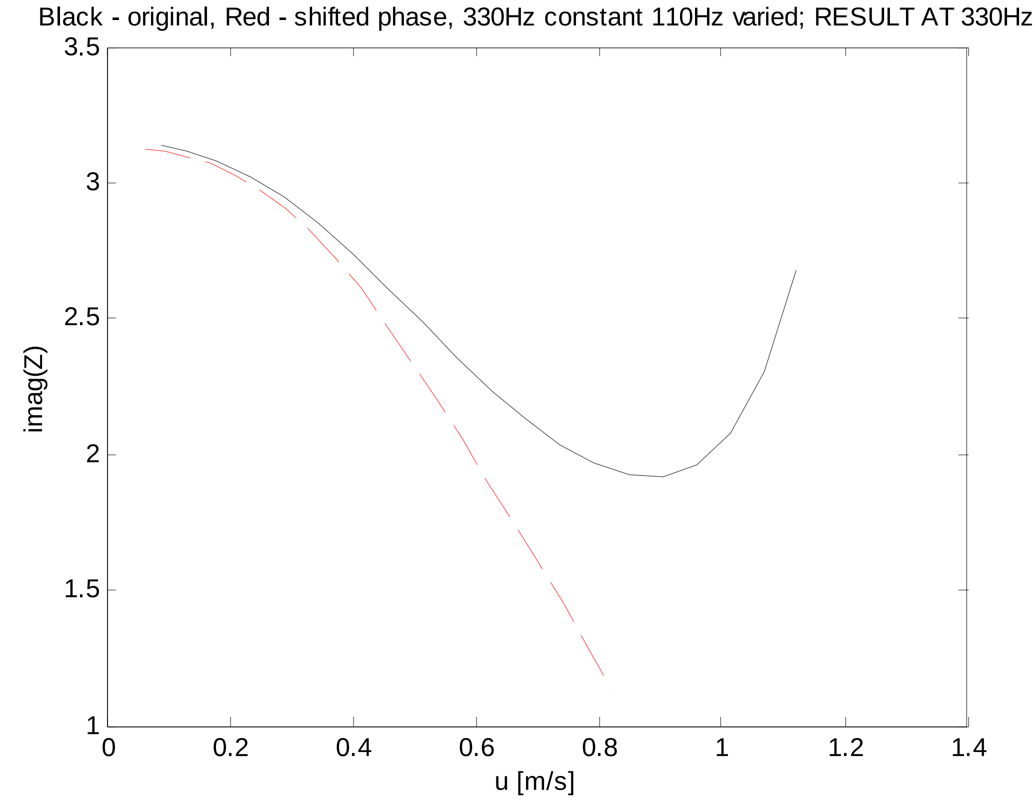
Black - original, Red - shifted phase, 330Hz constant 110Hz varied; RESULT AT 330Hz
imag(Z)
u [m/s]
3.5
3
2.5
2
1.5
1
0
0.2
0.4
0.6
0.8
1
1.2
1.4

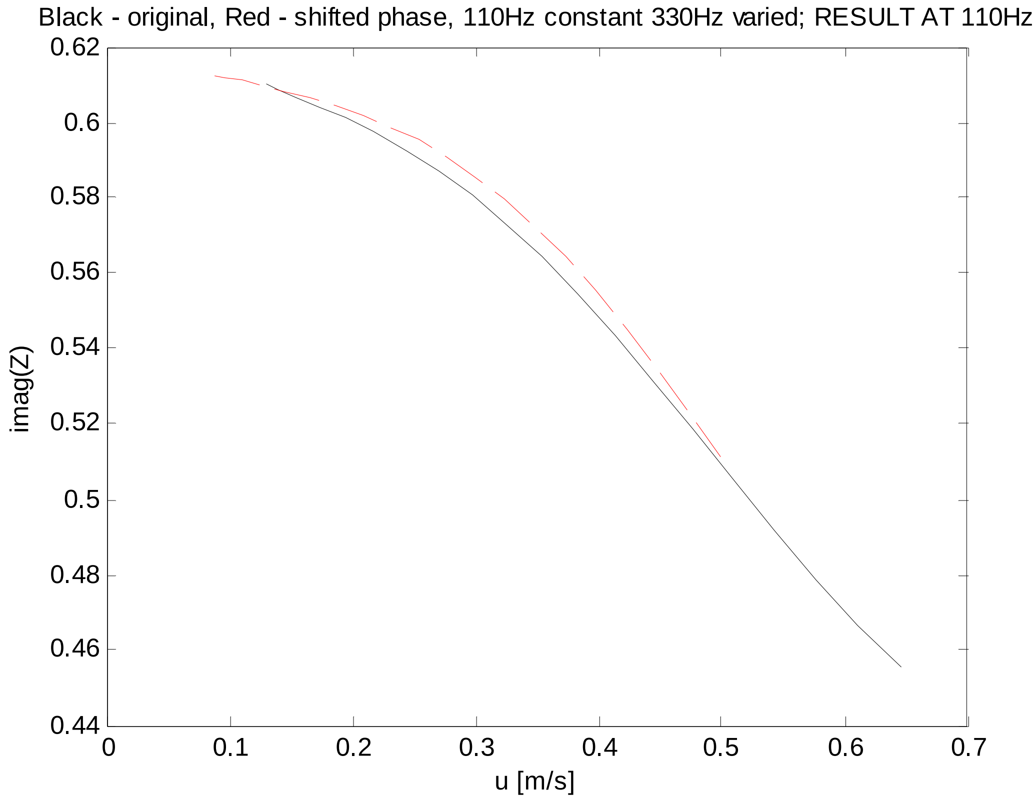
Black - original, Red - shifted phase, 110Hz constant 330Hz varied; RESULT AT 110Hz
0.62
0.6
0.58
0.56
0.54
0.52
0.5
0.48
0.46
0.44
imag(Z)
0
0.1
0.2
0.3
0.4
0.5
0.6
0.7
u [m/s]

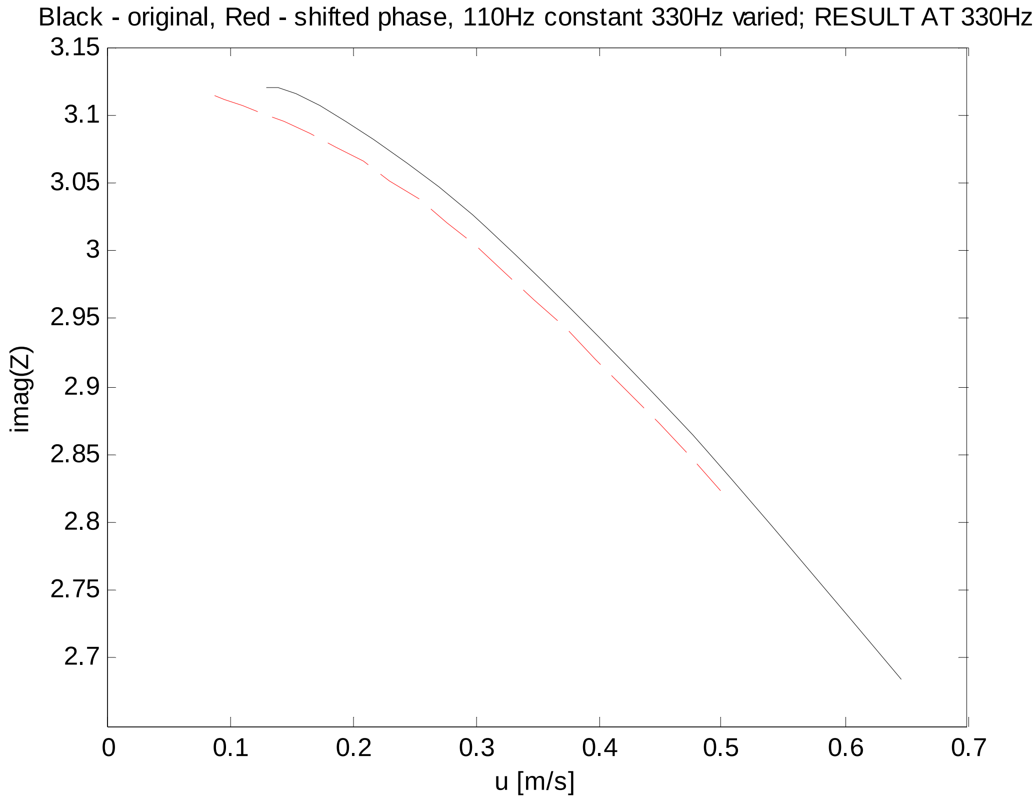
Black - original, Red - shifted phase, 110Hz constant 330Hz varied; RESULT AT 330Hz
3.15
3.1
3.05
3
2.95
2.9
2.85
2.8
2.75
2.7
imag(Z)
0
0.1
0.2
0.3
0.4
0.5
0.6
0.7
u [m/s]

# Attempt to use P-U probe method

A calibration factor which is independent of frequency could not be found by making two measurements with both methods on the same setup. The relation of acoustic impedance for two methods varied very much with changing excitation level according to following plots.

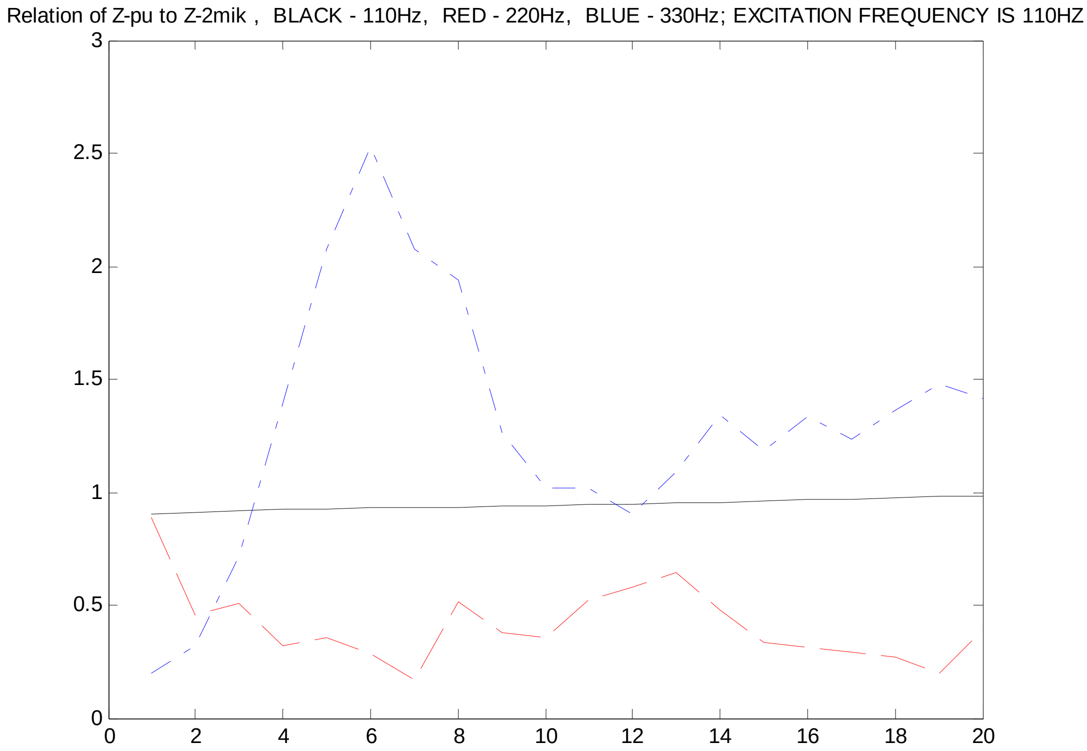

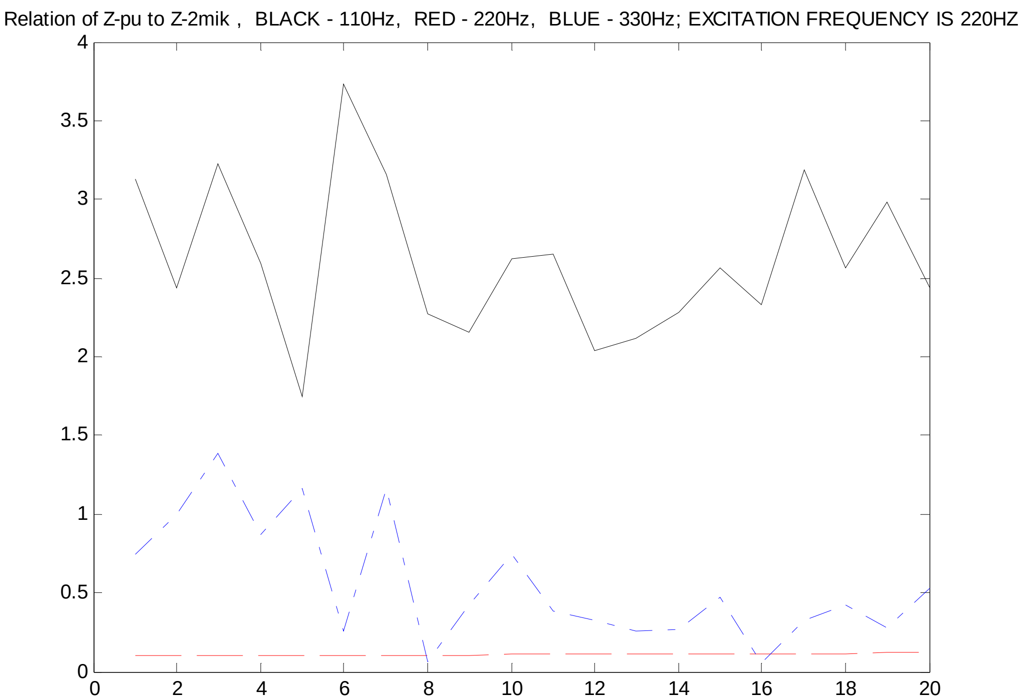


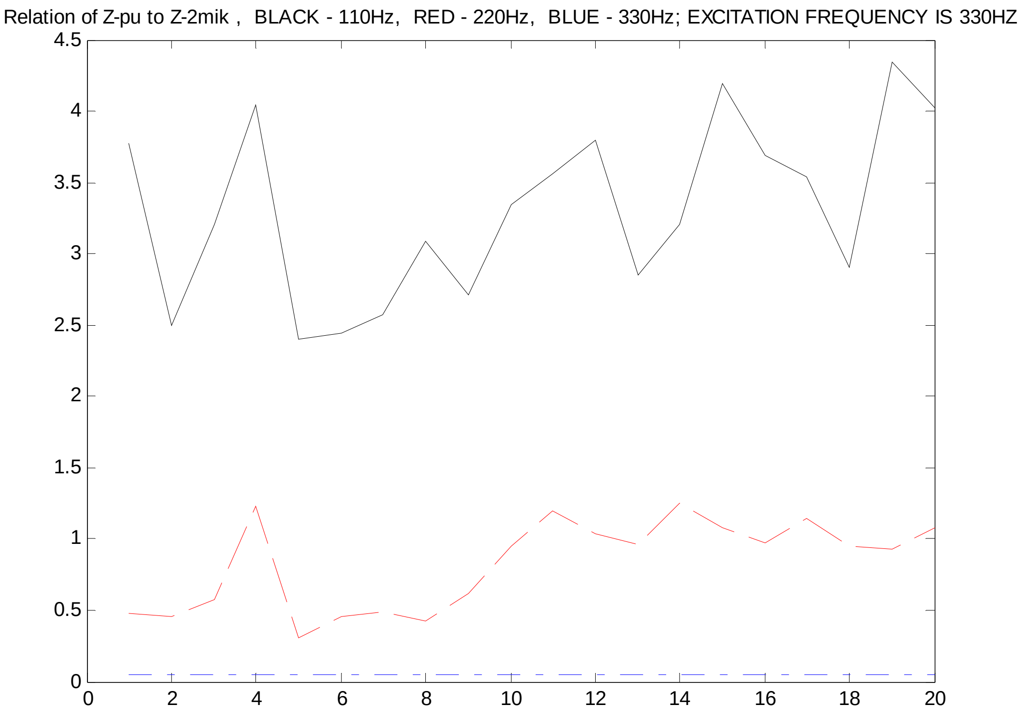


As can be seen the relation is quite constant at frequency which is the same as excitation frequency. By this conclusion a calibration factor consisting of parts for each frequency of interest could be calculated. Using that factor the following plots of acoustic properties for sample P4 measured with PU-method could be made. Here follows plots of comparison of same setup measured with both methods where the PU-probe was calibrated using data from the two-microphone method. The curves are quite similar except for the absolute value of the reflection coefficient, where abs(R) is increasing with increased sound level for the PU-method while it was decreasing for two-microphone method.

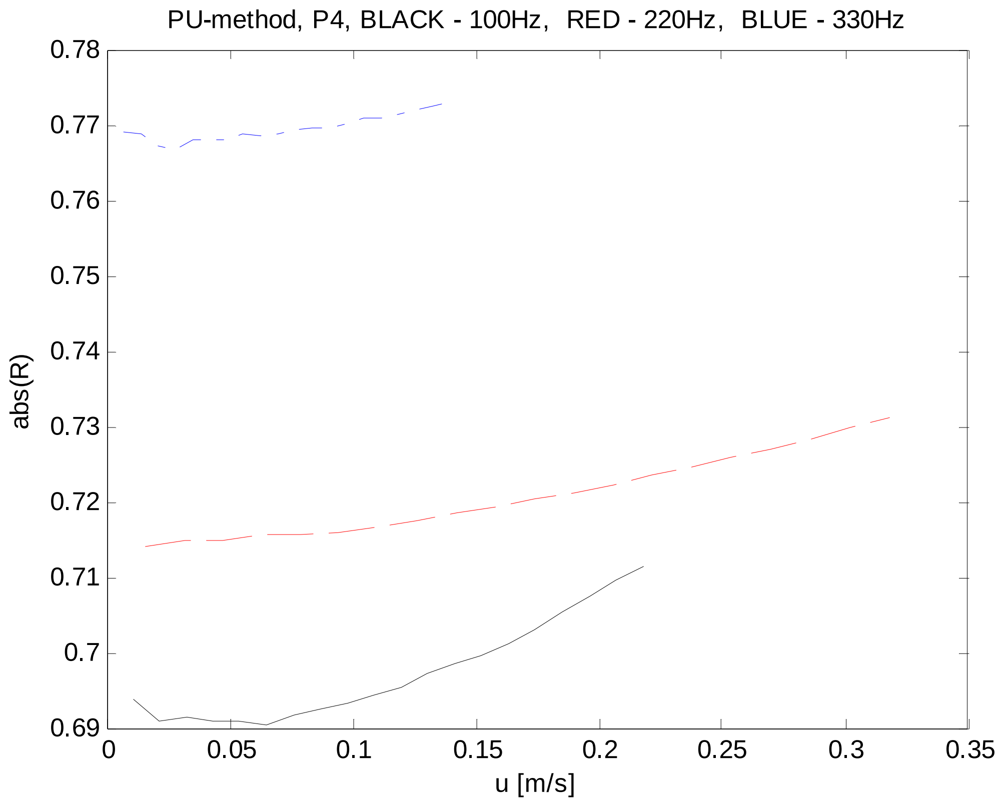


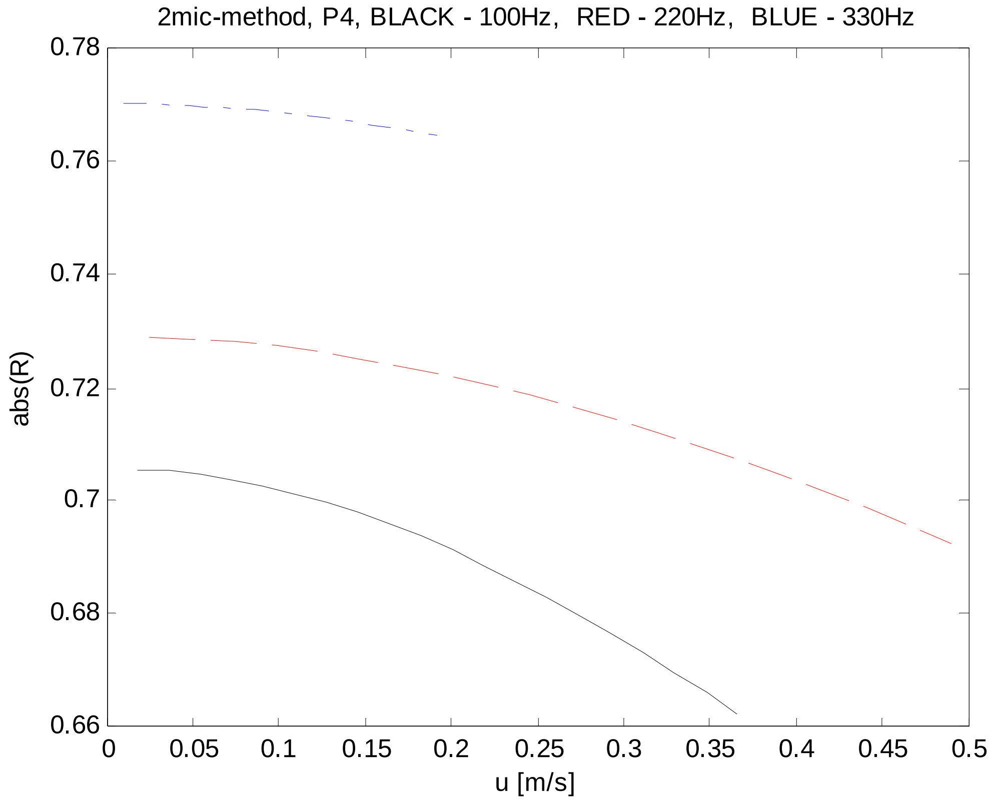

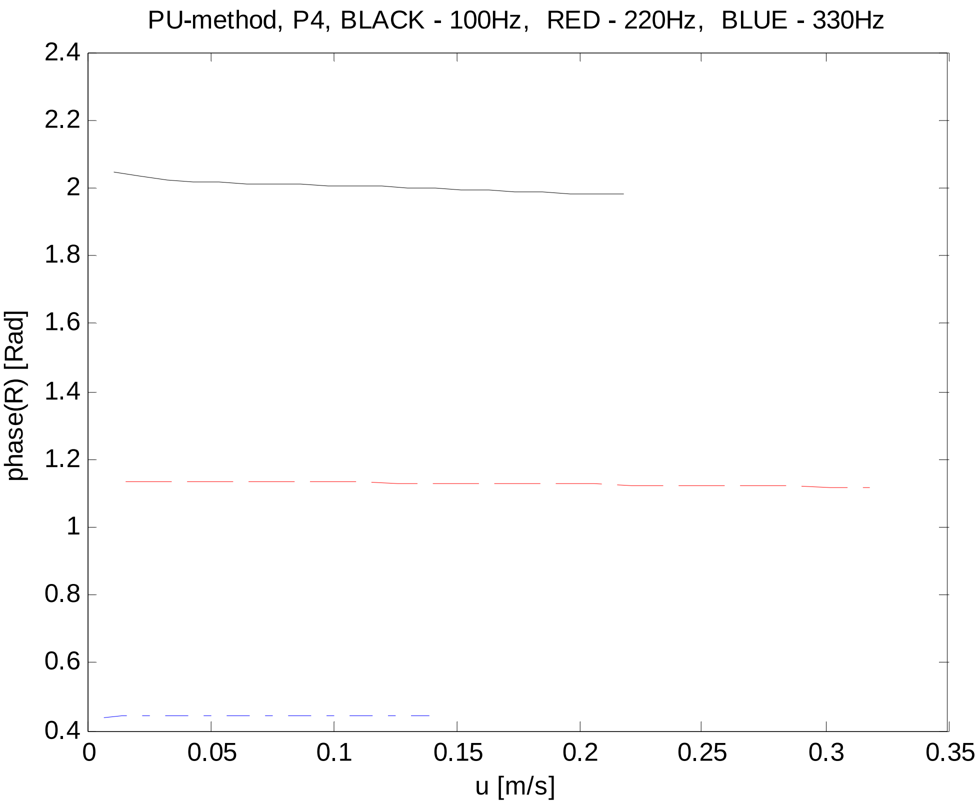
PU-method, P4, BLACK - 100Hz, RED - 220Hz, BLUE - 330Hz
phase(R) [Rad]
2.4
2.2
2
1.8
1.6
1.4
1.2
1
0.8
0.6
0.4
0
0.05
0.1
0.15
0.2
0.25
0.3
0.35
u [m/s]

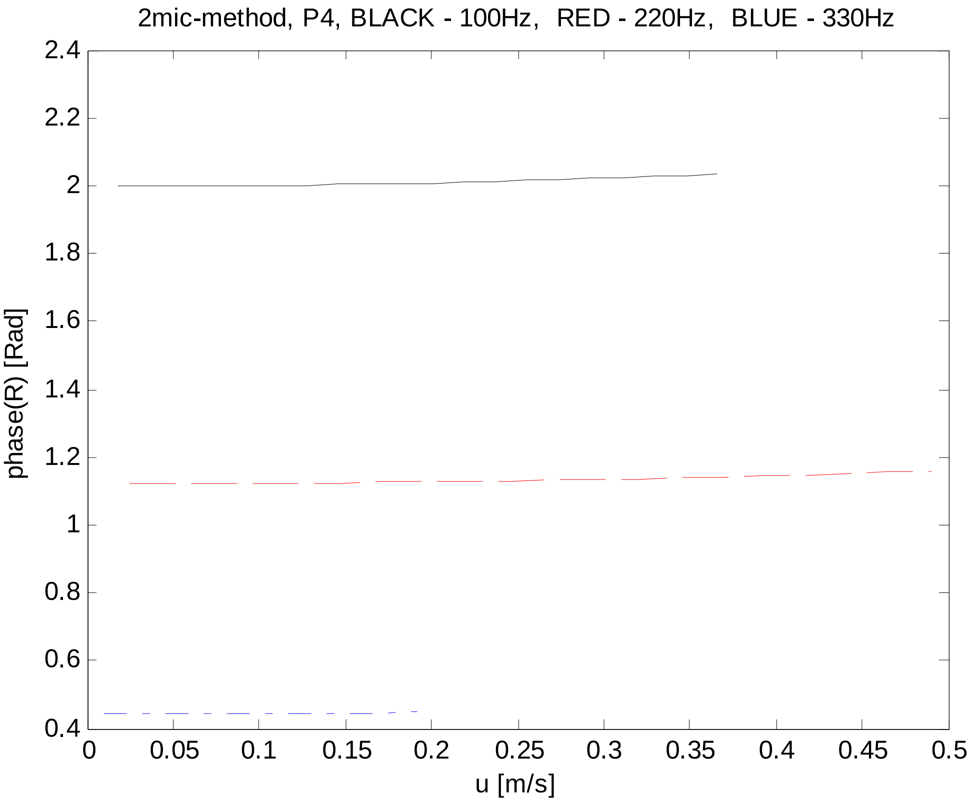
2mic-method, P4, BLACK - 100Hz, RED - 220Hz, BLUE - 330Hz
phase(R) [Rad]
2.4
2.2
2
1.8
1.6
1.4
1.2
1
0.8
0.6
0.4
0
0.05
0.1
0.15
0.2
0.25
0.3
0.35
0.4
0.45
0.5
u [m/s]

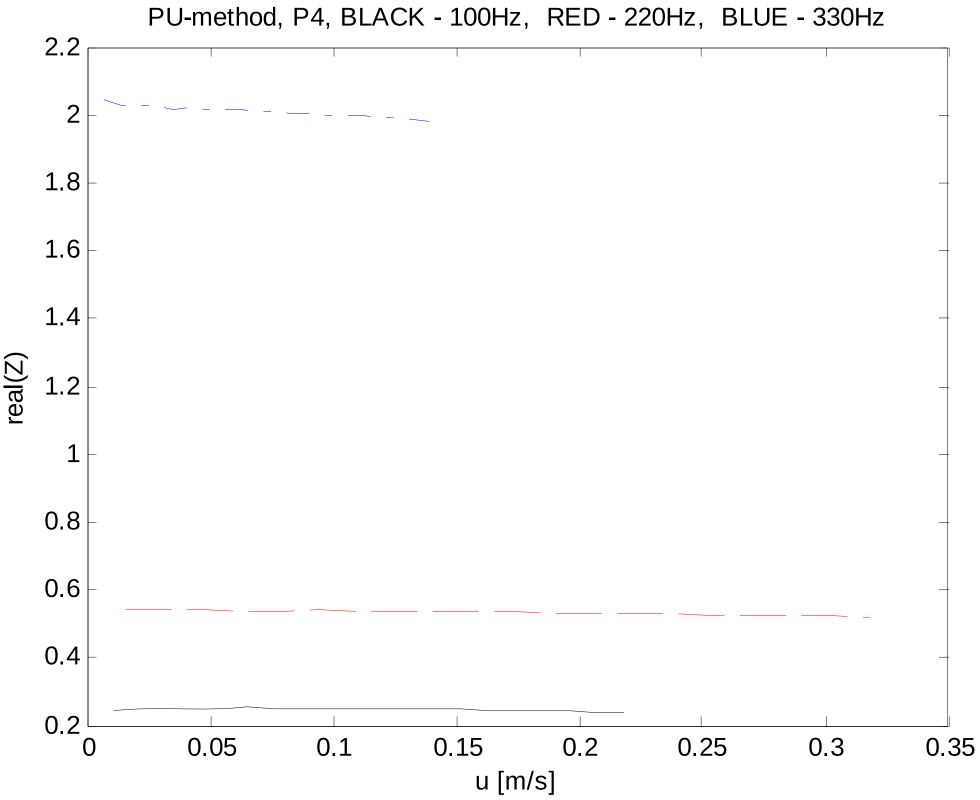
PU-method, P4, BLACK - 100Hz, RED - 220Hz, BLUE - 330Hz
real(Z)
u [m/s]

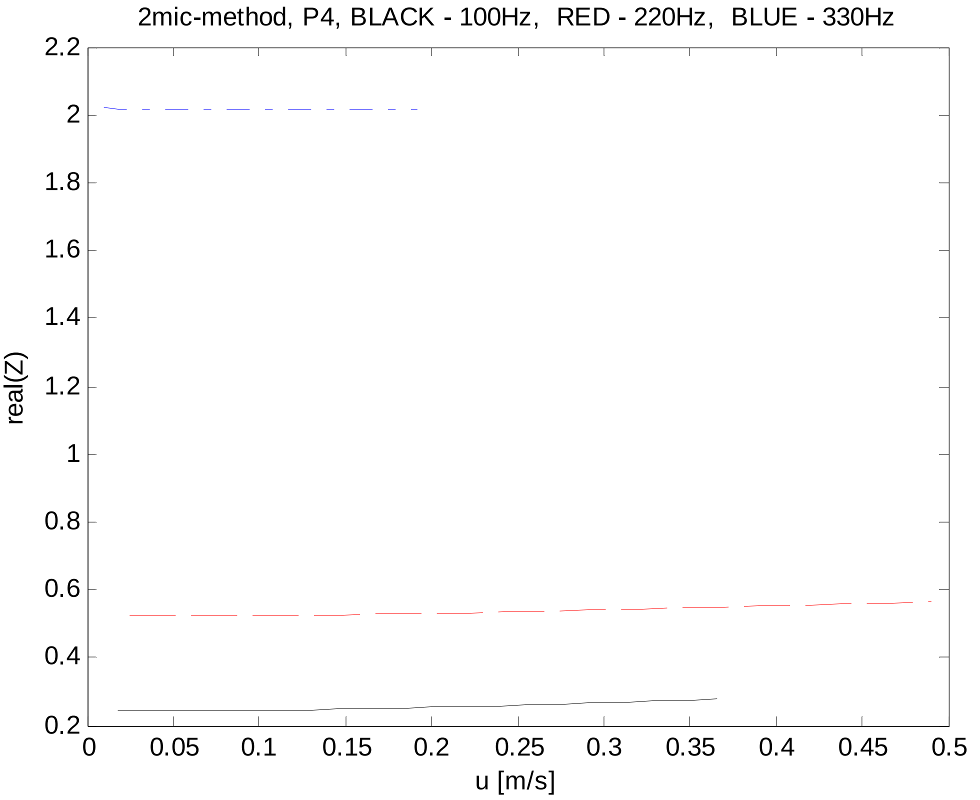
2mic-method, P4, BLACK - 100Hz, RED - 220Hz, BLUE - 330Hz
real(Z)
u [m/s]

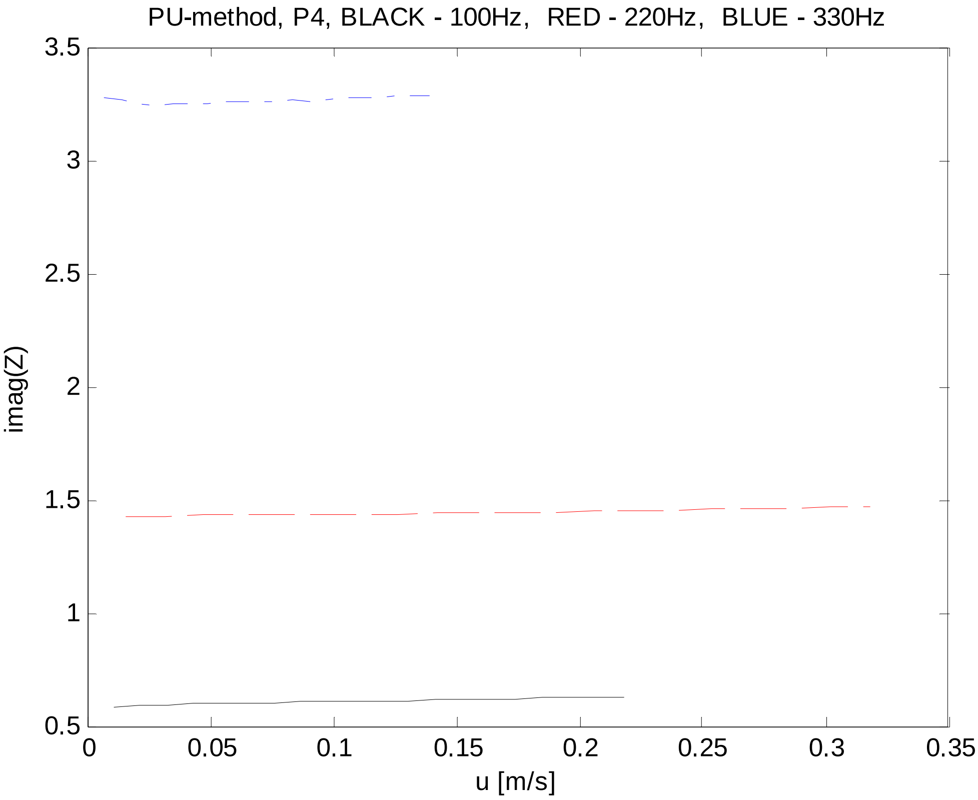
PU-method, P4, BLACK - 100Hz, RED - 220Hz, BLUE - 330Hz
imag(Z)
u [m/s]
3.5
3
2.5
2
1.5
1
0.5
0
0.05
0.1
0.15
0.2
0.25
0.3
0.35

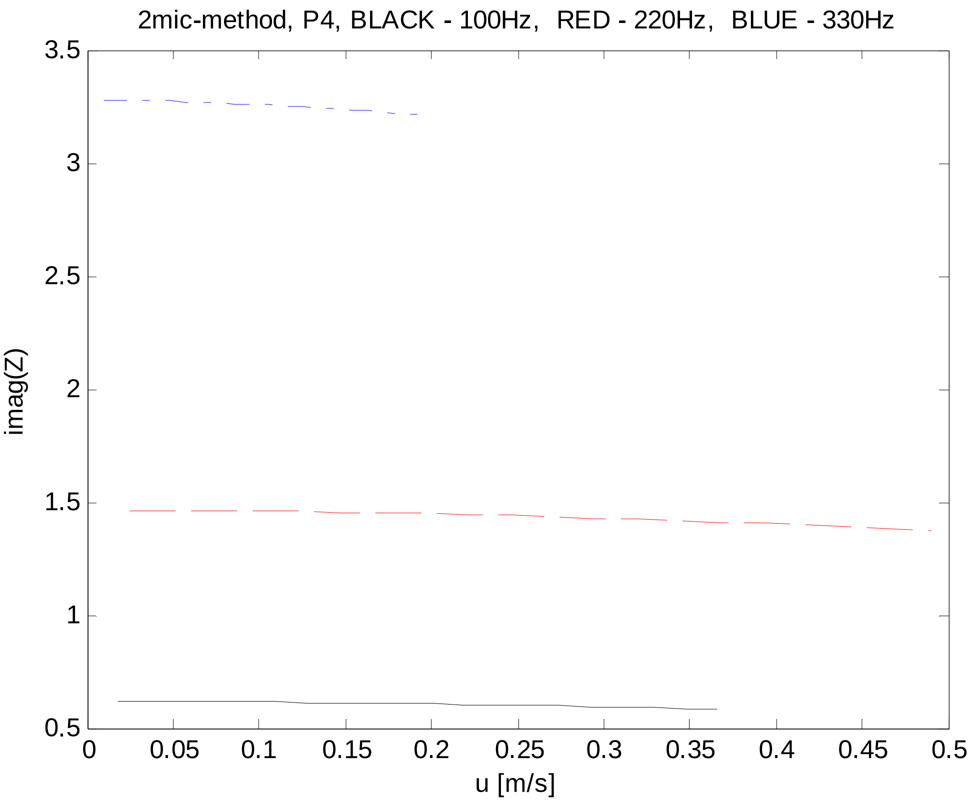
2mic-method, P4, BLACK - 100Hz, RED - 220Hz, BLUE - 330Hz
imag(Z)
u [m/s]
3.5
3
2.5
2
1.5
1
0.5
0
0.05
0.1
0.15
0.2
0.25
0.3
0.35
0.4
0.45
0.5

However, the calibration factor produced in this way was only good for the same sample which was used for factor calculation. Applied on other samples it is producing results which are completely different from the results received with the two-microphone method. Here are plots comparing two methods for samples P2 and P3.

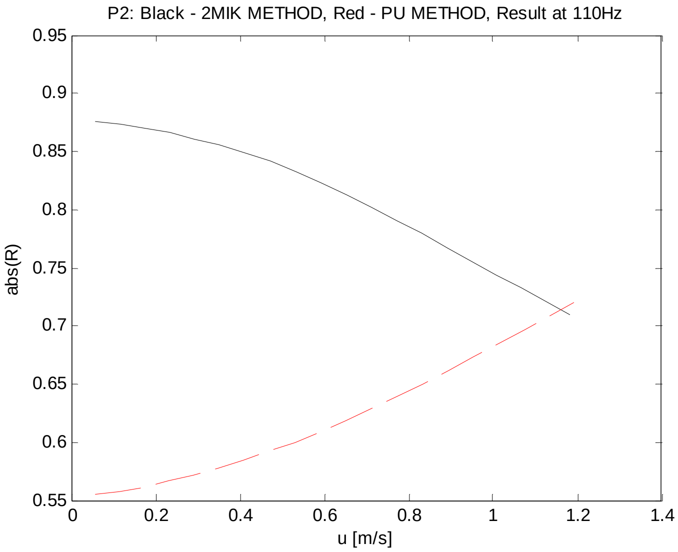


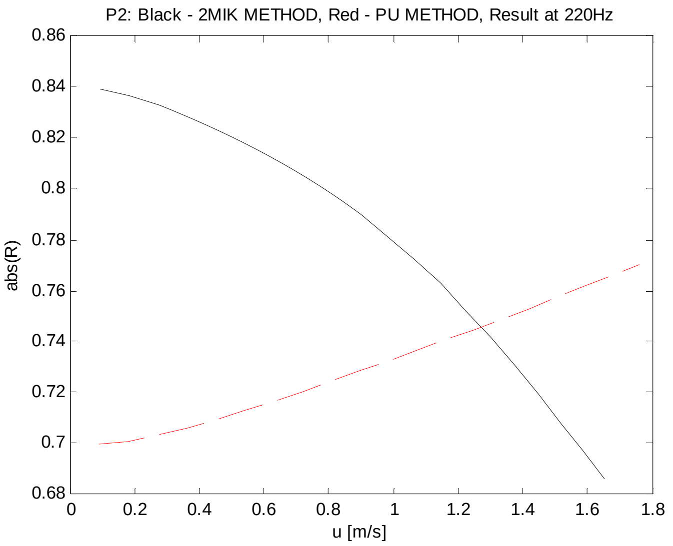


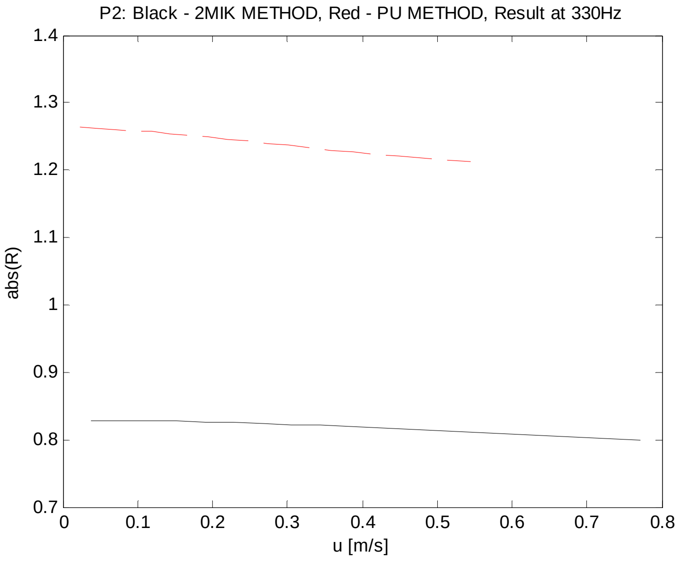

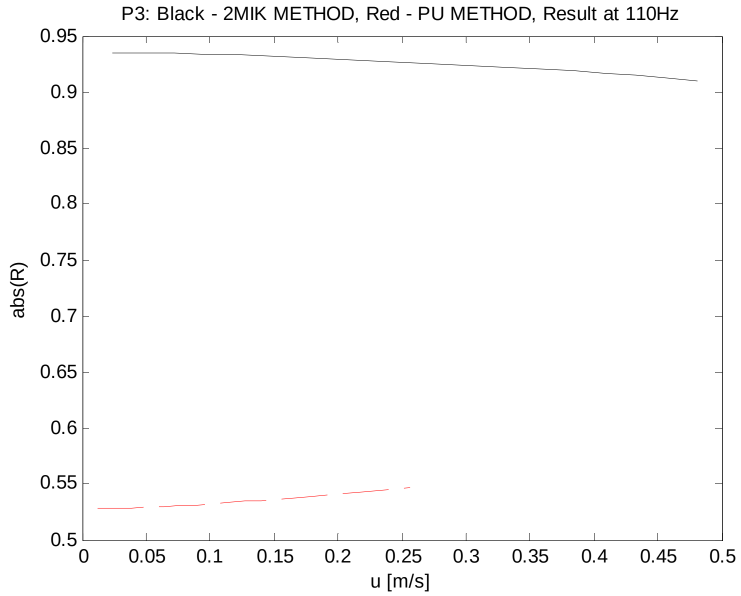
P3: Black - 2MIK METHOD, Red - PU METHOD, Result at 110Hz
abs(R)
u [m/s]
0.95
0.9
0.85
0.8
0.75
0.7
0.65
0.6
0.55
0.5
0
0.05
0.1
0.15
0.2
0.25
0.3
0.35
0.4
0.45
0.5

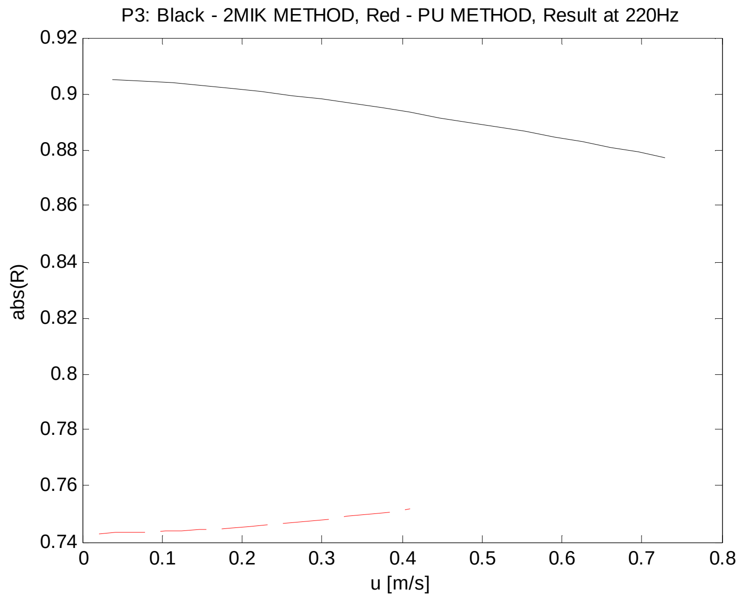
P3: Black - 2MIK METHOD, Red - PU METHOD, Result at 220Hz
abs(R)
u [m/s]
0.92
0.9
0.88
0.86
0.84
0.82
0.8
0.78
0.76
0.74
0
0.1
0.2
0.3
0.4
0.5
0.6
0.7
0.8

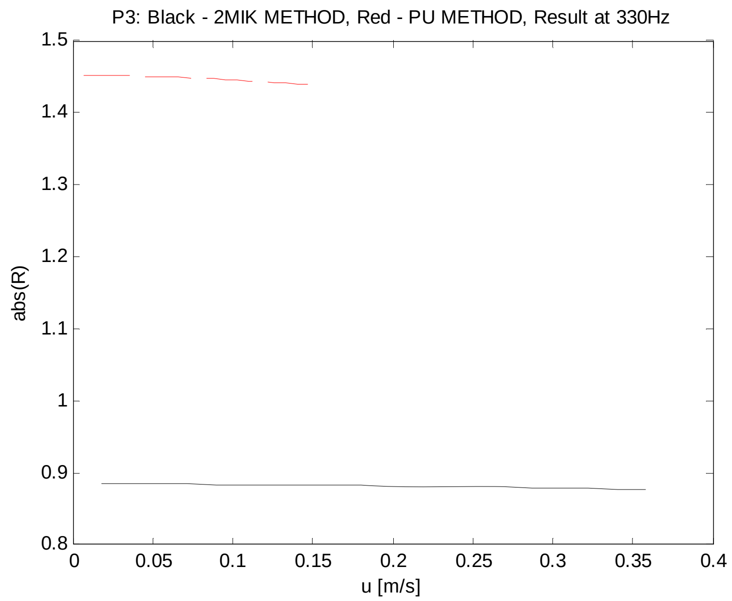
P3: Black - 2MIK METHOD, Red - PU METHOD, Result at 330Hz
abs(R)
u [m/s]
1.5
1.4
1.3
1.2
1.1
1
0.9
0.8
0
0.05
0.1
0.15
0.2
0.25
0.3
0.35
0.4

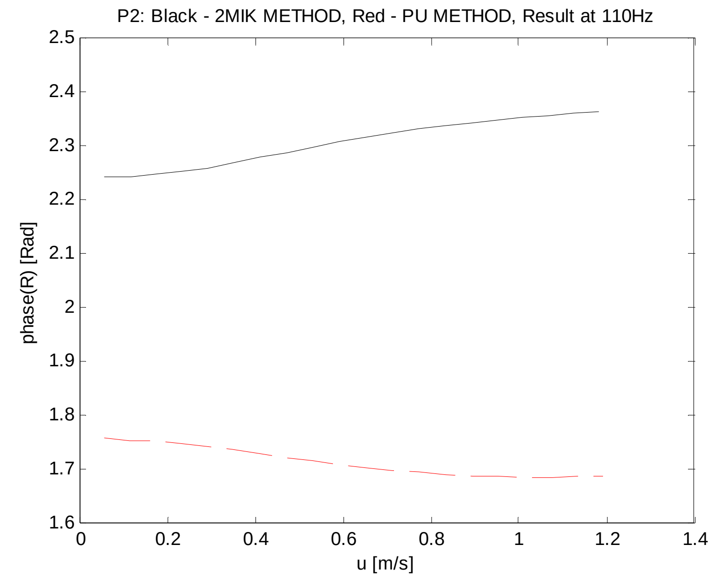
P2: Black - 2MIK METHOD, Red - PU METHOD, Result at 110Hz
phase(R) [Rad]
u [m/s]

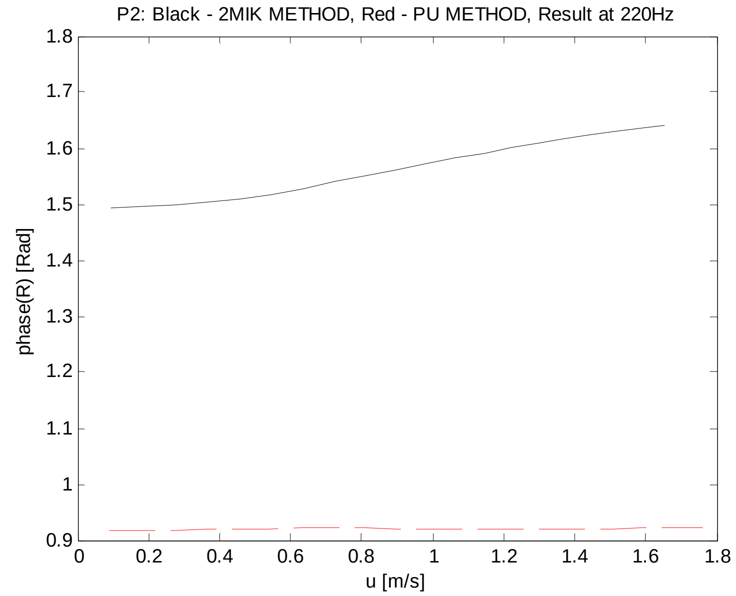
P2: Black - 2MIK METHOD, Red - PU METHOD, Result at 220Hz
phase(R) [Rad]
u [m/s]

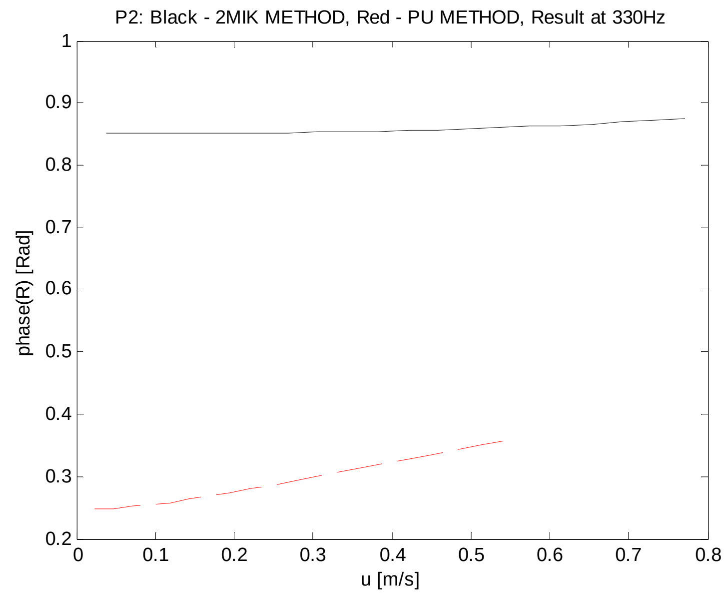
P2: Black - 2MIK METHOD, Red - PU METHOD, Result at 330Hz
phase(R) [Rad]
u [m/s]

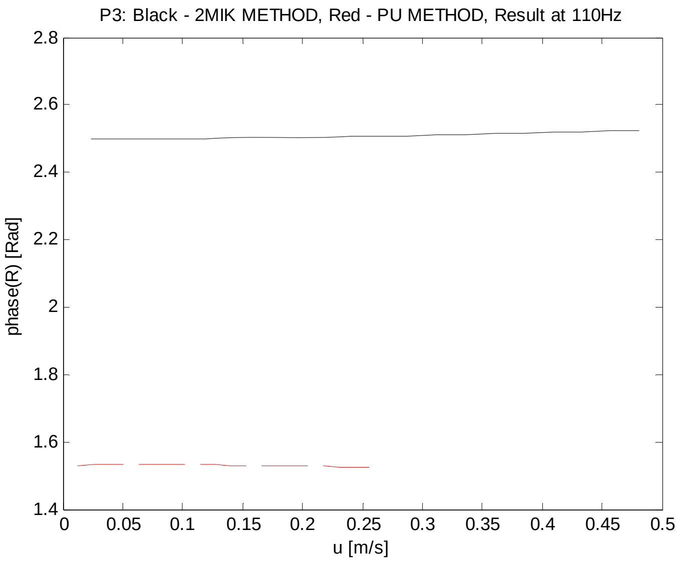
P3: Black - 2MIK METHOD, Red - PU METHOD, Result at 110Hz
phase(R) [Rad]
u [m/s]
2.8
2.6
2.4
2.2
2
1.8
1.6
1.4
0
0.05
0.1
0.15
0.2
0.25
0.3
0.35
0.4
0.45
0.5

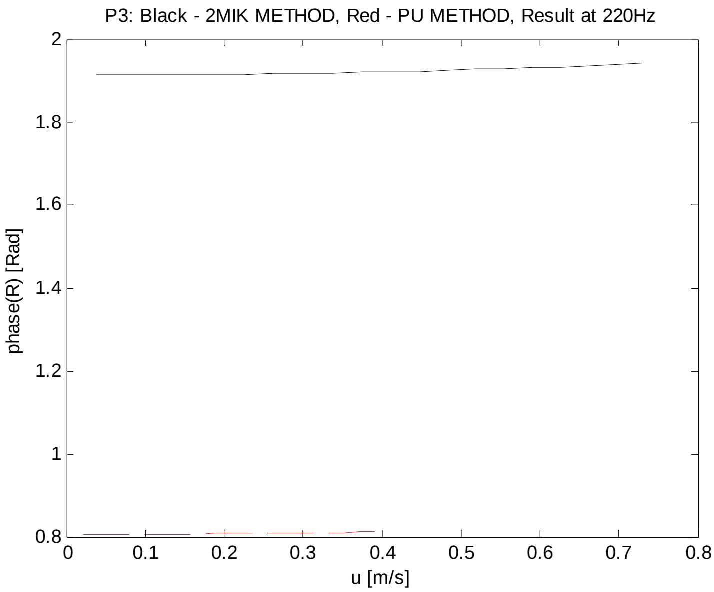
P3: Black - 2MIK METHOD, Red - PU METHOD, Result at 220Hz
phase(R) [Rad]
u [m/s]
2
1.8
1.6
1.4
1.2
1
0.8
0
0.1
0.2
0.3
0.4
0.5
0.6
0.7
0.8

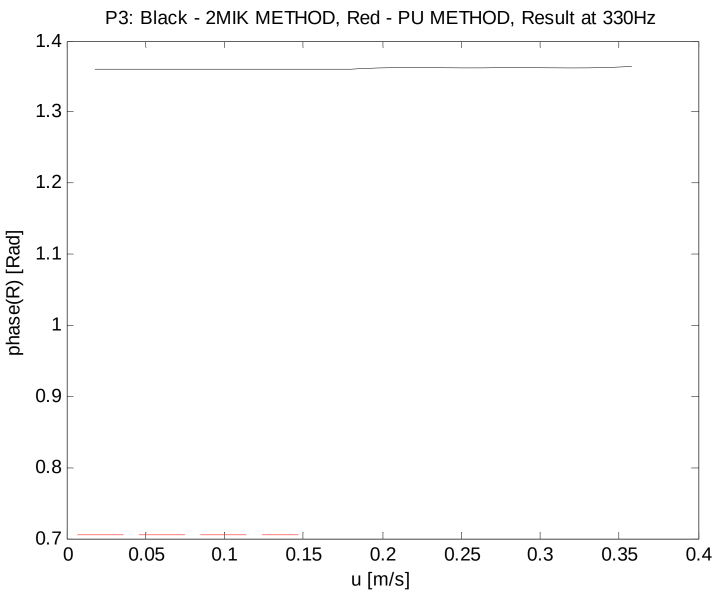
P3: Black - 2MIK METHOD, Red - PU METHOD, Result at 330Hz
phase(R) [Rad]
u [m/s]
1.4
1.3
1.2
1.1
1
0.9
0.8
0.7
0
0.05
0.1
0.15
0.2
0.25
0.3
0.35
0.4

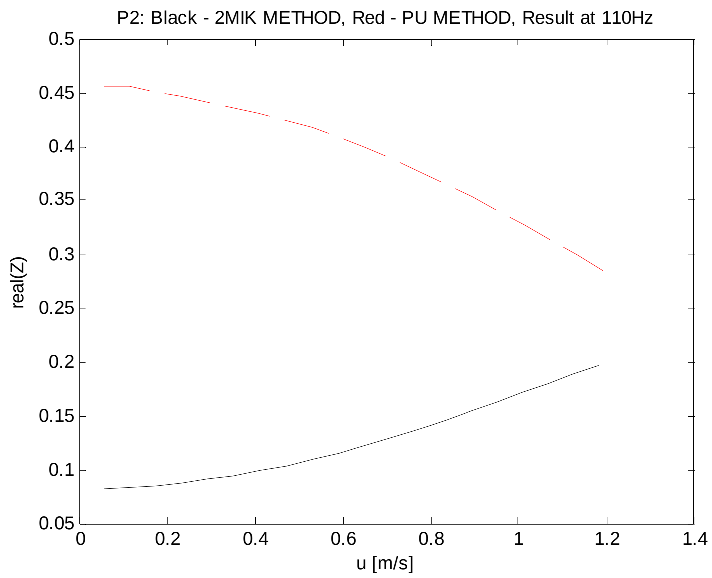
P2: Black - 2MIK METHOD, Red - PU METHOD, Result at 110Hz
real(Z)
u [m/s]
0.5
0.45
0.4
0.35
0.3
0.25
0.2
0.15
0.1
0.05
0
0.2
0.4
0.6
0.8
1
1.2
1.4

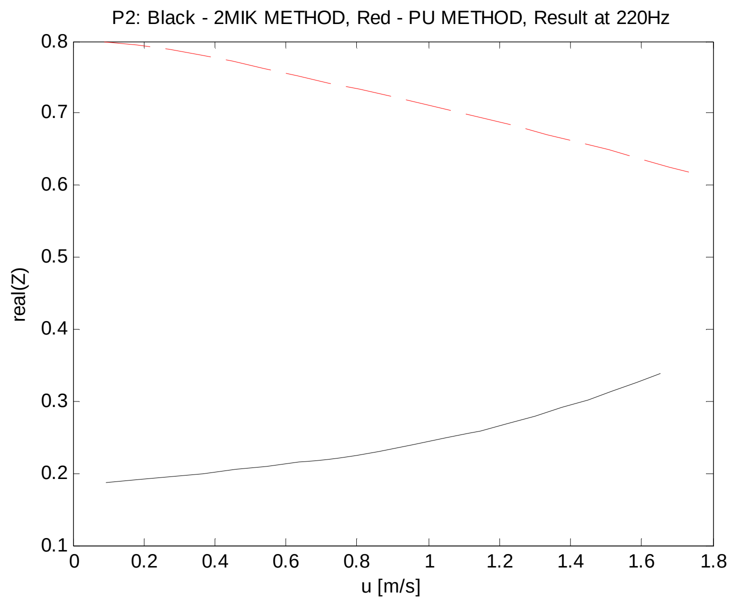
P2: Black - 2MIK METHOD, Red - PU METHOD, Result at 220Hz
real(Z)
u [m/s]
0.8
0.7
0.6
0.5
0.4
0.3
0.2
0.1
0
0.2
0.4
0.6
0.8
1
1.2
1.4
1.6
1.8

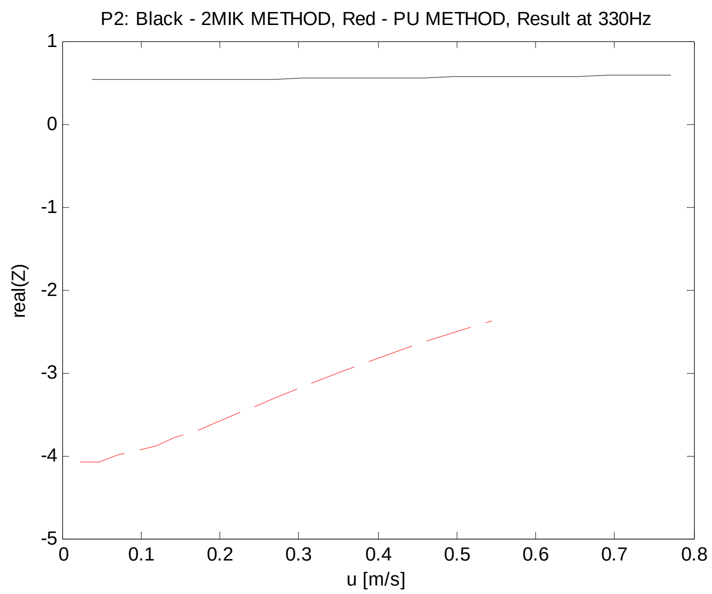
P2: Black - 2MIK METHOD, Red - PU METHOD, Result at 330Hz
real(Z)
u [m/s]
1
0
-1
-2
-3
-4
-5
0
0.1
0.2
0.3
0.4
0.5
0.6
0.7
0.8

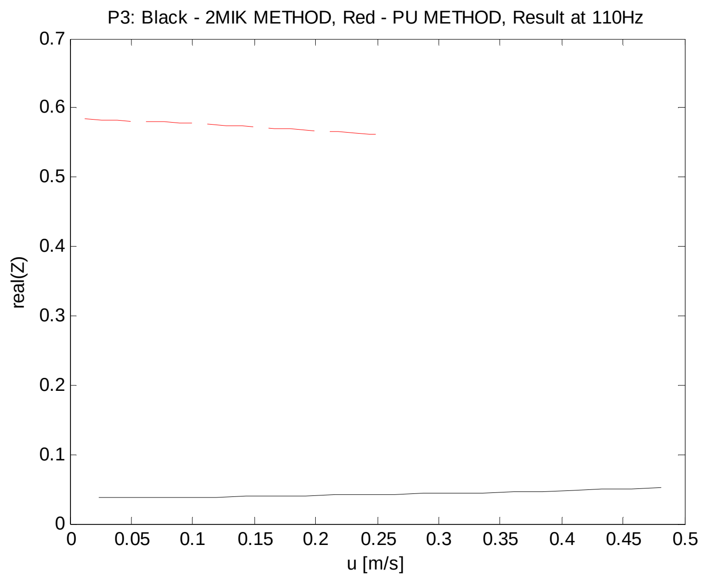
P3: Black - 2MIK METHOD, Red - PU METHOD, Result at 110Hz
real(Z)
u [m/s]
0
0.1
0.2
0.3
0.4
0.5
0.6
0.7
0.05
0.15
0.25
0.35
0.45

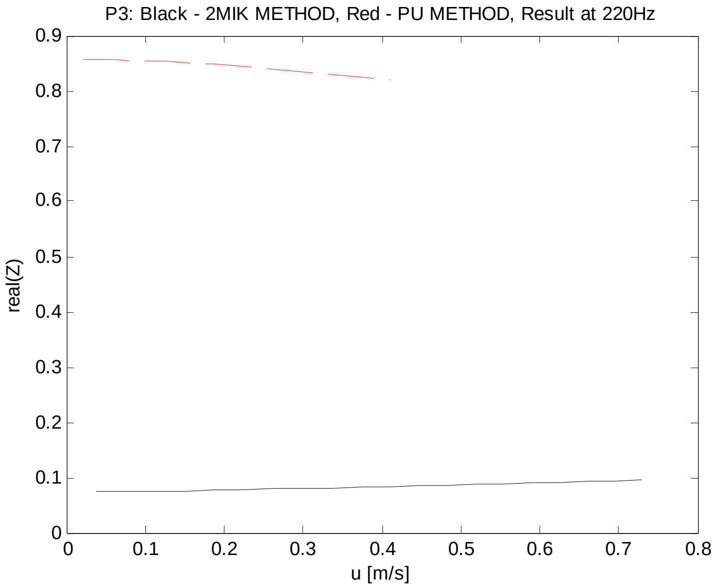
P3: Black - 2MIK METHOD, Red - PU METHOD, Result at 220Hz
real(Z)
u [m/s]
0
0.1
0.2
0.3
0.4
0.5
0.6
0.7
0.8
0.9

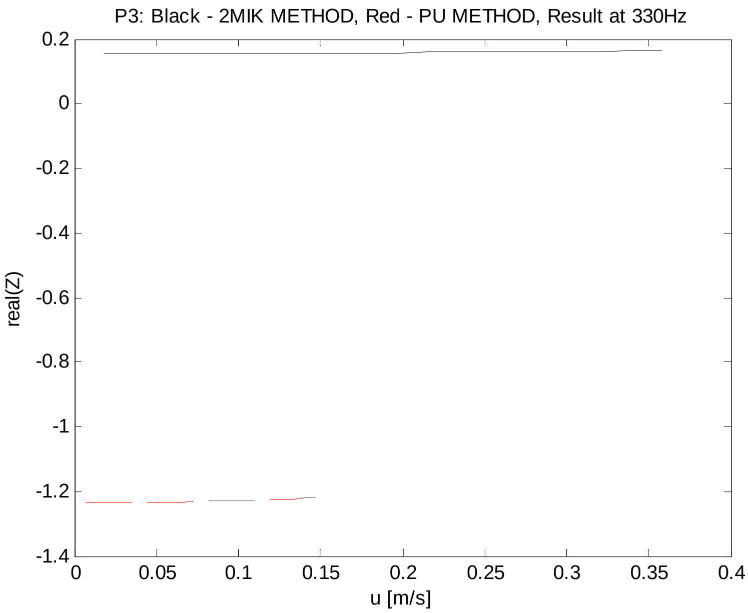
P3: Black - 2MIK METHOD, Red - PU METHOD, Result at 330Hz
real(Z)
u [m/s]
0.2
0
-0.2
-0.4
-0.6
-0.8
-1
-1.2
-1.4
0.05
0.1
0.15
0.2
0.25
0.3
0.35
0.4

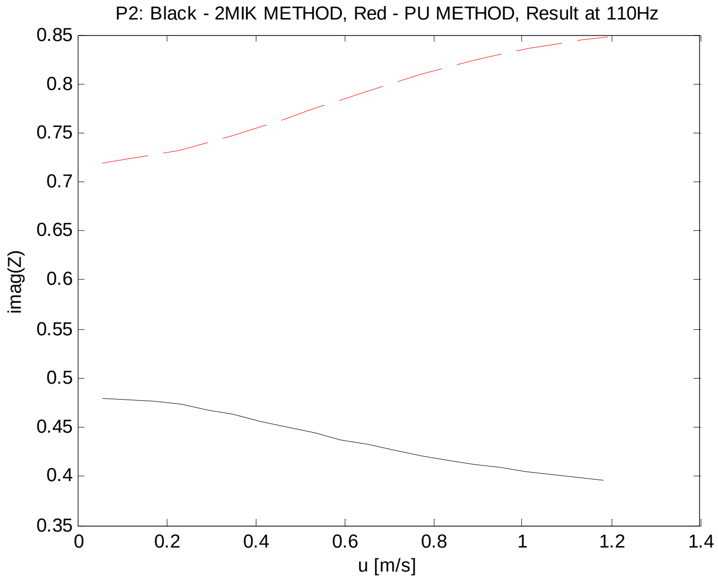
P2: Black - 2MIK METHOD, Red - PU METHOD, Result at 110Hz
imag(Z)
u [m/s]

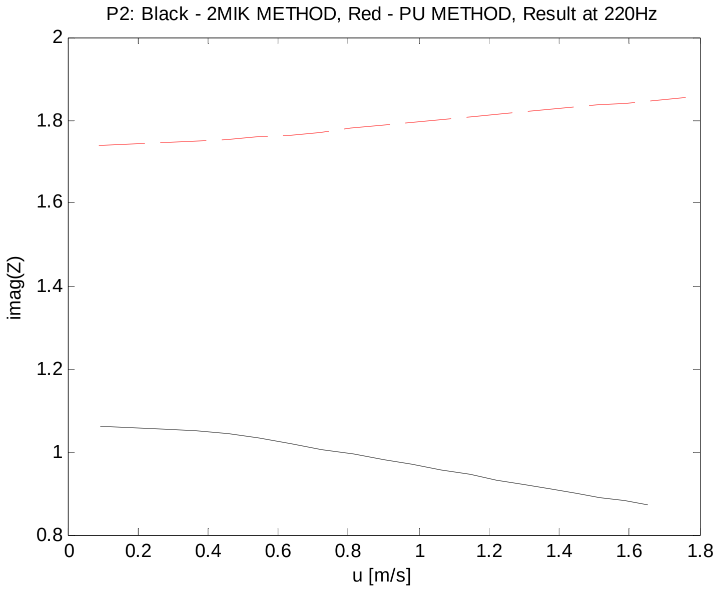
P2: Black - 2MIK METHOD, Red - PU METHOD, Result at 220Hz
imag(Z)
u [m/s]

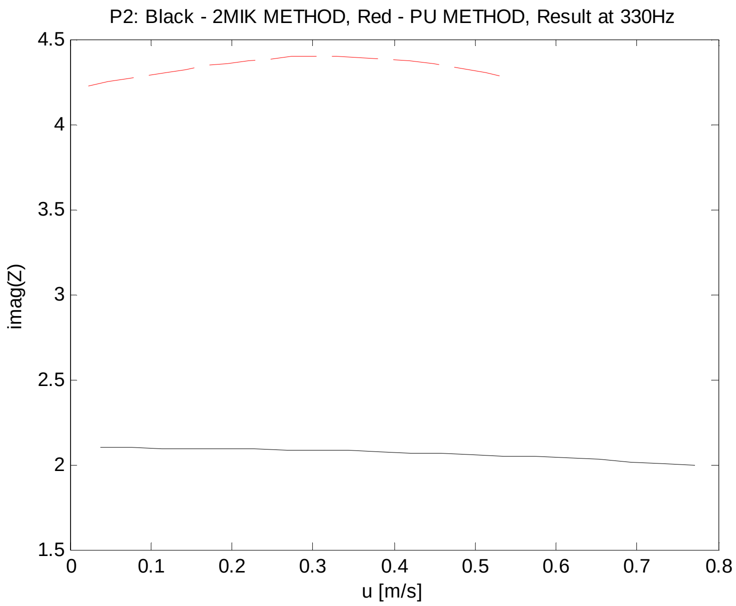
P2: Black - 2MIK METHOD, Red - PU METHOD, Result at 330Hz
imag(Z)
u [m/s]

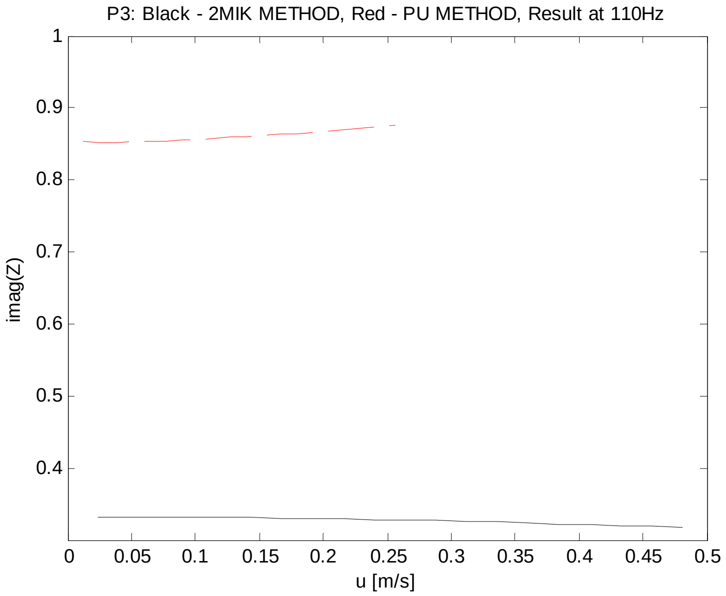

P3: Black - 2MIK METHOD, Red - PU METHOD, Result at 110Hz
imag(Z)
1
0.9
0.8
0.7
0.6
0.5
0.4
0
0.05
0.1
0.15
0.2
0.25
0.3
0.35
0.4
0.45
0.5
u [m/s]


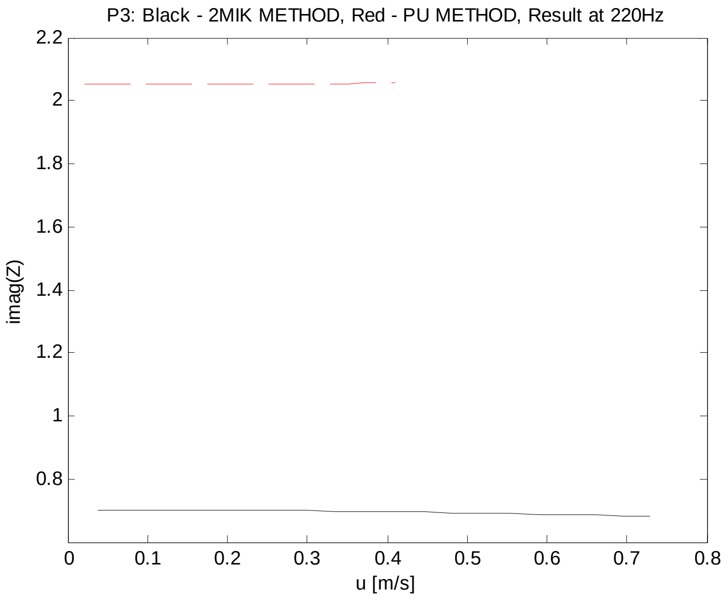

P3: Black - 2MIK METHOD, Red - PU METHOD, Result at 220Hz
imag(Z)
2.2
2
1.8
1.6
1.4
1.2
1
0.8
0
0.1
0.2
0.3
0.4
0.5
0.6
0.7
0.8
u [m/s]


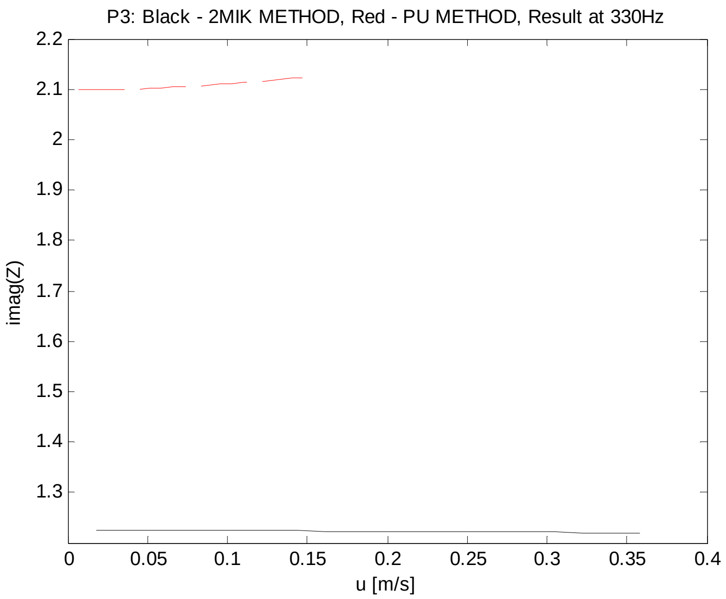

P3: Black - 2MIK METHOD, Red - PU METHOD, Result at 330Hz
imag(Z)
2.2
2.1
2
1.9
1.8
1.7
1.6
1.5
1.4
1.3
0
0.05
0.1
0.15
0.2
0.25
0.3
0.35
0.4
u [m/s]

The following aspects could have influenced the results. The holes for transducers were not tightened with rubber rings and holes not used were blocked by microphones used in two-microphone method. Because of the probe presence in the duct some disturbances in the original sound field have occurred. Data evaluation relied on moving measured impedances from the probe position to the sample position using linear theory.

It was mentioned in [Ref-6 JACOBSEN F. AND DE BREE H.-E. (2005)] that it was difficult to calibrate the Microflown sound intensity probe. It did not work to just calculate a compensation factor by a comparison of two measurements using two mentioned methods.

# 7. Conclusions

Acoustic properties of five samples have been investigated using impedance tube and two different measurement methods. Both single tone and two tone excitations involving harmonics have been used. Results include information about non-linear energy transfer between harmonics for tonal excitation and could be used for solving duct propagation problems through perforated pipes.

1. There is a nonlinear dependence of both reflection coefficient and acoustic impedance, in form of resistance and reactance, at the measurement frequency when the excitation is changed at other frequencies especially if the studied frequency is three times higher than the varied signal. The deviation is larger for the sample with higher particle velocity inside the holes.

2. If the excitation frequencies used in two-tone excitation are not exact harmonics it does not effect the acoustic properties measurement. The results will be approximately the same whether one of signals will be shifted 10Hz upwards or downwards in frequency.

3. In case of two-tonal excitation the shifted phase of the varied signal effects the impedance measurement.

4. For successful measurement of acoustic properties using the PU-method the sound intensity probe better calibration techniques must be used, perhaps calibration in an anechoic room or in a standing wave tube with rigid termination according to recommendations previously published in the literature. The calibration factor obtained by the technique used in this study is only good for the sample used in the comparison and also must be calculated for each frequency of excitation.

# 8. References:


1. BODEN H. 2008. On Impedance Measurements for Samples with Non-linear Acoustic Properties. AIAA Paper 2008-3016.

2. BODEN H. 2005. Experimental Investigation of Harmonic Interaction Effects for Perforates AIAA Paper 2005-2896.

3. ÅBOM M.. 2009. *An introduction to Flow Acoustics.* TRITA-AVE 2006:04. ISSN 1651-7660.

4. BODEN H., CARLSSON U., GLAV R. WALLIN H.P. AND ÅBOM M. 2001. *Ljud och Vibrationer.* Norstedts Tryckeri AB, Stockholm ISBN 91-7170-434-5.

5. BODEN H., GUO YING AND BORA TÖZUN HUSEYIN 2006. Experimental Investigation of Nonlinear Acoustic Properties for Perforates AIAA Paper 2006-2404.

6. JACOBSEN F. AND DE BREE H.-E. 2005. *A comparison of two different sound intensity measurement principles.,* submitted to J.Acoustical Society of AmericA.

7. JACOBSEN F. AND DE BREE H.-E. 2005. *Measurement of sound intensity: p-u probes versus p-p probes.*

8. BODEN H. AND ÅBOM M. 1986. *Influence of errors on the two-microphone method for measuring acoustic properties in ducts.* Journal of the Acoustical Society of America 79(2), 541-549

9. ÅBOM M. AND BODEN H. 1988. *Error analysis of two-microphone measurements in ducts with flow.* Journal of the Acoustical Society of America 83, 2429-2438

10. KUMAR S. 2007. *Linear Acoustic Modelling And Testing of Exhaust Mufflers.* Master of Science Thesis, KTH, Sweden